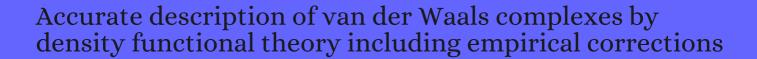
CITATION REPORT List of articles citing



DOI: 10.1002/jcc.20078 Journal of Computational Chemistry, 2004, 25, 1463-73.

Source: https://exaly.com/paper-pdf/37118687/citation-report.pdf

Version: 2024-04-28

This report has been generated based on the citations recorded by exaly.com for the above article. For the latest version of this publication list, visit the link given above.

The third column is the impact factor (IF) of the journal, and the fourth column is the number of citations of the article.

#	Paper	IF	Citations
2267	Interplay of Inter- and Intramolecular Interactions in Crystal Structures of 1,3,4-Thiadiazole Resorcinol Derivatives.		
2266	The Diverse Nature of Ion Speciation at the Nanoscale Hydrophobic/Water Interface.		
2265	First-Principles Treatment of Photoluminescence in Semiconductors.		
2264	Photoinduced Conversion of Cu Nanoclusters Self-Assembly Architectures from Ribbons to Spheres.		
2263	Boosted Reactivity of Ammonia Borane Dehydrogenation over Ni/Ni2P Heterostructure.		
2262	Visible-Light-Induced Living/Controlled Radical Copolymerization of 1-Octene and Acrylic Monomers Mediated by Organocobalt Complexes.		
2261	Combining Bidentate Lewis Acid Catalysis and Photochemistry: Formal Insertion of oXylene into an Enamine Double Bond.		
2260	In Situ Fabrication of NiMo Bimetal Sulfide Hybrid as an Efficient Electrocatalyst for Hydrogen Evolution over a Wide pH Range.		
2259	Metal-Free Catalytic Asymmetric Fluorination of Keto Esters Using a Combination of Hydrogen Fluoride (HF) and Oxidant: Experiment and Computation.		
2258	Unveiling the Mechanisms Leading to H2 Production Promoted by Water Decomposition on Epitaxial Graphene at Room Temperature.		
2257	Aluminum-Induced Interfacial Strengthening in Calcium Silicate Hydrates: Structure, Bonding, and Mechanical Properties.		
2256	Substituent Directed Phototransformations of BN-Heterocycles: Elimination vs Isomerization via Selective BC Bond Cleavage.		
2255	Carbon-Defect-Driven Electroless Deposition of Pt Atomic Clusters for Highly Efficient Hydrogen Evolution.		
2254	Selenium Substitution-Induced Hydration Changes of Crown Ethers As Tools for Probing Water Interactions with Supramolecular Macrocycles in Aqueous Solutions.		
2253	Elucidation of Chiral Symmetry Breaking in a Racemic Polymer System with Terahertz Vibrational Spectroscopy and Crystal Orbital Density Functional Theory.		
2252	Experimental and Theoretical Study on the Nature of Adsorbed Oxygen Species on Shaped Ceria Nanoparticles.		
2251	Crumpled Nitrogen-Doped Graphene-Wrapped Phosphorus Composite as a Promising Anode for Lithium-Ion Batteries.		

2250 Expanding the Origin of Stereocontrol in Propene Polymerization Catalysis.	
Single-Step Access to Long-Chain ,-Dicarboxylic Acids by Isomerizing Hydroxycarbonylation of Unsaturated Fatty Acids.	
2248 Syndioselective 3,4-Polymerization of 1Phenyl-1,3-Butadiene by Rare-Earth Metal Catalysts.	
Boron-carbon-nitride sheet as a novel surface for biological applications: insights from density functional theory.	
2246 Cooperative Electronic and Structural Regulation in a Bioinspired Allosteric Photoredox Catalyst.	
Comparative Experimental and Theoretical Study of the Fe L2,3-Edges Xray Absorption 2245 Spectroscopy in Three Highly Popular, Low-Spin Organoiron Complexes: [Fe(CO)5], [(5C5H5)Fe(CO)(-CO)]2, and [(5C5H5)2Fe].	
Comprehensive Study of the Thermochemistry of First-Row Transition Metal Compounds by Spin Component Scaled MP2 and MP3 Methods. 2004 , 23, 5581-5592	72
Highly Accurate Coupled Cluster Potential Energy Curves for the Benzene Dimer: Sandwich, T-Shaped, and Parallel-Displaced Configurations. 2004 , 108, 10200-10207	605
2242 Theoretische Chemie 2004. 2005 , 53, 287-293	О
2241 Modelling of hydrogen adsorption in the metal organic framework MOF5. 2005 , 317, 113-118	71
Van der Waals interactions in aromatic systems: structure and energetics of dimers and trimers of pyridine. 2005 , 6, 1554-8	142
2239 DFT study of fullerene dimers. 2005 , 6, 2625-32	21
Guanine quartet networks stabilized by cooperative hydrogen bonds. 2005 , 44, 2270-5	262
2237 Protonated isobutene in zeolites: tert-butyl cation or alkoxide?. 2005 , 44, 4769-71	98
Guanine Quartet Networks Stabilized by Cooperative Hydrogen Bonds. 2005 , 117, 2310-2315	63
Guanine Quartet Networks Stabilized by Cooperative Hydrogen Bonds. 2005, 117, 2310-2315 Protonated Isobutene in Zeolites: tert-Butyl Cation or Alkoxide?. 2005, 117, 4847-4849	63
	j

2232	Weak intermolecular interactions calculated with diffusion Monte Carlo. 2005 , 123, 184106	37
2231	Linear Response Properties Required to Simulate Vibrational Spectra of Biomolecules in Various Media: (R)-Phenyloxirane (A Comparative Theoretical and Spectroscopic Vibrational Study). 2005 , 91-124	11
2230	Proper gaussian basis sets for density functional studies of water dimers and trimers. 2005 , 109, 21471-5	34
2229	The X3LYP extended density functional accurately describes H-bonding but fails completely for stacking. 2005 , 7, 1624-6	135
2228	A Theoretical Investigation of the Geometries and Binding Energies of Molecular Tweezer and Clip Host-Guest Systems. 2005 , 1, 1110-8	61
2227	Design of density functionals that are broadly accurate for thermochemistry, thermochemical kinetics, and nonbonded interactions. 2005 , 109, 5656-67	1172
2226	Simple and complex lattices of N-alkyl fatty acid amides on a highly oriented pyrolytic graphite surface. 2005 , 21, 1364-70	25
2225	An Efficient a Posteriori Treatment for Dispersion Interaction in Density-Functional-Based Tight Binding. 2005 , 1, 841-7	251
2224	Stacked clusters of polycyclic aromatic hydrocarbon molecules. 2005 , 109, 2487-97	154
2223	Van der Waals complexes of polar aromatic molecules: unexpected structures for dimers of azulene. 2005 , 127, 14841-8	87
2222	A density-functional model of the dispersion interaction. 2005 , 123, 154101	902
2221	A post-Hartree-Fock model of intermolecular interactions. 2005 , 123, 24101	622
2220	Test of a nonempirical density functional: short-range part of the van der Waals interaction in rare-gas dimers. 2005 , 122, 114102	99
2219	Binding energy curves from nonempirical density functionals II. van der Waals bonds in rare-gas and alkaline-earth diatomics. 2005 , 109, 11015-21	79
2218	Prescription for the design and selection of density functional approximations: more constraint satisfaction with fewer fits. 2005 , 123, 62201	658
2217	Cooperativity in ionic liquids. 2006 , 124, 174506	146
2216	Density functional theory including dispersion corrections for intermolecular interactions in a large benchmark set of biologically relevant molecules. 2006 , 8, 5287-93	395
2215	A post-Hartree-Fock model of intermolecular interactions: inclusion of higher-order corrections. 2006 , 124, 174104	727

(2006-2006)

2214	functional and intermolecular perturbation theory approach. 2006 , 74,	95
2213	Coarse-grained interaction potentials for polyaromatic hydrocarbons. 2006 , 124, 054307	45
2212	Binding energies in benzene dimers: Nonlocal density functional calculations. 2006 , 124, 164105	149
2211	Dipolar interactions and hydrogen bonding in supramolecular aggregates: understanding cooperative phenomena for 1st hyperpolarizability. 2006 , 35, 1305-23	204
2210	Treating dispersion effects in extended systems by hybrid MP2:DFT calculationsprotonation of isobutene in zeolite ferrierite. 2006 , 8, 3955-65	210
2209	Semiempirical van der Waals correction to the density functional description of solids and molecular structures. 2006 , 73,	641
2208	Interaction energy of a water molecule with a single-layer graphitic surface modeled by hydrogenand fluorine-terminated clusters. 2006 , 110, 10501-6	36
2207	Stacking interactions as the principal design element in acyl-transfer catalysts. 2006 , 4, 4223-30	37
2206	On the accuracy of density functional theory in transition metal chemistry. 2006 , 102, 203	258
2205	Adsorption of Ar on graphite using London dispersion forces corrected Kohn-Sham density functional theory. 2006 , 73,	41
2204	Systematic errors in computed alkane energies using B3LYP and other popular DFT functionals. 2006 , 8, 3631-4	363
2203	Application of van der Waals density functional to an extended system: adsorption of benzene and naphthalene on graphite. 2006 , 96, 146107	343
2202	Interaction energy contributions of H-bonded and stacked structures of the AT and GC DNA base pairs from the combined density functional theory and intermolecular perturbation theory approach. 2006 , 128, 11730-1	174
2201	Time dependent density functional theory calculations for electronic circular dichroism spectra and optical rotations of conformationally flexible chiral donor-acceptor dyad. 2006 , 71, 9797-806	50
2200	Characterizing the potential energy surface of the water dimer with DFT: failures of some popular functionals for hydrogen bonding. 2006 , 110, 7268-71	46
2199	Density Functional Theoretical Studies of the Re K e Bonds in Re(Cp)(CO)(PF3)Xe and Re(Cp)(CO)2Xe. 2006 , 25, 5242-5248	11
2198	High-accuracy quantum mechanical studies of pi-pi interactions in benzene dimers. 2006 , 110, 10656-68	659
2197	Formation and destruction of polycyclic aromatic hydrocarbon clusters in the interstellar medium. 2006 , 460, 519-531	112

2196	DFT modeling of biological systems. 2006 , 243, 2500-2515		12
2195	Multicentered integrated QM:QM methods for weakly bound clusters: An efficient and accurate 2-body:many-body treatment of hydrogen bonding and van der Waals interactions. 2006 , 427, 185-191		60
2194	van der Waals corrections to density functional theory calculations: Methane, ethane, ethylene, benzene, formaldehyde, ammonia, water, PBE, and CPMD. 2006 , 327, 54-62		64
2193	Molecular quantum mechanics to biodynamics: Essential connections. 2006 , 764, 1-8		6
2192	Aliphatic C-H/pi interactions: Methane-benzene, methane-phenol, and methane-indole complexes. 2006 , 110, 10822-8		162
2191	Benchmark database of accurate (MP2 and CCSD(T) complete basis set limit) interaction energies of small model complexes, DNA base pairs, and amino acid pairs. 2006 , 8, 1985-93		1499
2190	Conformational changes in glycine tri- and hexapeptide. 2006 , 39, 23-34		16
2189	Semiempirical hybrid density functional with perturbative second-order correlation. 2006 , 124, 034108		2321
2188	Modelling of carbohydrate-aromatic interactions: ab initio energetics and force field performance. 2005 , 19, 887-901		55
2187	The SCC-DFTB method and its application to biological systems. 2006 , 116, 316-325		296
2186	Oligoethylene chains terminated by ferrocenyl end groups: synthesis, structural properties, and two-dimensional self-assembly on surfaces. 2006 , 12, 1618-28		34
2185	Origin of stereoinduction by chiral aminophosphane phosphinite ligands in enantioselective catalysis: asymmetric hydroformylation. 2006 , 12, 1457-67		34
2184	The importance of inter- and intramolecular van der Waals interactions in organic reactions: the dimerization of anthracene revisited. 2006 , 45, 625-9		116
2183	Seemingly simple stereoelectronic effects in alkane isomers and the implications for Kohn-Sham density functional theory. 2006 , 45, 4460-4		332
2182	Hybrid density functional theory for pi-stacking interactions: application to benzenes, pyridines, and DNA bases. <i>Journal of Computational Chemistry</i> , 2006 , 27, 491-504	3.5	226
2181	Semiempirical GGA-type density functional constructed with a long-range dispersion correction. Journal of Computational Chemistry, 2006 , 27, 1787-99	3.5	19063
2180	Carbon nanorings: A challenge to theoretical chemistry. 2006 , 7, 2503-7		34
2179	The Importance of Inter- and Intramolecular van der Waals Interactions in Organic Reactions: the Dimerization of Anthracene Revisited. 2006 , 118, 641-645		20

(2007-2006)

2178	Scheinbar einfache stereo-elektronische Effekte in Alkan-Isomeren und ihre Auswirkungen fildie Kohn-Sham-Dichtefunktionaltheorie. 2006 , 118, 4571-4575	52
2177	Intermolecular potentials of the methane dimer calculated with M ${ m I}$ ler-Plesset perturbation theory and density functional theory. 2006 , 125, 094312	39
2176	The use of atomic intrinsic polarizabilities in the evaluation of the dispersion energy. 2007 , 127, 224105	30
2175	Infrared photodissociation of a water molecule from a flexible molecule-H2O complex: rates and conformational product yields following XH stretch excitation. 2007 , 126, 134306	33
2174	Local and semilocal density functional computations for crystals of 1-alkyl-3-methyl-imidazolium salts. 2007 , 126, 144705	19
2173	Dispersion interactions within the Piris natural orbital functional theory: the helium dimer. 2007 , 126, 214103	41
2172	Calculations of the Stabilization Energies of the Building Blocks of Biomacromolecules. 2007,	1
2171	Mg2+ binding and archaeosine modification stabilize the G15 C48 Levitt base pair in tRNAs. 2007 , 13, 1427-36	70
2170	Library of dispersion-corrected atom-centered potentials for generalized gradient approximation functionals: Elements H, C, N, O, He, Ne, Ar, and Kr. 2007 , 75,	149
2169	Energetics of interlayer binding in graphite: The semiempirical approach revisited. 2007, 76,	57
2168	Computational Design of High Hydrogen Adsorption Efficiency in Molecular Bulflower 2007 , 111, 4487-4490	40
2167	Unraveling solvent-driven equilibria between alpha- and 3(10)-helices through an integrated spin labeling and computational approach. 2007 , 129, 11248-58	39
2166	Interaction of metal porphyrins with fullerene C60: a new insight. 2007 , 111, 4374-82	25
2165	Resolution of identity density functional theory augmented with an empirical dispersion term (RI-DFT-D): a promising tool for studying isolated small peptides. 2007 , 111, 1146-54	66
2164	Semi-empirical molecular orbital methods including dispersion corrections for the accurate prediction of the full range of intermolecular interactions in biomolecules. 2007 , 9, 2362-70	117
2163	Density functional theory with dispersion corrections for supramolecular structures, aggregates, and complexes of (bio)organic molecules. 2007 , 5, 741-58	636
2162	Non-covalent interactions in biomacromolecules. 2007 , 9, 5291-303	339
2161	Application of valence-bond techniques to the study of weakly bound complexes. The potential energy surface of the Ne-CH(4) system. 2007 , 9, 2457-69	4

2160	The Application of Modern Computational Chemistry Methods to Organometallic Systems. 2007, 639-669	3
2159	On calculating a polymer's enthalpy of formation with quantum chemical methods. 2007 , 111, 13869-72	6
2158	Noncovalent Interactions between Graphene Sheets and in Multishell (Hyper)Fullerenes. 2007 , 111, 11199-1	12 0 73
2157	Potassium intercalation in graphite: A van der Waals density-functional study. 2007, 76,	142
2156	A comparison between plane wave and Gaussian-type orbital basis sets for hydrogen bonded systems: formic acid as a test case. 2007 , 127, 154102	59
2155	Assessment of the MP2 method, along with several basis sets, for the computation of interaction energies of biologically relevant hydrogen bonded and dispersion bound complexes. 2007 , 111, 8257-63	160
2154	Density Functional and Semiempirical Molecular Orbital Methods Including Dispersion Corrections for the Accurate Description of Noncovalent Interactions Involving Sulfur-Containing Molecules. 2007 , 3, 1656-64	70
2153	Comparing the electron and hole mobilities in the 由nd phases of perylene: role of Btacking. 2007 , 17, 1933-1938	60
2152	Pseudohelical and helical primary structures of 1,2-spiroannelated four- and five-membered rings: syntheses and chiroptical properties. 2007 , 72, 9264-77	16
2151	Oxidative Dehydrogenation of Propane by Monomeric Vanadium Oxide Sites on Silica Support. 2007 , 111, 6041-6050	156
2150	Applications of Quantum Chemical Methods in Zeolite Science. 2007, 701-XXI	15
2149	Accurate theoretical determination of the structure of aromatic complexes is complicated: the phenol dimer and phenolmethanol cases. 2007 , 111, 5851-4	36
2148	Radical Cations of the Nucleic Bases and Radiation Damage to DNA: Ab Initio Study. 2007, 121-147	26
2147	Hydration and stability of nucleic acid bases and base pairs. 2007 , 9, 903-17	79
2146	Benchmark RI-MP2 database of nucleic acid base trimers: performance of different density functional models for prediction of structures and binding energies. 2007 , 9, 5000-8	60
2145	Evaluation of the adsorption free energy of light guest molecules in nanoporous host structures. 2007 , 9, 2697-705	11
2144	Experimental and theoretical study of the CD spectra and conformational properties of axially chiral 2,2'-, 3,3'-, and 4,4'-biphenol ethers. 2007 , 111, 4222-34	55
2143	Comparative performance of exchange and correlation density functionals in determining intermolecular interaction potentials of the methane dimer. 2007 , 111, 9586-90	16

(2007-2007)

2142	Predicting noncovalent interactions between aromatic biomolecules with London-dispersion-corrected DFT. 2007 , 111, 14346-54	61
2141	Quantum Chemical Adsorption Studies on the (110) Surface of the Mineral Goethite. 2007 , 111, 877-885	37
2140	Electron and hole mobilities in polymorphs of benzene and naphthalene: role of intermolecular interactions. 2007 , 126, 144710	68
2139	Quantum chemical study on the circular dichroism spectra and specific rotation of donor-acceptor cyclophanes. 2007 , 111, 7995-8006	39
2138	C-H bond activation by hyperconjugation with Al-C bonds and by chelating coordination of the hydride ion. 2007 , 129, 11259-64	29
2137	Ab Initio Modeling of Methanol Interaction with Single-Walled Carbon Nanotubes. 2007 , 111, 18917-18926	29
2136	Direct measurements of the interaction between pyrene and graphite in aqueous media by single molecule force spectroscopy: understanding the pi-pi interactions. 2007 , 23, 7911-5	114
2135	Structure of the naphthalene dimer from rare gas tagging. 2007 , 111, 4211-4	14
2134	Interaction between n-Alkane Chains: Applicability of the Empirically Corrected Density Functional Theory for Van der Waals Complexes. 2007 , 3, 755-63	86
2133	On the Convergence of the Physicochemical Properties of [n]Helicenes. 2007 , 111, 14948-14955	65
2132	Empirical Correction to Molecular Interaction Energies in Density Functional Theory (DFT) for Methane Hydrate Simulation. 2007 , 3, 1665-72	27
2131	Parametrization of an empirical correction term to density functional theory for an accurate description of pi-stacking interactions in nucleic acids. 2007 , 111, 13124-34	39
2130	Extension of the self-consistent-charge density-functional tight-binding method: third-order expansion of the density functional theory total energy and introduction of a modified effective coulomb interaction. 2007 , 111, 10861-73	221
2129	Density-functional, density-functional tight-binding, and wave function calculations on biomolecular systems. 2007 , 111, 5642-7	26
2128	Can the DFT-D method describe the full range of noncovalent interactions found in large biomolecules?. 2007 , 9, 448-51	120
2127	Weakly Bonded Complexes of Aliphatic and Aromatic Carbon Compounds Described with Dispersion Corrected Density Functional Theory. 2007 , 3, 1673-9	64
2126	CarParrinello Molecular Dynamics Simulations and Biological Systems. 2006, 133-171	17
2125	A combined experimental and theoretical study on the conformation of multiarmed chiral aryl ethers. 2007 , 72, 6998-7010	28

2124	Stereoelectronic Substituent Effects in Saturated Main Group Molecules: Severe Problems of Current Kohn-Sham Density Functional Theory. 2007 , 3, 42-5	74
2123	A new class of chiroptical molecular switches based on the redox-induced conformational changes. 2007 , 9, 3977-80	18
2122	Leading RNA tertiary interactions: structures, energies, and water insertion of A-minor and P-interactions. A quantum chemical view. 2007 , 111, 9153-64	38
2121	Vibrations and thermodynamics of clusters of polycyclic aromatic hydrocarbon molecules: the role of internal modes. 2007 , 111, 2999-3009	30
2120	Basis set limit coupled cluster study of h-bonded systems and assessment of more approximate methods. 2007 , 111, 11122-33	85
2119	Density Functionals for Noncovalent Interaction Energies of Biological Importance. 2007 , 3, 289-300	528
2118	Double-hybrid density functionals with long-range dispersion corrections: higher accuracy and extended applicability. 2007 , 9, 3397-406	890
2117	Van der Waals density functional: Self-consistent potential and the nature of the van der Waals bond. 2007 , 76,	909
2116	Efficient calculation of van der Waals dispersion coefficients with time-dependent density functional theory in real time: application to polycyclic aromatic hydrocarbons. 2007 , 127, 014107	28
2115	Rapid intramolecular heterolytic dihydrogen activation by a four-membered heterocyclic phosphane-borane adduct. 2007 , 5072-4	516
2114	Performance of the DFT-D method, paired with the PCM implicit solvation model, for the computation of interaction energies of solvated complexes of biological interest. 2007 , 9, 5555-60	59
2113	CH/pi interactions in DNA and proteins. A theoretical study. 2007 , 111, 9372-9	51
2112	London dispersion forces by range-separated hybrid density functional with second order perturbational corrections: the case of rare gas complexes. 2007 , 126, 044103	71
2111	Structure and Reactivity of Solid Catalysts [Quantum Chemical Approach. 2007 , 19-26	1
2110	DNA base trimers: empirical and quantum chemical ab initio calculations versus experiment in vacuo. 2007 , 13, 2067-77	26
2109	Highly diastereoselective lithiation and substitution of an (S)-prolinyl thiocarbamate via sterically homogeneous lithio(thiocarbamate): synthesis of enantiomerically pure prolinethiols. 2007 , 13, 6419-29	10
2108	Estimation of the kinetic acidity from substrate conformationstereochemical course of the deprotonation of cyclohexenyl carbamates. 2007 , 46, 1645-9	16
2107	Relative energy computations with approximate density functional theorya caveat!. 2007 , 46, 4217-9	171

2106 l	Homolytic substitution at phosphorus for the synthesis of alkyl and aryl phosphanes. 2007 , 46, 6533-6	56
	Vorhersage der kinetischen Acidit durch Konformationsanalyse der Substrate ßtereochemischer Verlauf der Deprotonierung von Cyclohexenylcarbamaten. 2007 , 119, 1672-1676	5
	Die Berechnung relativer Energien mit approximativer Dichtefunktionaltheorie leine Warnung. 2007 , 119, 4295-4297	26
2103	Homolytische Substitution am Phosphor zur Synthese von Alkyl- und Arylphosphanen. 2007 , 119, 6653-6656	17
2102	Density functional theory augmented with an empirical dispersion term. Interaction energies and geometries of 80 noncovalent complexes compared with ab initio quantum mechanics calculations. 3.5 Journal of Computational Chemistry, 2007, 28, 555-69	592
	A comparative quantum chemical study of the ruthenium catalyzed olefin metathesis. <i>Journal of Computational Chemistry</i> , 2007 , 28, 2275-85	58
2100 l	Decomposition Cascades of Dicoordinate Copper(I) Chalcogenides. 2007 , 2007, 5294-5299	6
2 099 <i>I</i>	Amphiphilic organic ion pairs in solution: a theoretical study. 2007 , 8, 1524-33	11
	nsufficient description of dispersion in B3LYP and large basis set superposition errors in MP2 calculations can hide peptide conformers. 2007 , 442, 42-46	106
	Vibrational dynamics of hydrogen-bonded HCN complexes with OH and NH acids: Computational OFT systematic study. 2007 , 107, 1170-1180	14
2096 I	nterplay of electrostatic and van der Waals forces in coronene dimer. 2007, 107, 1335-1343	42
2095	Ab Initio Study of Compressed 1,3,5,7-Tetranitro-1,3,5,7-tetraazacyclooctane (HMX), Cyclotrimethylenetrinitramine (RDX), 2,4,6,8,10,12-Hexanitrohexaazaisowurzitane (CL-20), 2,4,6-Trinitro-1,3,5-benzenetriamine (TATB), and Pentaerythritol Tetranitrate (PETN). 2007 , 111, 2787-2796	136
	Thermodynamics of reversible gas adsorption on alkali-metal exchanged zeolitesthe interplay of nfrared spectroscopy and theoretical calculations. 2007 , 9, 1421-37	90
	ntermolecular potentials of the silane dimer calculated with Hartree-Fock theory, Mller-Plesset perturbation theory, and density functional theory. 2007 , 111, 11922-9	10
	Long-range corrected density functional study on weakly bound systems: balanced descriptions of various types of molecular interactions. 2007 , 126, 234114	133
2091	Beyond a HartreeBock description of crystalline solids: the case of lithium hydride. 2007 , 117, 781-791	29
	Reparameterization of a meta-generalized gradient approximation functional by combining TPSS exchange with 1 correlation. 2007 , 118, 693-707	19
2089 I	Pi-pi stacking tackled with density functional theory. 2007 , 13, 1245-57	111

2088	MP2, DFT-D, and PCM study of the HMBIICNE complex: Thermodynamics, electric properties, and solvent effects. 2008 , 108, 1533-1545		10
2087	Identifying stabilizing key residues in proteins using interresidue interaction energy matrix. 2008 , 72, 402-13		30
2086	Structural importance of secondary interactions in molecules: origin of unconventional conformations of phosphine-borane adducts. 2008 , 14, 333-43		68
2085	Potential-energy and free-energy surfaces of glycyl-phenylalanyl-alanine (GFA) tripeptide: experiment and theory. 2008 , 14, 4886-98		44
2084	Characterization of three members of the electron-transfer series [Fe(pda)2]n (n=2-, 1-, 0) by spectroscopy and density functional theoretical calculations [pda=redox non-innocent derivatives of N,N'-bis(pentafluorophenyl)-o-phenylenediamide(2-, 1, 0)]. 2008 , 14, 7608-22		40
2083	Calculation of conformational energies and optical rotation of the most simple chiral alkane. 2008 , 20, 1009-15		33
2082	Investigation of the benzene-naphthalene and naphthalene-naphthalene potential energy surfaces: DFT/CCSD(T) correction scheme. 2008 , 9, 1702-8		45
2081	Highly accurate CCSD(T) and DFT-SAPT stabilization energies of H-bonded and stacked structures of the uracil dimer. 2008 , 9, 1636-44		108
2080	IRMPD spectroscopy of a protonated, phosphorylated dipeptide. 2008 , 9, 2564-73		33
2079	Quantum chemical investigation of exciton coupling: super-molecular calculations of a merocyanine dimer aggregate. 2008 , 9, 2467-70		30
2078	Evaluation of the intramolecular basis set superposition error in the calculations of larger molecules: [n]helicenes and Phe-Gly-Phe tripeptide. <i>Journal of Computational Chemistry</i> , 2008 , 29, 861-70	.5	62
2077	Calculation of weakly polar interaction energies in polypeptides using density functional and local Mler-Plesset perturbation theory. <i>Journal of Computational Chemistry</i> , 2008 , 29, 1344-52	.5	30
2076	Application of semiempirical long-range dispersion corrections to periodic systems in density functional theory. <i>Journal of Computational Chemistry</i> , 2008 , 29, 2088-97	.5	247
2075	Different Reactivity Patterns in the Reactions of the Homologous Trimethylelement Compounds EMe3 (E = Al, Ga, In) with Methylhydrazine. 2008 , 2008, 543-551		24
2074	Synthesis of Enantiopure Highly Functionalized Pyrrolizines and Indolizines from Natural Amino Acids: An Experimental and Theoretical Investigation. 2008 , 2008, 2808-2816		20
2073	Increased stability of C60 encapsulated in double walled carbon nanotubes. 2008, 455, 88-92		4
2072	Theoretical investigation of equilibrium and transition state structures, binding energies and barrier heights of water-encapsulated open-cage [59]fullerenone complexes. 2008 , 465, 48-52		11
2071	Magnetic interactions in dehydrogenated Guanine Lytosine base pair. 2008, 465, 285-289		10

(2009-2008)

2070	A commentary on Density functional calculation of hydrogen-filled C60 moleculesIby C-K. Yang [Carbon 2007;45(12):2451B3]. 2008 , 46, 704-705	13
2069	Reply to the Commentary on D ensity functional calculation of hydrogen-filled C60 molecules © 2008 , 46, 705	6
2068	Excited state dynamics in pyrrole water clusters: First-principles simulation. 2008, 343, 347-352	15
2067	Theoretical energetic and vibrational analysis of amide-templated pseudorotaxanes. 2008, 343, 186-199	9
2066	Hydrogen and dihydrogen bonding of transition metal hydrides. 2008 , 345, 95-102	28
2065	Weak intermolecular bonding in N,N?-dimethylethyleneurea dimers and N,N?-dimethylethyleneurealvater systems: The role of the dispersion effects in intermolecular interaction. 2008 , 354, 202-210	12
2064	Time-dependent density functional study of excimers and exciplexes of organic molecules. 2008 , 343, 362-371	67
2063	Hydrogen adsorption strength and sites in the metal organic framework MOF5: Comparing experiment and model calculations. 2008 , 351, 72-76	59
2062	Intermolecular potential calculations for polynuclear aromatic hydrocarbon clusters. 2008, 112, 6249-56	92
2061	Geometries of Third-Row Transition-Metal Complexes from Density-Functional Theory. 2008 , 4, 1449-59	363
2060	Configurationally labile lithiated O-benzyl carbamates: application in asymmetric synthesis and quantum chemical investigations on the equilibrium of diastereomers. 2008 , 3, 78-87	28
2059	Thermodynamic stability versus kinetic lability of ZnS4 core. 2010 , 5, 1445-54	4
2058	Modeling the interplay of inter- and intramolecular hydrogen bonding in conformational polymorphs. 2008 , 128, 244708	78
2057	Intermolecular pi-pi interactions in solids. 2008 , 10, 2611-5	42
2056	Long-range corrected hybrid density functionals with damped atom-atom dispersion corrections. 2008 , 10, 6615-20	7709
2055	Performance of B3LYP Density Functional Methods for a Large Set of Organic Molecules. 2008 , 4, 297-306	601
2054	Implementation and Performance of DFT-D with Respect to Basis Set and Functional for Study of Dispersion Interactions in Nanoscale Aromatic Hydrocarbons. 2008 , 4, 2030-48	149
2053	Equilibrium Molecular Dynamics Simulations. 2009 , 255-290	9

2052	OMx-D: semiempirical methods with orthogonalization and dispersion corrections. Implementation and biochemical application. 2008 , 10, 2159-66	87
2051	Melamine Structures on the Au(111) Surface. 2008, 112, 11476-11480	106
2050	Highly accurate first-principles benchmark data sets for the parametrization and validation of density functional and other approximate methods. Derivation of a robust, generally applicable, double-hybrid functional for thermochemistry and thermochemical kinetics. 2008 , 112, 12868-86	578
2049	Estimate of Benzenellriphenylene and Triphenylenellriphenylene Interactions: A Topic Relevant to Columnar Discotic Liquid Crystals. 2008 , 112, 9501-9509	11
2048	Nature and magnitude of aromatic stacking of nucleic acid bases. 2008 , 10, 2595-610	300
2047	Searching of potential energy curves for the benzene dimer using dispersion-corrected density functional theory. 2008 , 10, 2715-21	22
2046	Describing weak interactions of biomolecules with dispersion-corrected density functional theory. 2008 , 10, 2730-4	56
2045	Calculating stacking interactions in nucleic acid base-pair steps using spin-component scaling and local second order Mller-Plesset perturbation theory. 2008 , 10, 2785-91	45
2044	The interaction of carbohydrates and amino acids with aromatic systems studied by density functional and semi-empirical molecular orbital calculations with dispersion corrections. 2008 , 10, 2767-74	44
2043	B3LYP augmented with an empirical dispersion term (B3LYP-D*) as applied to molecular crystals. 2008 , 10, 405-410	642
2042	Role of interaction anisotropy in the formation and stability of molecular templates. 2008, 100, 156101	62
2041	Computational characterization and modeling of buckyball tweezers: density functional study of concave-convex pipi interactions. 2008 , 10, 2813-8	179
2040	Pi-stacking effect on levoglucosenone derived internal chiral auxiliaries. A case of complete enantioselectivity inversion on the Diels-Alder reaction. 2008 , 10, 3389-92	34
2039	Structures and interaction energies of stacked graphene-nucleobase complexes. 2008 , 10, 2722-9	231
2038	Assessment of Density Functionals for Intramolecular Dispersion-Rich Interactions. 2008, 4, 1610-9	65
2037	Empirical corrections to density functional theory highlight the importance of nonbonded intramolecular interactions in alkanes. 2008 , 112, 11495-500	46
2036	Physical origins of interactions in dimers of polycyclic aromatic hydrocarbons. 2008 , 10, 2735-46	115
2035	Assessment of the Performance of the M05-2X and M06-2X Exchange-Correlation Functionals for Noncovalent Interactions in Biomolecules. 2008 , 4, 1996-2000	555

(2008-2008)

2034	Toward the exact solution of the electronic Schrödinger equation for noncovalent molecular interactions: worldwide distributed quantum monte carlo calculations. 2008 , 112, 2104-9	45
2033	Probing phenylalanine/adenine pi-stacking interactions in protein complexes with explicitly correlated and CCSD(T) computations. 2008 , 112, 14291-5	42
2032	On the accuracy of density-functional theory exchange-correlation functionals for H bonds in small water clusters. II. The water hexamer and van der Waals interactions. 2008 , 129, 194111	204
2031	A Prototype for Graphene Material Simulation: Structures and Interaction Potentials of Coronene Dimers. 2008 , 112, 4061-4067	135
2030	Conformational Isomerism in the Isoreticular Metal Organic Framework Family: A Force Field Investigation. 2008 , 112, 14980-14987	43
2029	Self-consistent implementation of a nonlocal van der Waals density functional with a Gaussian basis set. 2008 , 129, 014106	71
2028	Accurate and efficient calculation of van der Waals interactions within density functional theory by local atomic potential approach. 2008 , 129, 154102	70
2027	Investigation of the benzene-dimer potential energy surface: DFT/CCSD(T) correction scheme. 2008 , 128, 114102	160
2026	Analysis of non-covalent interactions in (bio)organic molecules using orbital-partitioned localized MP2. 2008 , 10, 3327-34	51
2025	Popular Kohn-Sham density functionals strongly overestimate many-body interactions in van der Waals systems. 2008 , 78,	74
2024	On the mechanism of asymmetric allylation of aldehydes with allyltrichlorosilanes catalyzed by QUINOX, a chiral isoquinoline N-oxide. 2008 , 130, 5341-8	103
2023	Interactions in large, polyaromatic hydrocarbon dimers: application of density functional theory with dispersion corrections. 2008 , 112, 10968-76	131
2022	Exploring the Limit of Accuracy of the Global Hybrid Meta Density Functional for Main-Group Thermochemistry, Kinetics, and Noncovalent Interactions. 2008 , 4, 1849-68	784
2021	Benzene Dimer: High-Level Wave Function and Density Functional Theory Calculations. 2008 , 4, 1829-34	215
2020	The structure and binding energies of the van der Waals complexes of Ar and N2 with phenol and its cation, studied by high level ab initio and density functional theory calculations. 2008 , 128, 044313	22
2019	Stability and cations coordination of DNA and RNA 14-mer G-quadruplexes: a multiscale computational approach. 2008 , 112, 12115-23	32
2018	IR/UV spectra and quantum chemical calculations of Trp-Ser: stacking interactions between backbone and indole side-chain. 2008 , 10, 2844-51	33
2017	Tighter multipole-based integral estimates and parallel implementation of linear-scaling AO-MP2 theory. 2008 , 10, 3335-44	71

2016	Carbohydrate-protein recognition probed by density functional theory and ab initio calculations including dispersive interactions. 2008 , 10, 6500-8	43
2015	Improved supermolecular second order Mler-Plesset intermolecular interaction energies using time-dependent density functional response theory. 2008 , 128, 144112	116
2014	The non-covalent functionalisation of carbon nanotubes studied by density functional and semi-empirical molecular orbital methods including dispersion corrections. 2008 , 10, 128-35	28
2013	A QM/MM study of fluoroaromatic interactions at the binding site of carbonic anhydrase II, using a DFT method corrected for dispersive interactions. 2008 , 10, 2706-14	18
2012	Microscopic Characterization of the Interface between Aromatic Isocyanides and Au(111): A First-Principles Investigation. 2008 , 112, 6413-6421	34
2011	Adsorption of aromatic hydrocarbons and ozone at environmental aqueous surfaces. 2008 , 112, 4942-50	35
2010	On the importance of electron correlation effects for the intramolecular stacking geometry of a bis-thiophene derivative. 2008 , 112, 12469-74	22
2009	Origin of Enantioselective Hydrogenation of Ketones by RuH2(diphosphine)(diamine) Catalysts: A Theoretical Study. 2008 , 27, 1514-1523	47
2008	A quantum mechanical strategy to investigate the structure of liquids: the cases of acetonitrile, formamide, and their mixture. 2008 , 112, 6803-13	8
2007	Semiempirical double-hybrid density functional with improved description of long-range correlation. 2008 , 112, 2702-12	114
2006	Metahybrid density functional theory and correlated ab initio studies on microhydrated adenine-thymine base pairs. 2008 , 112, 9182-6	9
2005	Theoretical thermodynamics for large molecules: walking the thin line between accuracy and computational cost. 2008 , 41, 569-79	313
2005	Computational cost. 2008 , 41, 569-79 A combined theoretical and experimental study of the polymer inter-chain structure in	313
	computational cost. 2008 , 41, 569-79 A combined theoretical and experimental study of the polymer inter-chain structure in	
2004	A combined theoretical and experimental study of the polymer inter-chain structure in poly(phenylene vinylene) derivatives. 2008 , 1, 015006	4
2004	A combined theoretical and experimental study of the polymer inter-chain structure in poly(phenylene vinylene) derivatives. 2008, 1, 015006 Bond dissociation enthalpies of large aromatic carbon-centered radicals. 2008, 112, 13566-73 Electronic properties and stabilities of bulk and low-index surfaces of SnO in comparison with SnO2: A first-principles density functional approach with an empirical correction of van der Waals	32
2004	A combined theoretical and experimental study of the polymer inter-chain structure in poly(phenylene vinylene) derivatives. 2008, 1, 015006 Bond dissociation enthalpies of large aromatic carbon-centered radicals. 2008, 112, 13566-73 Electronic properties and stabilities of bulk and low-index surfaces of SnO in comparison with SnO2: A first-principles density functional approach with an empirical correction of van der Waals interactions. 2008, 77, Benzene Dimer: Dynamic Structure and Thermodynamics Derived from On-the-Fly ab initio DFT-D	4 32 98

1998	Statistical model for intermolecular adhesion in pi-conjugated polymers. 2008 , 100, 198303	3
1997	Adsorption and bonding mechanism of a N,N?-di(n-butyl)quinacridone monolayer studied by density functional theory including semiempirical dispersion corrections. 2008 , 78,	3
1996	Deriving molecular bonding from a macromolecular self-assembly using kinetic Monte Carlo simulations. 2008 , 77,	44
1995	Efficient computation of the dispersion interaction with density-functional theory. 2009, 79,	53
1994	Stacking of polycyclic aromatic hydrocarbons as prototype for graphene multilayers, studied using density functional theory augmented with a dispersion term. 2009 , 131, 194702	41
1993	Fluorescence quenching in an organic donor-acceptor dyad: a first principles study. 2009 , 131, 034310	14
1992	Density functional method including weak interactions: Dispersion coefficients based on the local response approximation. 2009 , 131, 224104	188
1991	Oscillations in meta-generalized-gradient approximation potential energy surfaces for dispersion-bound complexes. 2009 , 131, 034111	146
1990	Dispersion-corrected Mller-Plesset second-order perturbation theory. 2009 , 131, 094106	172
1989	A new all-round density functional based on spin states and S(N)2 barriers. 2009 , 131, 094103	104
1988	Surface stability and electronic structure of hydrogen- and fluorine-terminated diamond surfaces: A first principles investigation. 2009 , 24, 2461-2470	34
1987	Combined experimental and quantum chemical investigation of chiroptical properties of nicotinamide derivatives with and without intramolecular cation-pi interactions. 2009 , 113, 8754-64	31
1986	Study of the interaction between water and hydrogen sulfide with polycyclic aromatic hydrocarbons. 2009 , 130, 234307	26
1985	Approximating quantum many-body intermolecular interactions in molecular clusters using classical polarizable force fields. 2009 , 130, 164115	93
1984	Approximate Density Functionals: Which Should I Choose?. 2009,	14
1983	An efficient algorithm for the density-functional theory treatment of dispersion interactions. 2009 , 130, 124105	96
1982	Density functional theory study of multiply ionized weakly bound fullerene dimers. 2009 , 130, 224302	11
1981	The role of polymorphism in organic thin films: oligoacenes investigated from first principles. 2009 , 11, 125010	101

1980	Multimode simulation of dimer absorption spectra from first principles calculations: application to the 3,4,9,10-perylenetetracarboxylic diimide dimer. 2009 , 131, 154302	46
1979	Derivation of the dispersion energy as an explicit density- and exchange-hole functional. 2009 , 130, 084104	33
1978	Relativistic all-electron molecular dynamics simulations. 2009 , 130, 124103	26
1977	Modeling of high-order many-mode terms in the expansion of multidimensional potential energy surfaces: application to vibrational spectra. 2009 , 131, 014108	27
1976	Effects of pi-stacking interactions on the near carbon K-edge x-ray absorption fine structure: a theoretical study of the ethylene pentamer and the phthalocyanine dimer. 2009 , 130, 104305	11
1975	An organometallic route to long helicenes. 2009 , 106, 13169-74	110
1974	A Ditopic Ion-Pair Receptor Based on Stacked Nucleobase Quartets. 2009 , 121, 3335-3337	23
1973	Computing chiroptical properties with first-principles theoretical methods: background and illustrative examples. 2009 , 21 Suppl 1, E116-52	264
1972	Dihydrogen bonding: donor-acceptor bonding (AHHX) versus the H2 molecule (A-H2-X). 2009 , 15, 5814-22	31
1971	Fixing the chirality and trapping the transition state of helicene with atomic metal glue. 2009 , 15, 13210-8	29
1970	Ab initio study of the interactions between CO(2) and N-containing organic heterocycles. 2009 , 10, 374-83	164
1969	DFT/CCSD(T) investigation of the interaction of molecular hydrogen with carbon nanostructures. 2009 , 10, 1868-73	38
1968	Rectification in supramolecular zinc porphyrin/fulleropyrrolidine dyads self-organized on gold(111). 2009 , 10, 2633-41	11
1967	Theoretical study on hydrogen-bond effects in IR spectra of high- and low-temperature phases of nitric acid dihydrate. 2009 , 10, 3229-38	2
1966	Noncovalent interactions in supramolecular complexes: a study on corannulene and the double concave buckycatcher. <i>Journal of Computational Chemistry</i> , 2009 , 30, 51-6	69
1965	Can the hybrid meta GGA and DFT-D methods describe the stacking interactions in conjugated polymers?. <i>Journal of Computational Chemistry</i> , 2009 , 30, 1179-84	15
1964	Polarizable empirical force field for nitrogen-containing heteroaromatic compounds based on the classical Drude oscillator. <i>Journal of Computational Chemistry</i> , 2009 , 30, 1821-38	62
1963	Interaction energy and the shift in OH stretch frequency on hydrogen bonding for the H2O> H2O, CH3OH> H2O, and H2O> CH3OH dimers. <i>Journal of Computational Chemistry</i> , 2010 , 31, 963-72	11

(2009-2009)

1962	A ditopic ion-pair receptor based on stacked nucleobase quartets. 2009 , 48, 3285-7	64
1961	Modeling the noncovalent interactions at the metabolite binding site in purine riboswitches. 2009 , 15, 633-49	26
1960	Theoretical study of 1-(4-hexylcyclohexyl)-4-isothiocyanatobenzene: molecular properties and spectral characteristics. 2009 , 15, 935-43	8
1959	Performance of Becke's half-and-half functional for non-covalent interactions: energetics, geometries and electron densities. 2009 , 15, 1051-60	15
1958	Local electron correlation descriptions of the intermolecular stacking interactions between aromatic intercalators and nucleic acids. 2009 , 479, 279-283	23
1957	A local-MP2 approach to the ab initio study of electron correlation in crystals and to the simulation of vibrational spectra: the case of Ice XI. 2009 , 123, 327-335	13
1956	Influence of Estacking on the N7 and O6 proton affinity of guanine. 2009 , 123, 105-111	11
1955	Dispersion interactions in density-functional theory. 2009 , 22, 1127-1135	298
1954	MP2 and DFT study of IR spectra of TCNE-methylsubstituted benzene complexes: Is charge transfer important?. 2009 , 110, NA-NA	2
1953	A solution to the observed $Z' = 2$ preference in the crystal structures of hydrophobic amino acids. 2009 , 65, 393-400	38
1952	Weak intra- and intermolecular interactions in a binaphthol imine: an experimental charge-density study on (+/-)-8'-benzhydrylideneamino-1,1'-binaphthyl-2-ol. 2009 , 65, 757-69	30
1951	Modeling of a Trgert tweezer and its complexation properties. 2009 , 934, 117-122	16
1950	Model study on sorption of polycyclic aromatic hydrocarbons to goethite. 2009 , 330, 244-9	34
1949	IRDV double resonance spectra of pyrazine dimers: Competition between . 2009 , 467, 255-259	15
1948	CarbohydrateBromatic interactions: A computational and IR spectroscopic investigation of the complex, methyl \(\text{H-fucopyranoside} \) [toluene, isolated in the gas phase. 2009 , 471, 17-21	48
1947	Six-coordination in Chlorophylls: The fundamental role of dispersion energy. 2009 , 472, 243-247	24
1946	Solvent effect on EPR, molecular and electronic properties of semiquinone radical derived from 3,4-dihydroxybenzoic acid as model for humic acid transient radicals: High-field EPR and DFT studies. 2009 , 473, 160-166	32
1945	Interaction energies in monosubstituted-benzene dimers in parallel- and antiparallel-displaced conformations. 2009 , 474, 101-106	36

1944	Understanding Peierls distortion in one-dimensional infinite V-chain and V B z multi-decker complex. 2009 , 479, 133-136	3
1943	Molecular hydrogen encapsulation in spherophanes. 2009 , 480, 225-230	5
1942	Some comments on the DFT + D method. 2009 , 480, 327-329	13
1941	Stabilization of platinum nanoparticles on graphene by non-invasive functionalization. 2009 , 47, 2233-2238	16
1940	An assessment of theoretical methods for nonbonded interactions: comparison to complete basis set limit coupled-cluster potential energy curves for the benzene dimer, the methane dimer, benzene-methane, and benzene-H2S. 2009 , 113, 10146-59	345
1939	Isobaric-isothermal molecular dynamics simulations utilizing density functional theory: an assessment of the structure and density of water at near-ambient conditions. 2009 , 113, 11959-64	302
1938	Evidence for a rapid degenerate hetero-Cope-type rearrangement in [Cp*W(S)2S-CH2-CH=CH2]. 2009 , 4, 1830-1833	1
1937	The Effect of Confined Space on the Growth of Naphthalenic Species in a Chabazite-Type Catalyst: A Molecular Modeling Study. 2009 , 1, 373-378	41
1936	Accurate molecular van der Waals interactions from ground-state electron density and free-atom reference data. 2009 , 102, 073005	3885
1935	Infrared spectroscopy and hydrogen-bond dynamics of liquid water from centroid molecular dynamics with an ab initio-based force field. 2009 , 113, 13118-30	111
1934	Theoretical study of the catalysis of cyanohydrin formation by the cyclic dipeptide catalyst cyclo[(S)-His-(S)-Phe]. 2009 , 74, 1464-72	22
1933	Theoretical Study of Dispersion Binding of Hydrocarbon Molecules to Hydrogen-Terminated Silicon(100)-2 1 . 2009 , 113, 5681-5689	24
1932	Ligands for dinitrogen fixation at Schrock-type catalysts. 2009 , 48, 1638-48	54
1931	Van der Waals Interactions in Density-Functional Theory: Rare-Gas Diatomics. 2009 , 5, 719-27	131
1930	Self-consistent polarization density functional theory: application to argon. 2009 , 113, 2075-85	19
1929	Ion-pair binding energies of ionic liquids: can DFT compete with ab initio-based methods?. 2009 , 113, 7064-72	153
1928	Metal-phosphine bond strengths of the transition metals: a challenge for DFT. 2009 , 113, 11833-44	119
1927	Understanding ground- and excited-state properties of perylene tetracarboxylic acid bisimide crystals by means of quantum chemical computations. 2009 , 131, 15660-8	94

(2009-2009)

1926	Quantum chemical modeling of zeolite-catalyzed methylation reactions: toward chemical accuracy for barriers. 2009 , 131, 816-25	265
1925	Origin of the Argon Nanocoating Shift in the OH Stretching Fundamental of n-Propanol: A Combined Experimental and Quantum Chemical Study. 2009 , 113, 10929-10938	22
1924	An analysis of the different behavior of DNA and RNA through the study of the mutual relationship between stacking and hydrogen bonding. 2009 , 113, 4907-14	42
1923	Uncovering a Solvent-Controlled Preferential Growth of Buckminsterfullerene (C60) Nanowires. 2009 , 113, 6390-6397	27
1922	A systematic CCSD(T) study of long-range and noncovalent interactions between benzene and a series of first- and second-row hydrides and rare gas atoms. 2009 , 113, 1663-9	51
1921	Accurate calculations of intermolecular interaction energies using explicitly correlated coupled cluster wave functions and a dispersion-weighted MP2 method. 2009 , 113, 11580-5	141
1920	Binding in thiophene and benzothiophene dimers investigated by density functional theory with dispersion-correcting potentials. 2009 , 113, 5476-84	20
1919	Convergence of the CCSD(T) Correction Term for the Stacked Complex Methyl Adenine-Methyl Thymine: Comparison with Lower-Cost Alternatives. 2009 , 5, 1761-6	50
1918	Pentacene Binds Strongly to Hydrogen-Terminated Silicon Surfaces Via Dispersion Interactions. 2009 , 113, 9969-9973	12
1917	A potential surface for the interaction between water and coronene as a model for a hydrophobic surface. 2009 , 107, 1197-1207	14
1916	Understanding the role of intra- and intermolecular interactions in the formation of single- and double-helical structures of aromatic oligoamides: a computational study. 2009 , 113, 1335-42	21
1915	Density functional theory calculations of solid nitromethane under hydrostatic and uniaxial compressions with empirical van der Waals correction. 2009 , 113, 3610-4	34
1914	Computational, structural, and mechanistic analysis of the electrochemically driven pirouetting motion of a copper rotaxane. 2009 , 113, 6219-29	19
1913	Reference Quantum Chemical Calculations on RNA Base Pairs Directly Involving the 2'-OH Group of Ribose. 2009 , 5, 1166-79	26
1912	Accurate interaction energies at density functional theory level by means of an efficient dispersion correction. 2009 , 130, 174101	40
1911	Application of dispersion-corrected density functional theory. 2009 , 113, 10321-6	33
1910	Dispersion Corrected Atom-Centered Potentials for Phosphorus. 2009 , 5, 2930-4	15
1909	H/Br exchange in BBr3 by HSiR3 (R = H, CH3, C2H5): origin of DFT failures to describe a seemingly innocuous reaction barrier. 2009 , 113, 12035-43	12

1908	Phenylalanyl-Glycyl-Phenylalanine Tripeptide: A Model System for Aromatic-Aromatic Side Chain Interactions in Proteins. 2009 , 5, 2248-56	22
1907	DFT Study of the Hydrogen Spillover Mechanism on Pt-Doped Graphite. 2009 , 113, 14908-14915	114
1906	Weak interactions between trivalent pnictogen centers: computational analysis of bonding in dimers X3EEX3 (E = pnictogen, X = halogen). 2009 , 48, 6740-7	64
1905	Performance of Kinetic Energy Functionals for Interaction Energies in a Subsystem Formulation of Density Functional Theory. 2009 , 5, 3161-74	100
1904	Unified Inter- and Intramolecular Dispersion Correction Formula for Generalized Gradient Approximation Density Functional Theory. 2009 , 5, 2950-8	70
1903	Self-Assembly of Diacid Molecules: A Theoretical Approach of Molecular Interactions. 2009 , 113, 17566-1757	1 7
1902	Structural and Electronic Trends among Group 15 Elemental Nanotubes. 2009 , 113, 12220-12224	18
1901	Theoretical studies of RNA catalysis: hybrid QM/MM methods and their comparison with MD and QM. 2009 , 49, 202-16	74
1900	Stable "inverse" sandwich complex with unprecedented organocalcium(I): crystal structures of [(thf)(2)Mg(Br)-C(6)H(2)-2,4,6-Ph(3)] and [(thf)(3)Ca{mu-C(6)H(3)-1,3,5-Ph(3)}Ca(thf)(3)]. 2009 , 131, 2977-85	117
1899	Insight from first principles into the nature of the bonding between water molecules and 4d metal surfaces. 2009 , 130, 184707	84
1898	Implementation and Optimization of DFT-D/COSab with Respect to Basis Set and Functional: Application to Polar Processes of Furfural Derivatives in Solution. 2009 , 5, 2772-86	8
1897	Effects of hydration on the proton transfer mechanism in the adenine-thymine base pair. 2009 , 113, 7892-8	63
1896	Ab initio molecular dynamics study of supercritical carbon dioxide including dispersion corrections. 2009 , 131, 144506	25
1895	Long-range corrected double-hybrid density functionals. 2009 , 131, 174105	271
1894	Symmetry-Adapted Perturbation Theory Applied to Endohedral Fullerene Complexes: A Stability Study of H2@C60 and 2H2@C60. 2009 , 5, 1585-96	78
1893	The CrMn Interaction in syn-Facial [Tricarbonyl(benzyl)chromium]manganesetricarbonyl Complexes: A Non-Covalent MetalMetal Bond. 2009 , 28, 1001-1013	44
1892	Computations of Noncovalent Interactions. 2009, 1-38	38
1891	Efficient implementation of a van der Waals density functional: application to double-wall carbon nanotubes. 2009 , 103, 096102	1208

(2009-2009)

1890	Periodic DFT modeling of bulk and surface properties of MgCl2. 2009 , 11, 6525-32	46
1889	Importance of van der Waals interactions in liquid water. 2009 , 113, 1127-31	164
1888	Triplet excimer formation in platinum-based phosphors: a theoretical study of the roles of Pt-Pt bimetallic interactions and interligand pi-pi interactions. 2009 , 131, 11371-80	106
1887	What is the structure of kaolinite? Reconciling theory and experiment. 2009 , 113, 6756-65	55
1886	Ab initio study of hydrogen adsorption in MOF-5. 2009 , 131, 4143-50	206
1885	Carbohydrate-aromatic pi interactions: a test of density functionals and the DFT-D method. 2009 , 11, 3411-6	56
1884	Tuning the oxidation level, the spin state, and the degree of electron delocalization in homo- and heteroleptic bis(alpha-diimine)iron complexes. 2009 , 131, 1208-21	97
1883	Correction for dispersion and Coulombic interactions in molecular clusters with density functional derived methods: application to polycyclic aromatic hydrocarbon clusters. 2009 , 130, 244304	81
1882	Noncovalent interactions in a transition-metal triphenylphosphine complex: a density functional case study. 2009 , 48, 4622-4	132
1881	Density functional for van der Waals forces accounts for hydrogen bond in benchmark set of water hexamers. 2009 , 131, 046102	50
1880	Balance of Attraction and Repulsion in Nucleic-Acid Base Stacking: CCSD(T)/Complete-Basis-Set-Limit Calculations on Uracil Dimer and a Comparison with the Force-Field Description. 2009 , 5, 1524-44	44
1879	Understanding effects of molecular adsorption at a single-wall boron nitride nanotube interface from density functional theory calculations. 2009 , 20, 355705	45
1878	Importance of dispersion and electron correlation in ab initio protein folding. 2009, 113, 5290-300	61
1877	The method of local increments for the calculation of adsorption energies of atoms and small molecules on solid surfaces. Part I. A single Cu atom on the polar surfaces of ZnO. 2009 , 11, 11196-206	25
1876	Consequences of acid strength for isomerization and elimination catalysis on solid acids. 2009 , 131, 6554-65	115
1875	Van der Waals interactions in density functional theory using Wannier functions. 2009 , 113, 5224-34	72
1874	Anchoring the potential energy surface of the diacetylene dimer. 2009 , 107, 923-928	7
1873	Cooperativity in noncovalent interactions of biologically relevant molecules. 2009 , 11, 8440-7	45

1872	Second-Order Nonlinear Optical Properties of Transition-Metal-Trisubstituted PolyoxometalateDiphosphate Complexes: A DonorConjugated BridgeAcceptor Paradigm for Totally Inorganic Nonlinear Optical Materials. 2009, 113, 19672-19676	55
1871	Design of an organic zeolite toward the selective adsorption of small molecules at the dispersion corrected density functional theory level. 2009 , 113, 16472-8	17
1870	Density-based energy decomposition analysis for intermolecular interactions with variationally determined intermediate state energies. 2009 , 131, 164112	104
1869	Optimization and basis-set dependence of a restricted-open-shell form of B2-PLYP double-hybrid density functional theory. 2009 , 113, 9861-73	70
1868	On the Nature of Bonding in Lone Pair Electron Complexes: CCSD(T)/Complete Basis Set Limit Calculations. 2009 , 5, 1180-5	79
1867	Assessment of QM/MM scoring functions for molecular docking to HIV-1 protease. 2009 , 49, 913-24	41
1866	A density functional for sparse matter. 2009 , 21, 084203	313
1865	Fluorine substituent effects on dihydrogen bonding of transition metal hydrides. 2009 , 11, 7231-40	10
1864	Advances in atomistic simulations of mineral surfaces. 2009 , 19, 7807	29
1863	Modelling doped (Ni, Pd, Pt) sulfur-nitrolic systems as new motifs for storage of hydrogen. 2009 , 11, 11054-9	12
1862	The conformational landscape of 5-methoxytryptamine studied by rotationally resolved fluorescence spectroscopy and resonant ionization spectroscopy. 2009 , 11, 2433-40	8
1861	Electronic spectrum of tryptophan-phenylalanine. A correlated ab initio and time-dependent density functional theory study. 2009 , 113, 16443-8	15
1860	Supramolecular interactions of fullerenes with (Cl)Fe- and Mn porphyrins. A theoretical study. 2009 , 11, 6072-81	5
1859	Non-bonded force field for the interaction between metals and organic molecules: a case study of olefins on aluminum. 2009 , 11, 10195-203	12
1858	Metal-free dihydrogen activation chemistry: structural and dynamic features of intramolecular P/B pairs. 2009 , 1534-41	118
1857	Dispersion-corrected DFT calculations on C(60)-porphyrin complexes. 2009 , 11, 4365-74	23
1856	C60-derived nanobaskets: stability, vibrational signatures, and molecular trapping. 2009 , 20, 395701	7
1855	Reliable Electronic Structure Computations for Weak Noncovalent Interactions in Clusters. 2009 , 39-90	24

1854	Neural network approach to quantum-chemistry data: accurate prediction of density functional theory energies. 2009 , 131, 074104	107
1853	Role of dispersive interactions in layered materials: a periodic B3LYP and B3LYP-D* study of Mg(OH)2, Ca(OH)2 and kaolinite. 2009 , 19, 2564	70
1852	Hydrogen bonding and pi-stacking: how reliable are force fields? A critical evaluation of force field descriptions of nonbonded interactions. 2009 , 49, 944-55	146
1851	Comprehensive Energy Analysis for Various Types of Enteraction. 2009 , 5, 515-29	235
1850	Suitability of double hybrid density functionals and their dispersion-corrected counterparts in producing the potential energy curves for CO2-Rg (Rg: He, Ne, Ar and Kr) systems. 2009 , 113, 1377-83	13
1849	Interaction of substituted aromatic compounds with graphene. 2009 , 25, 210-5	233
1848	CH/pi interaction in benzene and substituted derivatives with halomethane: a combined density functional and dispersion-corrected density functional study. 2009 , 113, 10113-8	27
1847	Reaction enthalpies using the neural-network-based X1 approach: the important choice of input descriptors. 2009 , 113, 3285-90	18
1846	Evaluation of MP2, DFT, and DFT-D methods for the prediction of infrared spectra of peptides. 2009 , 113, 6301-7	44
1845	Second-order nonlinear optical properties of trisubstituted Keggin and Wells-Dawson polyoxometalates: density functional theory investigation of the inorganic donor-conjugated bridge-acceptor structure. 2009 , 48, 8115-9	46
1844	Quantum Mechanical Studies of Noncovalent DNAProtein Interactions. 2010, 307-336	2
1843	Communications: Intramolecular basis set superposition error as a measure of basis set incompleteness: can one reach the basis set limit without extrapolation?. 2010 , 132, 211103	30
1842	Third-Generation Hydrogen-Bonding Corrections for Semiempirical QM Methods and Force Fields. 2010 , 6, 3808-3816	187
1841	TAMkin: a versatile package for vibrational analysis and chemical kinetics. 2010 , 50, 1736-50	127
1840	On the Structure and Geometry of Biomolecular Binding Motifs (Hydrogen-Bonding, Stacking, X-H WFT and DFT Calculations. 2010 , 6, 66-80	166
1839	DFT study on the catalytic reactivity of a functional model complex for intradiol-cleaving dioxygenases. 2010 , 114, 5878-85	21
1838	Noncovalent interactions in extended systems described by the effective fragment potential method: theory and application to nucleobase oligomers. 2010 , 114, 12739-54	91
1837	A Transferable H-Bonding Correction for Semiempirical Quantum-Chemical Methods. 2010 , 6, 344-52	222

1836	A consistent and accurate ab initio parametrization of density functional dispersion correction (DFT-D) for the 94 elements H-Pu. 2010 , 132, 154104	23773
1835	Mutual relationship between stacking and hydrogen bonding in DNA. Theoretical study of guanine-cytosine, guanine-5-methylcytosine, and their dimers. 2010 , 114, 10217-27	68
1834	The effect of pi-stacking, H-bonding, and electrostatic interactions on the ionization energies of nucleic acid bases: adenine-adenine, thymine-thymine and adenine-thymine dimers. 2010 , 12, 2292-307	83
1833	Adenine versus guanine quartets in aqueous solution: dispersion-corrected DFT study on the differences in Estacking and hydrogen-bonding behavior. 2010 , 125, 245-252	110
1832	Hydrogen physisorption in metal®rganic frameworks: concepts and quantum chemical calculations. 2010 , 127, 259-270	13
1831	Performance of the M06-L density functional for a folded Tyr©ly conformer. 2010, 485, 40-44	13
1830	On the performance of van der Waals corrected-density functional theory in describing the atomic hydrogen physisorption on graphite. 2010 , 500, 283-286	23
1829	Structure of sodiated octa-glycine: IRMPD spectroscopy and molecular modeling. 2010 , 21, 728-38	44
1828	DFT molecular dynamics (DFTMD) simulations of carbohydrates: COSMO solvated \(\text{\text{maltose}}\). 2010 , 953, 61-82	7
1827	Differential stabilization of adenine quartets by anions and cations. 2010 , 15, 387-97	16
1826	Mechanical Response and Energy-Dissipation Processes in Oligothiophene Monolayers Studied with First-Principles Simulations. 2010 , 39, 295-309	6
1825	Assembly of cyclic hydrocarbons from ethene and propene in acid zeolite catalysis to produce active catalytic sites for MTO conversion. 2010 , 271, 67-78	79
1824	On the reliability of the AMBER force field and its empirical dispersion contribution for the description of noncovalent complexes. 2010 , 11, 2399-408	29
1823	Experimental and Theoretical Conformational Analysis of 5-Benzylimidazolidin-4-one Derivatives II a P laygroundIfor Studying Dispersion Interactions and a Windshield-WiperIEffect in Organocatalysis. 2010 , 93, 1-16	57
1822	Can DFT methods correctly and efficiently predict the coordination number of copper(I) complexes? A case study. <i>Journal of Computational Chemistry</i> , 2010 , 31, 75-83	16
1821	Atomistic insight into chondroitin-6-sulfate glycosaminoglycan chain through quantum mechanics calculations and molecular dynamics simulation. <i>Journal of Computational Chemistry</i> , 2010 , 31, 1670-80 ^{3.5}	9
1820	Assessment of density functionals with long-range and/or empirical dispersion corrections for conformational energy calculations of peptides. <i>Journal of Computational Chemistry</i> , 2010 , 31, 2915-23 $^{3.5}$	44
1819	Subvalent Organometallic Compounds of the Alkaline Earth Metals in Low Oxidation States. 2010 , 2010, 197-216	45

1818	The Preparation and Structure of [Pt(S2N2){P(OR)nR?3fi}2] and [Pt(SeSN2)[{P(OMe)nPh3fi}2] (n = 0fi). 2010 , 2010, 3185-3194	3
1817	Intermediates involved in the oxidation of nitrogen monoxide: photochemistry of the cis-N(2)O(2)O(2) complex and of sym-N(2)O(4) in solid Ne matrices. 2010 , 16, 1506-20	40
1816	Modulation of stacking interactions by transition-metal coordination: ab initio benchmark studies. 2010 , 16, 5391-9	19
1815	A computational study of rhodium pincer complexes with classical and nonclassical hydride centres as catalysts for the hydroamination of ethylene with ammonia. 2010 , 16, 9203-14	22
1814	Supramolecular Catalysis in the Organic Solid State through Dry Grinding. 2010 , 122, 4369-4373	22
1813	Nanotexture Switching of Single-Layer Hexagonal Boron Nitride on Rhodium by Intercalation of Hydrogen Atoms. 2010 , 122, 6256-6260	2
1812	Switchable Open-Cage Fullerene for Water Encapsulation. 2010 , 122, 10131-10134	24
1811	Supramolecular catalysis in the organic solid state through dry grinding. 2010 , 49, 4273-7	100
1810	Nanotexture switching of single-layer hexagonal boron nitride on rhodium by intercalation of hydrogen atoms. 2010 , 49, 6120-4	62
1809	Switchable open-cage fullerene for water encapsulation. 2010 , 49, 9935-8	67
1808	Computing dispersion interactions in density functional theory. 2010 , 3, 1417-1430	37
1807	Theoretical prediction of a peptide binding to major histocompatibility complex II. 2010 , 29, 240-5	5
1806	Evaluation of dispersion-corrected density functional theory (B3LYP-DCP) for compounds of biochemical interest. 2010 , 29, 178-87	18
1805	An evaluation of the GLYCAM06 and MM3 force fields, and the PM3-D* molecular orbital method for modelling prototype carbohydrate-aromatic interactions. 2010 , 29, 321-5	13
1804	Infrared spectroscopic characterization of the oxidative dehydrogenation of propane by V4O10+. 2010 , 297, 102-106	29
1803	Assessment of density functionals for predicting the infrared spectrum of sodiated octa-glycine. 2010 , 297, 152-161	21
1802	Atomistic theoretical models for nanoporous hybrid materials. 2010 , 129, 304-318	46
1801	Interaction of CO, CO2 and CH4 with mesoporous organosilica: Periodic DFT calculations with dispersion corrections. 2010 , 129, 62-67	21

1800	Could N-(diethylcarbamothioyl)benzamide be a good ionophore for sensor membranes?. 2010 , 981, 86-92	20
1799	A performance study of density functional theory with empirical dispersion corrections and spin-component scaled second-order MllerPlesset perturbation theory on adsorbateDeolite interactions. 2010, 945, 85-88	11
1798	Hydrogen bonding interactions in cysteinellrea complexes: Theoretical studies of structures, properties and topologies. 2010 , 960, 98-105	9
1797	Theoretical study of tautomerization and isomerization of methylamino- and phenylamino-substituted cyclic azaphospholines, oxaphospholines and thiaphospholines in gas and aqueous phases. 2010 , 962, 101-107	5
1796	Adsorption of Xe atoms on the TiO2(110) surface: A density functional study. 2010 , 604, 428-434	13
1795	NWChem: A comprehensive and scalable open-source solution for large scale molecular simulations. 2010 , 181, 1477-1489	3430
1794	Assessment of approximate quantum chemical methods for calculating the interaction energy of nucleic acid bases with graphene and carbon nanotubes. 2010 , 484, 295-298	34
1793	Hydrogen adsorption sites and energies in 2D and 3D covalent organic frameworks. 2010 , 489, 86-91	25
1792	Alkane dimers interaction: A semi-local MGGA functional study. 2010 , 492, 183-186	17
1791	Interaction of the alcohol molecules methanol and ethanol with single-walled carbon nanotubes [] A computational study. 2010 , 498, 345-348	7
1790	DFT study of polymorphism of the DNA double helix at the level of dinucleoside monophosphates. 2010 , 110, n/a-n/a	2
1789	Electric field enhanced hydrogen storage on polarizable materials substrates. 2010 , 107, 2801-6	194
1788	Ultraviolet laser ionization studies of 1-fluoronaphthalene clusters and density functional theory calculations. 2010 , 19, 123602	1
1787	Van der Waals density functional from multipole dispersion interactions. 2010 , 132, 014110	10
1786	Structure and binding in crystals of cagelike molecules: hexamine and platonic hydrocarbons. 2010 , 132, 134705	33
1785	Free energy surface of two- and three-dimensional transitions of Au 12 nanoclusters obtained by ab initio metadynamics. 2010 , 81,	24
1784	A Computational Study of the Molecular Recognition of Nucleic Acid Bases by Poly(vinyldiaminotriazine). 2010 , 295, 125-130	1
1783	Density functional theory approach to noncovalent interactions via monomer polarization and Pauli blockade. 2010 , 104, 163001	31

1782	interactions. 2010 , 132, 094106	39
1781	Structure and energetics of azobenzene on Ag(111): benchmarking semiempirical dispersion correction approaches. 2010 , 104, 036102	214
1780	From localized orbitals to material properties: building classical force fields for nonmetallic condensed matter systems. 2010 , 104, 138301	32
1779	Long-range van der Waals attraction and alkali-metal lattice constants. 2010 , 81,	61
1778	Local response dispersion method. II. Generalized multicenter interactions. 2010 , 133, 194101	82
1777	INTERACTION IN BENZENE DIMER STUDIED USING DENSITY FUNCTIONAL THEORY AUGMENTED WITH AN EMPIRICAL DISPERSION TERM. 2010 , 09, 109-123	4
1776	Recent advances in the visible and UV spectroscopy of metal dication complexes. 2010 , 29, 555-588	20
1775	Basis set dependence of the doubly hybrid XYG3 functional. 2010 , 133, 104105	39
1774	Correcting for dispersion interaction and beyond in density functional theory through force matching. 2010 , 133, 174115	23
1773	The Vibrational Infrared Spectra of 1-Methyl-3-methylimidazolium Dimethylphosphate. Is the Dispersion-Corrected Functional Important in Intermolecular DFT Calculation of Ionic Liquids?. 2010 , 43, 513-522	4
1772	Quantum mechanics based force field for carbon (QMFF-Cx) validated to reproduce the mechanical and thermodynamics properties of graphite. 2010 , 133, 134114	16
1771	Experimental measurement of the van der Waals binding energy of X-O2 clusters (X=Xe, CH3I, C3H6, C6H12). 2010 , 133, 194306	8
1770	Determination of the experimental equilibrium structure of solid nitromethane using path-integral molecular dynamics simulations. 2010 , 132, 094502	11
1769	Range-separated density-functional theory with random phase approximation applied to noncovalent intermolecular interactions. 2010 , 132, 244108	113
1768	The crucial role of dispersion in the cohesion of nonbridged binuclear Os> Cr and Os> W adducts. 2010 , 49, 2911-9	69
1767	Intriguing pi(+)-pi Interaction in crystal packing. 2010 , 114, 4166-70	48
1766	Van der waals interactions in molecular assemblies from first-principles calculations. 2010 , 114, 1944-52	48
1765	Combining density functional theory (DFT) and pair distribution function (PDF) analysis to solve the structure of metastable materials: the case of metakaolin. 2010 , 12, 3239-45	112

1764	Transition state models for probing stereoinduction in Evans chiral auxiliary-based asymmetric aldol reactions. 2010 , 132, 12319-30	48
1763	Probing substituent effects in aryl-aryl interactions using stereoselective Diels-Alder cycloadditions. 2010 , 132, 3304-11	159
1762	Predicting Organic Crystal Lattice Energies with Chemical Accuracy. 2010 , 1, 3480-3487	174
1761	Cluster Structures: Bridging Experiment and Theory. 2010 , 1, 151-218	
1760	Opposite regiospecific ring opening of 2-(cyanomethyl)aziridines by hydrogen bromide and benzyl bromide: experimental study and theoretical rationalization. 2010 , 75, 4530-41	53
1759	Hydrostatic and uniaxial compression studies of 1,3,5-triamino- 2,4,6-trinitrobenzene using density functional theory with van der Waals correction. 2010 , 107, 113524	34
1758	Adsorption of small aromatic molecules on the (111) surfaces of noble metals: A density functional theory study with semiempirical corrections for dispersion effects. 2010 , 132, 224701	201
1757	Two- and three-body interatomic dispersion energy contributions to binding in molecules and solids. 2010 , 132, 234109	180
1756	Weak Chemical Interaction and van der Waals Forces: A Combined Density Functional and Intermolecular Perturbation Theory [Application to Graphite and Graphitic Systems. 2010 , 45-79	5
1755	The Relevance of Dispersion Interactions for the Stability of Oxide Phases. 2010 , 114, 22718-22726	55
1754	Stability of Hydrocarbons of the Polyhedrane Family Containing Bridged CH Groups: A Case of Failure of the Colle-Salvetti Correlation Density Functionals. 2010 , 6, 3442-55	16
1753	Using Nonempirical Semilocal Density Functionals and Empirical Dispersion Corrections to Model Dative Bonding in Substituted Boranes. 2010 , 6, 1825-33	20
1752	Formation and structure of the potassium complex of valinomycin in solution studied by Raman optical activity spectroscopy. 2010 , 12, 11021-32	53
1751	Benchmark calculations of water-acene interaction energies: Extrapolation to the water-graphene limit and assessment of dispersion-corrected DFT methods. 2010 , 12, 6375-81	98
1750	Designing molecular switches based on DNA-base mispairing. 2010 , 114, 15311-8	53
1749	Equations of state for energetic materials from density functional theory with van der Waals, thermal, and zero-point energy corrections. 2010 , 97, 251908	57
1748	The effects of perfluorination on carbohydrate-pi interactions: computational studies of the interaction of benzene and hexafluorobenzene with fucose and cyclodextrin. 2010 , 12, 7959-67	23
1747	van der Waals Interactions in Density-Functional Theory: Intermolecular Complexes. 2010 , 6, 1081-1088	137

1746	Branched alkanes have contrasting stabilities. 2010 , 12, 3070-3	33
1745	Medium effect on the rotational barrier of N,N,N'-trimethylurea and N,N,N'-trimethylthiourea: experimental and theoretical study. 2010 , 114, 6423-30	4
1744	Hydrophobic Behavior of Dehydroxylated Silica Surfaces: A B3LYP Periodic Study. 2010 , 114, 19984-19992	22
1743	A New Empirical Correction to the AM1 Method for Macromolecular Complexes. 2010 , 6, 2153-66	21
1742	Effects of London dispersion on the isomerization reactions of large organic molecules: a density functional benchmark study. 2010 , 12, 6940-8	110
1741	Hydrogen in the Metal®rganic Framework Cr MIL-53. 2010 , 114, 10648-10655	43
1740	Interactions Studied with Electronic Structure Methods: The Ethyne Methyl Isocyanide Complex and Thioanisole. 2010 , 6, 2687-700	7
1739	A density functional theory approach to noncovalent interactions via interacting monomer densities. 2010 , 12, 14686-92	5
1738	Mechanism of the hydride transfer between Anabaena Tyr303Ser FNR(rd)/FNR(ox) and NADP+/H. A combined pre-steady-state kinetic/ensemble-averaged transition-state theory with multidimensional tunneling study. 2010 , 114, 3368-79	25
1737	Ligand effects in bimetallic high oxidation state palladium systems. 2010 , 49, 11249-53	36
1736	Zooming into pi-stacked manifolds of nucleobases: ionized states of dimethylated uracil dimers. 2010 , 114, 2001-9	17
1735	Quantum chemical study of conformational fingerprints in the photoelectron spectra and (e, 2e) electron momentum distributions of n-hexane. 2010 , 114, 4400-17	32
1734	Molecular Crystals: A Test System for Weak Bonding 2010 , 114, 20523-20530	14
1733	Assessment of DFT and DFT-D for Potential Energy Surfaces of Rare Gas Trimers-Implementation and Analysis of Functionals and Extrapolation Procedures. 2010 , 6, 1951-65	7
1732	Intramolecular proton transfer in calixphyrin derivatives. 2010 , 114, 3649-54	6
1731	An Error and Efficiency Analysis of Approximations to MIlerBlesset Perturbation Theory. 2010 , 6, 3681-3687	12
1730	Theoretical study of chlorophyll a hydrates formation in aqueous organic solvents. 2010, 114, 681-7	20
1729	Configurationally labile enantioenriched lithiated 3-arylprop-2-enyl carbamates: joint experimental and quantum chemical investigations on the equilibrium of epimers. 2010 , 75, 5716-20	7

1728	Experimental and Theoretical Studies on the Chiroptical Properties of DonorAcceptor Binaphthyls. Effects of Dynamic Conformer Population on Circular Dichroism. 2010 , 1, 1809-1812	22
1727	Understanding the Resonance Raman Scattering of Donor-Acceptor Complexes using Long-Range Corrected DFT. 2010 , 6, 2845-55	20
1726	Intramolecular pi-pi stacking interactions in 2-substituted N,N-dibenzylaziridinium ions and their regioselectivity in nucleophilic ring-opening reactions. 2010 , 75, 885-96	64
1725	Hole Mobility for Thin-Film Organic Molecular Solids in the Presence of Defects or Surface Adsorbates: Theory and Implications for Gas Detection. 2010 , 114, 12173-12189	9
1724	NMR-spectroscopic and solid-state investigations of cometal-free asymmetric conjugate addition: a dinuclear paracyclophaneimine zinc methyl complex. 2010 , 132, 12899-905	28
1723	A DFT and ab initio benchmarking study of metal-alkane interactions and the activation of carbon-hydrogen bonds. 2010 , 114, 1843-51	31
1722	Interactions of Cyclotrimethylene Trinitramine (RDX) with Metal@rganic Framework IRMOF-1. 2010 , 114, 3732-3736	11
1721	Geometry Optimization of Large and Flexible van der Waals Dimers: A Fragmentation-Reconstruction Approach. 2010 , 6, 2536-46	6
1720	Competing thermal electrocyclic ring-closure reactions of (2Z)-hexa-2,4,5-trienals and their Schiff bases. Structural, kinetic, and computational studies. 2010 , 75, 4453-62	15
1719	Ionization-Induced Structural Changes in Uracil Dimers and Their Spectroscopic Signatures. 2010 , 6, 705-17	19
1718	Simulations of ICl-(CO2)n photodissociation: effects of structure, excited state charge flow, and solvent dynamics. 2010 , 114, 1347-56	3
		9
1717	Stacking and spreading interaction in N-heteroaromatic systems. 2010 , 114, 9606-16	55
1717 1716	Stacking and spreading interaction in N-heteroaromatic systems. 2010 , 114, 9606-16 Microhydration of the selenite dianion: a theoretical study of structures, hydration energies, and electronic stabilities of $SeO(3)(2-)(H(2)O)(n)$ (n = 0-6, 9) clusters. 2010 , 114, 8948-60	
, , ,	Microhydration of the selenite dianion: a theoretical study of structures, hydration energies, and	55
1716	Microhydration of the selenite dianion: a theoretical study of structures, hydration energies, and electronic stabilities of SeO(3)(2-)(H(2)O)(n) (n = 0-6, 9) clusters. 2010 , 114, 8948-60 Applications of Screened Hybrid Density Functionals with Empirical Dispersion Corrections to Rare	55 8
1716 1715	Microhydration of the selenite dianion: a theoretical study of structures, hydration energies, and electronic stabilities of SeO(3)(2-)(H(2)O)(n) (n = 0-6, 9) clusters. 2010 , 114, 8948-60 Applications of Screened Hybrid Density Functionals with Empirical Dispersion Corrections to Rare Gas Dimers and Solids. 2010 , 6, 864-72	55 8 16
1716 1715 1714	Microhydration of the selenite dianion: a theoretical study of structures, hydration energies, and electronic stabilities of SeO(3)(2-)(H(2)O)(n) (n = 0-6, 9) clusters. 2010 , 114, 8948-60 Applications of Screened Hybrid Density Functionals with Empirical Dispersion Corrections to Rare Gas Dimers and Solids. 2010 , 6, 864-72 Importance of the Inclusion of Dispersion in the Modeling of Asphaltene Dimers. 2010 , 24, 6468-6475 Origin of the Enhanced Interaction of Molecular Hydrogen with Extraframework Cu+ and FeO+	55 8 16

1710	Probing the hydration structure of polarizable halides: a multiedge XAFS and molecular dynamics study of the iodide anion. 2010 , 114, 12926-37	68
1709	Conformation Elucidation of Tethered Donor A cceptor Binaphthyls from the Anisotropy Factor of a Charge-Transfer Band. 2010 , 1, 2402-2405	17
1708	An Assessment of Density Functional Methods for Potential Energy Curves of Nonbonded Interactions: The XYG3 and B97-D Approximations. 2010 , 6, 727-34	86
1707	A System-Dependent Density-Based Dispersion Correction. 2010 , 6, 1990-2001	118
1706	Hydrogen generation from alcohols catalyzed by ruthenium-triphenylphosphine complexes: multiple reaction pathways. 2010 , 132, 8056-70	202
1705	Conformational Energies of DNA Sugar P hosphate Backbone: Reference QM Calculations and a Comparison with Density Functional Theory and Molecular Mechanics. 2010 , 6, 3817-3835	17
1704	Experimental and theoretical investigation of the aromatic-aromatic interaction in isolated capped dipeptides. 2010 , 114, 2973-82	49
1703	Toward Molecular Nanowires Self-Assembled on an Insulating Substrate: Heptahelicene-2-carboxylic acid on Calcite (101 4). 2010 , 114, 1547-1552	72
1702	Inclusion of Dispersion Effects Significantly Improves Accuracy of Calculated Reaction Barriers for Cytochrome P450 Catalyzed Reactions. 2010 , 1, 3232-3237	137
1701	Stabilization and structure calculations for noncovalent interactions in extended molecular systems based on wave function and density functional theories. 2010 , 110, 5023-63	666
1700	Mono- versus dinuclear Pt(II) 6-(5-trifluoromethyl-pyrazol-3-yl)-2,2'-bipyridine complexes: synthesis, characterization, and remarkable difference in luminescent properties. 2010 , 49, 1372-83	48
1699	Thermochemical benchmarking of hydrocarbon bond separation reaction energies: Jacob's ladder is not reversed!. 2010 , 108, 2655-2666	45
1698	DSD-BLYP: A General Purpose Double Hybrid Density Functional Including Spin Component Scaling and Dispersion Correction 2010 , 114, 20801-20808	261
1697	Molecular modeling of phenothiazine derivatives: self-assembling properties. 2010 , 114, 12479-89	15
1696	How Well Can Kohn-Sham DFT Describe the HO2 + O3 Reaction?. 2010 , 6, 2751-61	20
1695	Density functional theory analysis and spectral studies on amyloid peptide Abeta(28-35) and its mutants A30G and A30I. 2010 , 170, 439-50	5
1694	Toward DNA Conductivity: A Theoretical Perspective. 2010 , 1, 1881-1894	57
1693	Accurate correlated calculation of the intermolecular potential surface in the coronene dimer. 2010 , 108, 249-257	66

1692	Binding of pollutant aromatics on carbon nanotubes and graphite. 2010 , 50, 585-8	16
1691	Empirically corrected DFT and semi-empirical methods for non-bonding interactions. 2010 , 12, 307-22	71
1690	Hydroxyapatite as a key biomaterial: quantum-mechanical simulation of its surfaces in interaction with biomolecules. 2010 , 12, 6309-29	120
1689	Environmental effects in computational spectroscopy: accuracy and interpretation. 2010 , 11, 1812-32	47
1688	Interaction of the Explosive Molecules RDX and TATP with IRMOF-8. 2010 , 114, 7535-7540	18
1687	Periodic density functional theory calculations for 3-dimensional polyacetylene with empirical dispersion terms. 2010 , 12, 3289-93	23
1686	Molecular packing and charge transport parameters in crystalline organic semiconductors from first-principles calculations. 2010 , 12, 9381-8	56
1685	Performance of the Empirical Dispersion Corrections to Density Functional Theory: Thermodynamics of Hydrocarbon Isomerizations and Olefin Monomer Insertion Reactions. 2010 , 6, 477-90	41
1684	Accurate dispersion interactions from standard density-functional theory methods with small basis sets. 2010 , 12, 6092-8	46
1683	Nature of bonding in group 13 dimetallenes: a delicate balance between singlet diradical character and closed shell interactions. 2010 , 49, 10992-1000	37
1682	DFT/CC investigation of physical adsorption on a graphite (0001) surface. 2010 , 12, 6438-44	89
1681	Stereoselectivity in Oxyallyl-Furan 4+3 Cycloadditions: Control of Intermediate Conformations and Dispersive Stabilisation with Evans' Oxazolidinones. 2010 , 1, 387-392	60
1680	Frontiers in electronic structure theory. 2010 , 132, 110902	126
1679	Interactions of graphene sheets deduced from properties of polycyclic aromatic hydrocarbons. 2010 , 132, 044704	108
1678	Study of the interaction between short alkanethiols from ab initio calculations. 2010 , 12, 7555-65	16
1677	Ionization of cytosine monomer and dimer studied by VUV photoionization and electronic structure calculations. 2010 , 12, 2860-72	58
1676	Study of polycyclic aromatic hydrocarbons adsorbed on graphene using density functional theory with empirical dispersion correction. 2010 , 12, 6483-91	72
1675	Improved description of the structure of molecular and layered crystals: ab initio DFT calculations with van der Waals corrections. 2010 , 114, 11814-24	737

1674	Quantum-chemical simulation of solid-state NMR spectra: the example of a molecular tweezer host g uest complex. 2010 , 108, 333-342	15
1673	Ab Initio Study of Xe Adsorption on Graphene. 2010 , 114, 3544-3548	47
1672	Comparative Study of Selected Wave Function and Density Functional Methods for Noncovalent Interaction Energy Calculations Using the Extended S22 Data Set. 2010 , 6, 2365-76	194
1671	Binding of polycyclic aromatic hydrocarbons and graphene dimers in density functional theory. 2010 , 12, 013017	51
1670	Theoretical Study of the Hydrolysis of Pentameric Aluminum Complexes. 2010 , 6, 993-1007	17
1669	Competitive H-bonding synthons in organic hydrazides. 2010 , 12, 1186-1193	12
1668	Role of dispersive interactions in the CO adsorption on MgO(001): periodic B3LYP calculations augmented with an empirical dispersion term. 2010 , 12, 6382-6	58
1667	Theoretical Chemistry of Zeolite Reactivity. 2010 , 301-334	3
1666	A DFT periodic study on the interaction between O2 and cation exchanged chabazite MCHA ($M = H+$, Na+ or Cu+): effects in the triplet-singlet energy gap. 2010 , 12, 442-52	16
1665	Structure of the gas-phase glycine tripeptide. 2010 , 12, 3463-73	21
1664	Inclusion complexes of buckycatcher with C(60) and C(70). 2010 , 12, 7091-7	95
1663	Azobenzene versus 3,3',5,5'-tetra-tert-butyl-azobenzene (TBA) at Au(111): characterizing the role of spacer groups. 2010 , 12, 6404-12	44
1662	A highly ordered, aromatic bidentate self-assembled monolayer on Au(111): a combined experimental and theoretical study. 2010 , 12, 6445-54	19
1661	The complexes of halothane with benzene: the temperature dependent direction of the complexation shift of the aliphatic C-H stretching. 2010 , 12, 14034-44	56
1660	The 1,4-phenylenediisocyanide dimer: gas-phase properties and insights into organic self-assembled monolayers. 2010 , 12, 82-96	4
1659	Simultaneous adsorption of benzene and dioxygen in CuHY zeolites as a precursor process to the aerobic oxidation of benzene to phenol. 2010 , 12, 6345-51	11
1658	Investigations of the water clusters of the protected amino acid Ac-Phe-OMe by applying IR/UV double resonance spectroscopy: microsolvation of the backbone. 2010 , 12, 3511-21	34
1657	Role of van der Waals interaction in forming molecule-metal junctions: flat organic molecules on the Au(111) surface. 2010 , 12, 4759-67	103

1656	Ab initio study of van der Waals and hydrogen-bonded molecular crystals with a periodic local-MP2 method. 2010 , 12, 2429	48
1655	Structural changes in the water tetramer. A combined Monte Carlo and DFT study. 2010 , 12, 13657-66	13
1654	A comparative study of the binding of QSY 21 and Rhodamine 6G fluorescence probes to DNA: structure and dynamics. 2010 , 12, 9677-84	16
1653	Large-scale compensation of errors in pairwise-additive empirical force fields: comparison of AMBER intermolecular terms with rigorous DFT-SAPT calculations. 2010 , 12, 10476-93	65
1652	Reference MP2/CBS and CCSD(T) quantum-chemical calculations on stacked adenine dimers. Comparison with DFT-D, MP2.5, SCS(MI)-MP2, M06-2X, CBS(SCS-D) and force field descriptions. 2010 , 12, 3522-34	78
1651	The origin of the conformational preference of N,N'-diaryl-N,N'-dimethyl ureas. 2010 , 12, 15056-64	28
1650	Interpretation of the ultrafast photoinduced processes in pentacene thin films. 2010, 132, 3431-9	54
1649	Accurate Intermolecular Interaction Energies from a Combination of MP2 and TDDFT Response Theory. 2010 , 6, 168-78	140
1648	Solvent and temperature effects on diastereodifferentiating PaternEBIhi reaction of chiral alkyl cyanobenzoates with diphenylethene upon direct versus charge-transfer excitation. 2010 , 75, 5461-9	33
1647	Assessment of the performance of common density functional methods for describing the interaction energies of (H2O)6 clusters. 2010 , 132, 134303	64
1646	Theoretical study of the adsorption of C1-C4 primary alcohols in H-ZSM-5. 2010 , 12, 9481-93	62
1645	Modelling the binding of HIV-reverse transcriptase and nevirapine: an assessment of quantum mechanical and force field approaches and predictions of the effect of mutations on binding. 2010 , 12, 7117-25	26
1644	Experimental and computational study of the ring opening of tricyclic oxanorbornenes to polyhydro isoindole phosphonates. 2010 , 8, 3644-54	14
1643	Stability of noble-gas hydrocarbons in an organic liquid-like environment: HXeCCH in acetylene. 2011 , 13, 19601-6	26
1642	Liquid structures of water, methanol, and hydrogen fluoride at ambient conditions from first principles molecular dynamics simulations with a dispersion corrected density functional. 2011 , 13, 19943-50	59
1641	Electronic structure and metalthetal communication in (CpM)2(as-indacene) and (CpM)2(s-indacene) (M = Mn, Fe, Co, Ni) complexes: a DFT investigation. 2011 , 35, 2136	6
1640	Dispersion interactions of carbohydrates with condensate aromatic moieties: theoretical study on the CH-Interaction additive properties. 2011 , 13, 14215-22	25
1639	Chiral recognition between 1-(4-fluorophenyl)ethanol and 2-butanol: higher binding energy of homochiral complexes in the gas phase. 2011 , 13, 818-24	5

1638	Energetics and dynamics of proton transfer reactions along short water wires. 2011 , 13, 13207-15	43
1637	Heating a bowl of single-molecule-soup: structure and desorption energetics of water-encapsulated open-cage [60] fullerenoid anions in the gas-phase. 2011 , 13, 9818-23	29
1636	The fragmentation-recombination mechanism of the enzyme glutamate mutase studied by QM/MM simulations. 2011 , 133, 10195-203	29
1635	Axial chirality of donor-donor, donor-acceptor, and tethered 1,1'-binaphthyls: a theoretical revisit with dynamics trajectories. 2011 , 115, 5488-95	36
1634	Structure of the indole-benzene dimer revisited. 2011 , 115, 9485-92	28
1633	The structure and interaction energies of the weak complexes of CHClF2 and CHF3 with HCCH: a test of density functional theory methods. 2011 , 13, 4388-92	23
1632	[6]Saddlequat: a [6]helquat captured on its racemization pathway. 2011 , 2, 2314-2320	35
1631	Transition from one-dimensional water to ferroelectric ice within a supramolecular architecture. 2011 , 108, 3481-6	89
1630	Isolated monohydrates of a model peptide chain: effect of a first water molecule on the secondary structure of a capped phenylalanine. 2011 , 133, 3931-42	60
1629	Polarized Molecular Orbital Model Chemistry. II. The PMO Method. 2011 , 7, 857-867	24
1628	Energetics of direct and water-mediated proton-coupled electron transfer. 2011 , 133, 19040-3	27
1627	Competitive photocyclization/rearrangement of 4-aryl-1,1-dicyanobutenes controlled by intramolecular charge-transfer interaction. Effect of medium polarity, temperature, pressure, excitation wavelength, and confinement. 2011 , 10, 1405-14	12
1626	Energetics and structure of organic molecules embedded in single-wall carbon nanotubes from first principles: The example of benzene. 2011 , 84,	13
1625	Effects of Charge Localization on the Orbital Energies of Bithiophene Clusters. 2011 , 115, 17558-17563	6
1624	Sensitivity Analysis of Cluster Models for Calculating Adsorption Energies for Organic Molecules on Mineral Surfaces. 2011 , 115, 10044-10055	12
1623	Selectivity in Garratt-Braverman cyclization: an experimental and computational study. 2011 , 13, 888-91	27
1622	Silanol-Related and Unspecific Adsorption of Molecular Ammonia on Highly Dehydrated Silica. 2011 , 115, 23344-23353	17
1621	Impact of molecular flexibility on binding strength and self-sorting of chiral Eurfaces. 2011 , 133, 9580-91	87

1620	Nuclear shieldings with the SSB-D functional. 2011 , 115, 1250-6	16
1619	Fully computational lead-development of fluoro-olefin polymerization catalysts. 2011 , 115, 13885-95	5
1618	Ab Initio Modeling of Donor-Acceptor Interactions and Charge-Transfer Excitations in Molecular Complexes: The Case of Terthiophene-Tetracyanoquinodimethane. 2011 , 7, 2068-77	38
1617	Aldimines generated from aza-Wittig reaction between bis(iminophosphoranes) derived from 1,1'-diazidoferrocene and aromatic or heteroaromatic aldehydes: electrochemical and optical behaviour towards metal cations. 2011 , 40, 12548-59	19
1616	Singular Value Decomposition for Analyzing Temperature- and Pressure-Dependent Radial Distribution Functions: Decomposition into Grund RDFs (GRDFs). 2011 , 7, 3035-9	2
1615	Noncovalent interactions between modified cytosine and guanine DNA base pair mimics investigated by terahertz spectroscopy and solid-state density functional theory. 2011 , 115, 14391-6	22
1614	On the Nature of Interlayer Interactions in a System of Two Graphene Fragments. 2011 , 115, 24666-24673	29
1613	Theoretical study on the regioselectivity of the B80 buckyball in electrophilic and nucleophilic reactions using DFT-based reactivity indices. 2011 , 115, 9069-80	29
1612	Method of local increments for the calculation of adsorption energies of atoms and small molecules on solid surfaces. 2. CO/MgO(001). 2011 , 115, 7153-60	27
1611	Interchain Interactions Mediated by Br Adsorbates in Arrays of Metal©rganic Hybrid Chains on Ag(111). 2011 , 115, 14834-14838	62
1610	Alkanethiol Adsorption on Platinum: Chain Length Effects on the Quality of Self-Assembled Monolayers. 2011 , 115, 17788-17798	29
1609	Application of London-Type Dispersion Corrections in Solid-State Density Functional Theory for Predicting the Temperature-Dependence of Crystal Structures and Terahertz Spectra. 2011 , 11, 2006-2010	19
1608	Effect of nitrogen adsorption on the mid-infrared spectrum of water clusters. 2011 , 115, 6218-25	22
1607	Charge density analysis of 2-methyl-4-nitro-1-phenyl-1H-imidazole-5-carbonitrile: an experimental and theoretical study of C?NIC?N interactions. 2011 , 115, 12941-52	21
1606	On the role of London dispersion forces in biomolecular structure determination. 2011 , 115, 8038-46	35
1605	How is a co-methyl intermediate formed in the reaction of cobalamin-dependent methionine synthase? Theoretical evidence for a two-step methyl cation transfer mechanism. 2011 , 115, 4066-77	39
1604	VOPO4[H2O: a stacking faults structure studied by X-ray powder diffraction and DFT-D calculations. 2011 , 50, 4378-83	11
1603	Visualizing Halogen Bonds in Planar Supramolecular Systems. 2011 , 115, 2297-2301	61

1602	Experimental and theoretical study on molecular aggregation and its effect on the photo-physical properties of the mesogenic bi-1,3,4-thiadiazole derivative. 2011 , 13, 9697-705	7
1601	Comparison of intermolecular interaction energies from SAPT and DFT including empirical dispersion contributions. 2011 , 115, 11321-30	44
1600	Free energy simulations of a GTPase: GTP and GDP binding to archaeal initiation factor 2. 2011 , 115, 6749-63	26
1599	On the Geometry and Electronic Structure of the As-DNA Backbone. 2011 , 2, 389-392	9
1598	Analysis of the Reaction between O2and Nitrogen-Containing Char Using the Density Functional Theory. 2011 , 25, 670-675	19
1597	Charge Transfer in Molecular Complexes with 2,3,5,6-Tetrafluoro-7,7,8,8-tetracyanoquinodimethane (F4-TCNQ): A Density Functional Theory Study. 2011 , 23, 5149-5159	87
1596	Do Short CHM (M = Cu(I), Ag(I)) Distances Represent Agostic Interactions in Pincer-Type Complexes? Unusual NHC Transmetalation from Cu(I) to Ag(I). 2011 , 30, 3302-3310	51
1595	Modeling Charge Resonance in Cationic Molecular Clusters: Combining DFT-Tight Binding with Configuration Interaction. 2011 , 7, 44-55	42
1594	Adsorption of Gases in Microporous Organic Molecular Crystal, a Multiscale Computational Investigation. 2011 , 115, 4935-4942	13
1593	Vibrational and thermodynamic properties of ℍMX: a first-principles investigation. 2011 , 134, 204509	21
1592	Molecular calipers control atomic separation at a metal surface. 2011 , 11, 4113-7	17
1591	Density functional theory study of pyrophyllite and M-montmorillonites (M = Li, Na, K, Mg, and Ca): role of dispersion interactions. 2011 , 115, 9695-703	55
1590	On the Mechanism of Cyclopropanation Reactions Catalyzed by a Rhodium(I) Catalyst Bearing a Chelating Imine-Functionalized NHC Ligand: A Computational Study. 2011 , 30, 6562-6571	13
1589	Cation-cation "attraction": when London dispersion attraction wins over Coulomb repulsion. 2011 , 50, 2619-28	112
1588	A step beyond the Feltham-Enemark notation: spectroscopic and correlated ab initio computational support for an antiferromagnetically coupled M(II)-(NO)- description of Tp*M(NO) (M = Co, Ni). 2011 , 133, 18785-801	83
1587	Toward an Understanding of the Specific Ion Effect Using Density Functional Theory. 2011 , 2, 1088-1093	102
1586	Density Functional Theory Study of Alkane-Alkoxide Hydride Transfer in Zeolites. 2011 , 1, 105-115	33
1585	When do molecular bowls encapsulate metal cations?. 2011 , 115, 4968-75	40

1584	Weak Molecular Interactions Studied with Parallel Implementations of the Local Pair Natural Orbital Coupled Pair and Coupled Cluster Methods. 2011 , 7, 76-87	127
1583	Overcoming lability of extremely long alkane carbon-carbon bonds through dispersion forces. 2011 , 477, 308-11	298
1582	Aryl C-H amination by diruthenium nitrides in the solid state and in solution at room temperature: experimental and computational study of the reaction mechanism. 2011 , 133, 13138-50	56
1581	First-principles calculations of the structural and dynamic properties, and the equation of state of crystalline iodine oxides I2O4, I2O5, and I2O6. 2011 , 134, 204501	6
1580	Computational Insights into Palladium-Mediated Allylic Substitution Reactions. 2011, 65-93	22
1579	Electronic structure and chemical bond in naphthalene and anthracene. 2011 , 13, 5679-86	45
1578	Differences in structure, energy, and spectrum between neutral, protonated, and deprotonated phenol dimers: comparison of various density functionals with ab initio theory. 2011 , 13, 991-1001	33
1577	Van der Waals effects in ab initio water at ambient and supercritical conditions. 2011 , 135, 154503	127
1576	Dispersion interactions in room-temperature ionic liquids: results from a non-empirical density functional. 2011 , 135, 154505	18
1575	The calculation of intermolecular interaction energies. 2011 , 107, 148	24
1575 1574	The calculation of intermolecular interaction energies. 2011, 107, 148 Approximate Density Functionals: Which Should I Choose?. 2011,	24
1574	Approximate Density Functionals: Which Should I Choose?. 2011 , Evaluation of a combination of local hybrid functionals with DFT-D3 corrections for the calculation	3
1574 1573	Approximate Density Functionals: Which Should I Choose?. 2011 , Evaluation of a combination of local hybrid functionals with DFT-D3 corrections for the calculation of thermochemical and kinetic data. 2011 , 115, 8990-6	3 25
1574 1573 1572	Approximate Density Functionals: Which Should I Choose?. 2011, Evaluation of a combination of local hybrid functionals with DFT-D3 corrections for the calculation of thermochemical and kinetic data. 2011, 115, 8990-6 Electronic structures of silver oxides. 2011, 84, Structural and Vibrational Properties of Liquid Water from van der Waals Density Functionals. 2011	3 25 51
1574 1573 1572 1571	Approximate Density Functionals: Which Should I Choose?. 2011, Evaluation of a combination of local hybrid functionals with DFT-D3 corrections for the calculation of thermochemical and kinetic data. 2011, 115, 8990-6 Electronic structures of silver oxides. 2011, 84, Structural and Vibrational Properties of Liquid Water from van der Waals Density Functionals. 2011, 7, 3054-61 Synthesis, structural, and photophysical investigation of diimine triscarbonyl Re(I) tetrazolato	3 25 51 134
1574 1573 1572 1571 1570	Approximate Density Functionals: Which Should I Choose?. 2011, Evaluation of a combination of local hybrid functionals with DFT-D3 corrections for the calculation of thermochemical and kinetic data. 2011, 115, 8990-6 Electronic structures of silver oxides. 2011, 84, Structural and Vibrational Properties of Liquid Water from van der Waals Density Functionals. 2011, 7, 3054-61 Synthesis, structural, and photophysical investigation of diimine triscarbonyl Re(I) tetrazolato complexes. 2011, 50, 1229-41	3 25 51 134 71

1566	A potent ruthenium(II) antitumor complex bearing a lipophilic levonorgestrel group. 2011, 50, 9164-71	65
1565	Protein-ligand interaction energies with dispersion corrected density functional theory and high-level wave function based methods. 2011 , 115, 11210-20	73
1564	Density functional theory studies of interactions of ruthenium-arene complexes with base pair steps. 2011 , 115, 11293-302	21
1563	A Parameter-Free Density Functional That Works for Noncovalent Interactions. 2011 , 2, 983-989	124
1562	Carbon-tuned bonding method significantly enhanced the hydrogen storage of BN-Li complexes. 2011 , 3, 4824-9	17
1561	Hydrogen bond dynamics in heavy water studied with quantum dynamical simulations. 2011 , 13, 19865-75	12
1560	First principle kinetic studies of zeolite-catalyzed methylation reactions. 2011 , 133, 888-99	133
1559	Theoretical investigation into the mechanism of reductive elimination from bimetallic palladium complexes. 2011 , 50, 6449-57	45
1558	Solvation Structure and Dynamics of Ni(2+)(aq) from First Principles. 2011 , 7, 2937-46	10
1557	Ab initio van der waals interactions in simulations of water alter structure from mainly tetrahedral to high-density-like. 2011 , 115, 14149-60	78
1556	Electronic Structure of Organic Materials Investigated by Quantum Chemical Calculations. 2011 , 1-22	
1555	Density Functional Theory for Transition Metal Chemistry: The Case of a Water-Splitting Ruthenium Cluster. 2011 , 137-163	2
1554	Accurate Dispersion-Corrected Density Functionals for General Chemistry Applications. 2011, 1-16	1
1553	Heats of Adsorption of CO and CO2 in Metal \square rganic Frameworks: Quantum Mechanical Study of CPO-27-M (M = Mg, Ni, Zn). 2011 , 115, 21777-21784	112
1552	Temperature-dependent infrared spectroscopy of water from a first-principles approach. 2011 , 115, 6861-71	23
1551	Does DFT-D estimate accurate energies for the binding of ligands to metal complexes?. 2011 , 40, 11176-83	72
1550	Redox noninnocence of nitrosoarene ligands in transition metal complexes. 2011 , 50, 5763-76	49
1549	Quantification of binding affinities of essential sugars with a tryptophan analogue and the ubiquitous role of C-H m interactions. 2011 , 13, 6517-30	24

1548	Supramolecular assemblies involving anion[and lone pair[Interactions: experimental observation and theoretical analysis. 2011, 13, 4519	75
1547	DFT Study on the Mechanism of the Activation and Cleavage of CO2 by (NHC)CuEPh3 (E = Si, Ge, Sn). 2011 , 30, 1340-1349	60
1546	Shell-Models for Multi-Layer Carbon Nano-Particles. 2011 , 585-602	2
1545	N-HIIIIhydrogen-bonding and large-amplitude tipping vibrations in jet-cooled pyrrole-benzene. 2011 , 13, 14110-8	26
1544	Polymorphism of a Model Arylboronic Azaester: Combined Experimental and Computational Studies. 2011 , 11, 1835-1845	25
1543	Organometallic reactivity: the role of metal-ligand bond energies from a computational perspective. 2011 , 40, 11184-91	48
1542	Like-charge guanidinium pairing from molecular dynamics and ab initio calculations. 2011 , 115, 11193-201	48
1541	Current approaches to predicting molecular organic crystal structures. 2011 , 17, 3-52	169
1540	Theoretical evaluation of structural models of the S2 state in the oxygen evolving complex of Photosystem II: protonation states and magnetic interactions. 2011 , 133, 19743-57	249
1539	Application of London-type dispersion corrections to the solid-state density functional theory simulation of the terahertz spectra of crystalline pharmaceuticals. 2011 , 13, 4250-9	70
1538	A DFT study of substituent effects in corannulene dimers. 2011 , 13, 21139-45	41
1537	CO2 adsorption on TiO2(110) rutile: insight from dispersion-corrected density functional theory calculations and scanning tunneling microscopy experiments. 2011 , 134, 104707	83
1536	Performance of Density Functional Theory and Mller-Plesset Second-Order Perturbation Theory for Structural Parameters in Complexes of Ru. 2011 , 7, 2325-32	116
1535	Dispersion corrections essential for the study of chemical reactivity in fullerenes. 2011 , 115, 3491-6	108
1534	Adsorption and diffusion of water on graphene from first principles. 2011 , 84,	188
1533	Structural and electronic properties of the graphene/Al/Ni(111) intercalation system. 2011 , 13, 113028	95
1532	DFT study of the interaction free energy of Dromplexes of fullerenes with buckybowls and viologen dimers. 2011 , 35, 1453	32
1531	Origins of stereoselectivity in optically pure phenylethaniminopyridine tris-chelates M(NN')3(n+) (M = Mn, Fe, Co, Ni and Zn). 2011 , 40, 10416-33	73

1530	The Mathematics and Topology of Fullerenes. 2011 ,	24
1529	Tin Monoxide: Structural Prediction from First Principles Calculations with van der Waals Corrections. 2011 , 115, 19916-19924	79
1528	Ab initio studies of aromatic excimers using multiconfiguration quasi-degenerate perturbation theory. 2011 , 115, 7687-99	60
1527	Enhanced Hydrogen Storage on Li Functionalized BC3 Nanotube. 2011 , 115, 6136-6140	36
1526	Binding of 6-mer single-stranded homo-nucleotides to poly(3,4-ethylenedioxythiophene): specific hydrogen bonds with guanine. 2011 , 7, 9922	13
1525	On the physisorption of water on graphene: a CCSD(T) study. 2011 , 13, 12041-7	152
1524	Accurate Interaction Energies for Problematic Dispersion-Bound Complexes: Homogeneous Dimers of NCCN, P2, and PCCP. 2011 , 7, 2842-51	41
1523	Obtaining Good Performance With Triple-EType Basis Sets in Double-Hybrid Density Functional Theory Procedures. 2011 , 7, 2852-63	52
1522	Electronic structure of 2,2'-bipyridine organotransition-metal complexes. Establishing the ligand oxidation level by density functional theoretical calculations. 2011 , 50, 9773-93	146
1521	Noncovalent interactions in paired DNA nucleobases investigated by terahertz spectroscopy and solid-state density functional theory. 2011 , 115, 9467-78	43
1520	DSD-PBEP86: in search of the best double-hybrid DFT with spin-component scaled MP2 and dispersion corrections. 2011 , 13, 20104-7	304
1519	Density Functional Theory. 2011 , 255-368	3
1518	Accurate Molecular Crystal Lattice Energies from a Fragment QM/MM Approach with On-the-Fly Ab Initio Force Field Parametrization. 2011 , 7, 3733-42	111
1517	Towards large-scale, fully ab initio calculations of ionic liquids. 2011 , 13, 4189-207	115
1516	Neutral carbene analogues of group 13 elements: the dimerization reaction to a biradicaloid. 2011 , 50, 2629-33	18
1515	Efficient and Accurate Double-Hybrid-Meta-GGA Density Functionals-Evaluation with the Extended GMTKN30 Database for General Main Group Thermochemistry, Kinetics, and Noncovalent Interactions. 2011 , 7, 291-309	841
1514	Dimerization of Radical-Anions: Nitride Clusterfullerenes versus Empty Fullerenes. 2011 , 2, 1592-1600	20
1513	Real-world predictions from ab initio molecular dynamics simulations. 2012 , 307, 109-53	74

1512	Chapter 4:Polymorph Prediction of Small Organic Molecules, Co-crystals and Salts. 2011, 44-88	1
1511	Dispersion interactions in density-functional theory: an adiabatic-connection analysis. 2011 , 135, 194109	18
1510	Physics-based scoring of protein-ligand interactions: explicit polarizability, quantum mechanics and free energies. 2011 , 3, 683-98	11
1509	Polymorphism of Crystalline 4-Amino-2-Nitroacetanilide. 2011 , 11, 2074-2083	10
1508	Nature of adhesion of condensed organic films on platinum by first-principles simulations. 2011 , 13, 11827-37	7
1507	Comprehensive Benchmarking of a Density-Dependent Dispersion Correction. 2011 , 7, 3567-77	322
1506	Interaction of metal ions with biomolecular ligands: how accurate are calculated free energies associated with metal ion complexation?. 2011 , 115, 11394-402	36
1505	Local nature of substituent effects in stacking interactions. 2011 , 133, 10262-74	356
1504	On the Binding Strength Sequence for Nucleic Acid Bases and C(60) with Density Functional and Dispersion-corrected Density Functional Theories: Whether C(60) could protect nucleic acid bases from radiation-induced damage?. 2011 , 115, 3220-3228	24
1503	Anthracene-resorcin[4]arene-based capsules: synthesis and photoswitchable features. 2011 , 9, 7491-9	24
1502	Comparison of the performance of dispersion-corrected density functional theory for weak hydrogen bonds. 2011 , 13, 13942-50	119
1501	Electronic and Magnetic Properties of the Graphene- Ferromagnet Interfaces: Theory vs. Experiment. 2011 ,	2
1500	Self-Consistent-Charge Density Functional Tight-Binding Method: An Efficient Approximation of Density Functional Theory. 2011 , 287-307	5
1499	An introduction to quantum chemical methods applied to drug design. 2011 , 3, 1061-78	
1498	MNDO-Like Semiempirical Molecular Orbital Theory and Its Application to Large Systems. 2011 , 259-286	18
1497	Principles of Density Functional Theory: Equilibrium and Nonequilibrium Applications. 2011 , 1-44	
1496	Silver(I)-mediated Hoogsteen-type base pairs. 2011 , 105, 1398-404	56
1495	The ground states of iron(III) porphines: role of entropy-enthalpy compensation, Fermi correlation, dispersion, and zero-point energies. 2011 , 105, 1286-92	24

(2011-2011)

1494	Theoretical studies on the dimerization of substituted paraphenylenediamine radical cations. 2011 , 83, 368-78	3
1493	ConvexBoncave stacking of curved conjugated networks: Benchmark calculations on the corannulene dimer. 2011 , 512, 155-160	63
1492	Effects of the dispersion interaction in liquid water. 2011 , 513, 59-62	20
1491	Conventional and density-fitting local Mller P lesset theory calculations of C60 and its endohedral H2@C60 and 2H2@C60 complexes. 2011 , 513, 236-240	8
1490	2D vs. 3D titanium dioxide: Role of dispersion interactions. 2011 , 516, 72-75	18
1489	Structures of the xyloseWater complex: Energetics, transitions between conformers and spectroscopy. 2011 , 518, 49-54	9
1488	A combined quantum chemical and crystallographic study on the oxidized binuclear center of cytochrome c oxidase. 2011 , 1807, 769-78	30
1487	Stabilization of the peroxy intermediate in the oxygen splitting reaction of cytochrome cbb(3). 2011 , 1807, 813-8	14
1486	Experimental and theoretical IR study of methanol and ethanol conversion over H-SAPO-34. 2011 , 177, 12-24	37
1485	Perspective on the structure of liquid water. 2011 , 389, 1-34	249
1485 1484	Perspective on the structure of liquid water. 2011 , 389, 1-34 Proline-based chiral stationary phases: a molecular dynamics study of the interfacial structure. 2011 , 1218, 6331-47	249
. ,	Proline-based chiral stationary phases: a molecular dynamics study of the interfacial structure.	
1484	Proline-based chiral stationary phases: a molecular dynamics study of the interfacial structure. 2011, 1218, 6331-47 A thorough benchmark of density functional methods for general main group thermochemistry,	22
1484	Proline-based chiral stationary phases: a molecular dynamics study of the interfacial structure. 2011, 1218, 6331-47 A thorough benchmark of density functional methods for general main group thermochemistry, kinetics, and noncovalent interactions. 2011, 13, 6670-88 Assessment of the Performance of DFT and DFT-D Methods for Describing Distance Dependence of	1347
1484 1483 1482	Proline-based chiral stationary phases: a molecular dynamics study of the interfacial structure. 2011, 1218, 6331-47 A thorough benchmark of density functional methods for general main group thermochemistry, kinetics, and noncovalent interactions. 2011, 13, 6670-88 Assessment of the Performance of DFT and DFT-D Methods for Describing Distance Dependence of Hydrogen-Bonded Interactions. 2011, 7, 88-96 Assessment of Popular DFT and Semiempirical Molecular Orbital Techniques for Calculating Relative Transition State Energies and Kinetic Product Distributions in Enantioselective	1347 342
1484 1483 1482	Proline-based chiral stationary phases: a molecular dynamics study of the interfacial structure. 2011, 1218, 6331-47 A thorough benchmark of density functional methods for general main group thermochemistry, kinetics, and noncovalent interactions. 2011, 13, 6670-88 Assessment of the Performance of DFT and DFT-D Methods for Describing Distance Dependence of Hydrogen-Bonded Interactions. 2011, 7, 88-96 Assessment of Popular DFT and Semiempirical Molecular Orbital Techniques for Calculating Relative Transition State Energies and Kinetic Product Distributions in Enantioselective Organocatalytic Reactions. 2011, 7, 3586-95 A van der Waals density functional study of adenine on graphene: single-molecular adsorption and	22 1347 342 63
1484 1483 1482 1481 1480	Proline-based chiral stationary phases: a molecular dynamics study of the interfacial structure. 2011, 1218, 6331-47 A thorough benchmark of density functional methods for general main group thermochemistry, kinetics, and noncovalent interactions. 2011, 13, 6670-88 Assessment of the Performance of DFT and DFT-D Methods for Describing Distance Dependence of Hydrogen-Bonded Interactions. 2011, 7, 88-96 Assessment of Popular DFT and Semiempirical Molecular Orbital Techniques for Calculating Relative Transition State Energies and Kinetic Product Distributions in Enantioselective Organocatalytic Reactions. 2011, 7, 3586-95 A van der Waals density functional study of adenine on graphene: single-molecular adsorption and overlayer binding. 2011, 23, 135001 Density-functional approaches to noncovalent interactions: a comparison of dispersion corrections	13473426340

1476	Do H-bond features of silica surfaces affect the H2O and NH3 adsorption? Insights from periodic B3LYP calculations. 2011 , 115, 11221-8	18
1475	Degrees of Freedom in Polypeptides and Proteins. 2011 , 27-54	
1474	X-ray emission spectroscopy evidences a central carbon in the nitrogenase iron-molybdenum cofactor. 2011 , 334, 974-7	659
1473	On the accuracy of DFT-SAPT, MP2, SCS-MP2, MP2C, and DFT+Disp methods for the interaction energies of endohedral complexes of the C(60) fullerene with a rare gas atom. 2011 , 13, 732-43	77
1472	Approximations to complete basis set-extrapolated, highly correlated non-covalent interaction energies. 2011 , 135, 134318	69
1471	Dispersion-corrected density functional theory comparison of hydrogen adsorption on boron-nitride and carbon nanotubes. 2011 , 84,	23
1470	Forces and currents in carbon nanostructures: are we imaging atoms?. 2011 , 106, 176101	74
1469	Prediction of the Unknown Crystal Structure of Creatine Using Fully Quantum Mechanical Methods. 2011 , 11, 5733-5740	33
1468	Calculations of complexes of 9-diphenylaminoacridine fluorescent indicator with analyte molecules using density functional theory with dispersion correction. 2011 , 6, 298-302	
1467	Noncovalent interactions in biochemistry. 2011 , 1, 3-17	184
• •	Noncovalent interactions in biochemistry. 2011 , 1, 3-17 Density functional theory with London dispersion corrections. 2011 , 1, 211-228	184
1466		<u> </u>
1466	Density functional theory with London dispersion corrections. 2011 , 1, 211-228 DNA insertion in and wrapping around carbon nanotubes. 2011 , 1, 902-919 Substrate binding and activation in the active site of cytochrome contributes adensity.	1645
1466 1465	Density functional theory with London dispersion corrections. 2011 , 1, 211-228 DNA insertion in and wrapping around carbon nanotubes. 2011 , 1, 902-919 Substrate binding and activation in the active site of cytochrome c nitrite reductase: a density	1645 5
1466 1465 1464	Density functional theory with London dispersion corrections. 2011 , 1, 211-228 DNA insertion in and wrapping around carbon nanotubes. 2011 , 1, 902-919 Substrate binding and activation in the active site of cytochrome c nitrite reductase: a density functional study. 2011 , 16, 417-30 Oxygen cleavage with manganese and iron in ribonucleotide reductase from Chlamydia	1645 5 36
1466 1465 1464 1463	Density functional theory with London dispersion corrections. 2011, 1, 211-228 DNA insertion in and wrapping around carbon nanotubes. 2011, 1, 902-919 Substrate binding and activation in the active site of cytochrome c nitrite reductase: a density functional study. 2011, 16, 417-30 Oxygen cleavage with manganese and iron in ribonucleotide reductase from Chlamydia trachomatis. 2011, 16, 553-65 Atomistic simulations of materials for optical chemical sensors: DFT-D calculations of molecular interactions between gas-phase analyte molecules and simple substrate models. 2011, 17, 1855-62	1645 5 36 24
1466 1465 1464 1463 1462	Density functional theory with London dispersion corrections. 2011, 1, 211-228 DNA insertion in and wrapping around carbon nanotubes. 2011, 1, 902-919 Substrate binding and activation in the active site of cytochrome c nitrite reductase: a density functional study. 2011, 16, 417-30 Oxygen cleavage with manganese and iron in ribonucleotide reductase from Chlamydia trachomatis. 2011, 16, 553-65 Atomistic simulations of materials for optical chemical sensors: DFT-D calculations of molecular interactions between gas-phase analyte molecules and simple substrate models. 2011, 17, 1855-62 Hydrogen bonding interactions in noradrenaline-DMSO complexes: DFT and QTAIM studies of	1645 5 36 24

1458	Ion beam induced defects in graphene: Raman spectroscopy and DFT calculations. 2011 , 993, 506-509	22
1457	Solvent induced structural dynamics of ruthenium pentacarbonyl in benzene. 2011 , 508, 43-48	4
1456	Graphene on ferromagnetic surfaces and its functionalization with water and ammonia. 2011 , 6, 214	22
1455	The stability and reactivity of activated acryloylcarbamates as reagents for the synthesis of N-1 substituted thymine and uracil (an NMR and DFT study. 2011 , 24, 423-430	2
1454	Control of self-assembled 2D nanostructures by methylation of guanine. 2011 , 7, 939-49	18
1453	Atomic radii in molecules for use in a polarizable force field. 2011 , 111, 1763-1772	8
1452	1H, 13C, 15N NMR coordination shifts in Fe(II), Ru(II) and Os(II) cationic complexes with 2,2':6',2?-terpyridine. 2011 , 49, 237-41	14
1451	Validation of DFT-based methods for predicting qualitative thermochemistry of large polyaromatics. 2011 , 12, 1100-8	8
1450	Acetylene???furan trimer formation at 0.37 K as a model for ultracold aggregation of non- and weakly polar molecules. 2011 , 12, 2009-17	7
1449	Structural analysis of an isolated cyclic tetrapeptide and its monohydrate by combined IR/UV spectroscopy. 2011 , 12, 1981-8	35
1448	Isolated gramicidin peptides probed by IR spectroscopy. 2011 , 12, 1816-21	34
1447	Reduction potentials and acidity constants of Mn superoxide dismutase calculated by QM/MM free-energy methods. 2011 , 12, 3337-47	34
1446	System-dependent dispersion coefficients for the DFT-D3 treatment of adsorption processes on ionic surfaces. 2011 , 12, 3414-20	188
1445	Generation of potential energy surfaces in high dimensions and their haptic exploration. 2011 , 12, 3204-13	21
1444	Empirical hydrogen-bond potential functionsan old hat reconditioned. 2011 , 12, 3131-42	22
1443	Substituent effects on non-covalent interactions with aromatic rings: insights from computational chemistry. 2011 , 12, 3116-30	116
1442	Benchmarking density functional methods against the S66 and S66x8 datasets for non-covalent interactions. 2011 , 12, 3421-33	252
1441	Inter- and intramolecular dispersion interactions. <i>Journal of Computational Chemistry</i> , 2011 , 32, 1117-27 3.5	32

1440	The shape of gaseous n-butylbenzene: assessment of computational methods and comparison with experiments. <i>Journal of Computational Chemistry</i> , 2011 , 32, 1550-60	3.5	6
1439	Effect of the damping function in dispersion corrected density functional theory. <i>Journal of Computational Chemistry</i> , 2011 , 32, 1456-65	3.5	10429
1438	Accurate quantum-chemical description of gold complexes with pyridine and its derivatives. <i>Journal of Computational Chemistry</i> , 2011 , 32, 1839-45	3.5	15
1437	Assessment of TD-DFT- and TD-HF-based approaches for the prediction of exciton coupling parameters, potential energy curves, and electronic characters of electronically excited aggregates. <i>Journal of Computational Chemistry</i> , 2011 , 32, 1971-81	3.5	64
1436	Harmonic vibrational frequencies: scale factors for pure, hybrid, hybrid meta, and double-hybrid functionals in conjunction with correlation consistent basis sets. <i>Journal of Computational Chemistry</i> , 2011 , 32, 2339-47	3.5	49
1435	Zinc-homocysteine binding in cobalamin-dependent methionine synthase and its role in the substrate activation: DFT, ONIOM, and QM/MM molecular dynamics studies. <i>Journal of Computational Chemistry</i> , 2011 , 32, 3154-67	3.5	13
1434	Electric Control of Magnetization and Interplay between Orbital Ordering and Ferroelectricity in a Multiferroic Metal (Drganic Framework. 2011 , 123, 5969-5972		50
1433	Two-Dimensional Molecular Porous Networks Formed by Trimesic Acid and 4,4?-Bis(4-pyridyl)biphenyl on Au(111) through Hierarchical Hydrogen Bonds: Structural Systematics and Control of Nanopore Size and Shape. 2011 , 123, 7704-7708		3
1432	Electric control of magnetization and interplay between orbital ordering and ferroelectricity in a multiferroic metal-organic framework. 2011 , 50, 5847-50		223
1431	Two-dimensional molecular porous networks formed by trimesic acid and 4,4'-bis(4-pyridyl)biphenyl on Au(111) through hierarchical hydrogen bonds: structural systematics and control of nanopore size and shape. 2011 , 50, 7562-6		54
1430	Eland Elactams through palladium-catalyzed intramolecular allylic alkylation: enantioselective synthesis, NMR Investigation, and DFT rationalization. 2011 , 17, 2885-96		33
1429	Three-dimensional potential energy surface of selected carbohydrates' CH/ldispersion interactions calculated by high-level quantum mechanical methods. 2011 , 17, 5680-90		26
1428	Contiguous metal-mediated base pairs comprising two Ag(I) ions. 2011 , 17, 6533-44		104
1427	Mechanistic insights into ring-closing enyne metathesis with the second-generation Grubbs-Hoveyda catalyst: a DFT study. 2011 , 17, 7506-20		55
1426	CO2 and formate complexes of phosphine/borane frustrated Lewis pairs. 2011 , 17, 9640-50		135
1425	Competitive reactions of organophosphorus radicals on coke surfaces. 2011 , 17, 12027-36		21
1424	Theoretical simulations elucidate the role of naphthalenic species during methanol conversion within H-SAPO-34. 2011 , 17, 9083-93		31
1423	Neutral nickel oligo- and polymerization catalysts: the importance of alkyl phosphine intermediates in chain termination. 2011 , 17, 14628-42		15

1422	Telomere structure and stability: covalency in hydrogen bonds, not resonance assistance, causes cooperativity in guanine quartets. 2011 , 17, 12612-22	114
1421	Experimental and theoretical investigations of circular dichroism of donor-acceptor 1,1'-binaphthyls: influence of substitution on the coupling amplitude and cotton effect of the charge-transfer band. 2011 , 23 Suppl 1, E22-7	6
1420	Continuum modeling of van der Waals interactions between carbon onion layers. 2011 , 49, 1620-1627	23
1419	Surface-enhanced Raman Scattering Study on 1D-2D Graphene-based Structures. 2011 , 49, 3149-3157	18
1418	TDDFT study on the second-order nonlinear optical properties of a series of mono- and di-nuclear [60]fullerene complexes. 2011 , 963, 98-103	2
1417	Proline- and thioproline-derived enamines: The theoretical study of torsional and ring-puckering conformations. 2011 , 964, 133-140	2
1416	Dispersion energy effects on methane interaction within zeolite straight micropores: A computational investigation. 2011 , 967, 191-198	7
1415	Classical and quantum mechanical rainbow-scattering of fast He atoms from a KCl(001) surface. 2011 , 269, 799-803	9
1414	Catalytic synthesis of vinylphosphanes via calcium-mediated intermolecular hydrophosphanylation of alkynes and butadiynes. 2011 , 696, 216-227	33
1413	On the mechanism of the reaction of white phosphorus with silylenes. 2011 , 40, 7193-200	9
1412	Hydrogen bonded structure and dynamics of liquid-vapor interface of water-ammonia mixture: an ab initio molecular dynamics study. 2011 , 135, 114510	35
1411	Organic-inorganic compounds with strong nonlinear optical properties based on 2,4,6-trimethylpyridinium and tetrahedral BF4[hetworks. 2011 , 83,	5
1410	Importance of anisotropy in the evaluation of dispersion interactions. 2011 , 83,	16
1409	Electronic properties of the graphene/6H-SiC(0001[) interface: A first-principles study. 2011 , 84,	27
1408	Ground state of graphene slabs in an external electric field. 2011 , 84,	1
1407	Rainbow scattering under axial surface channeling from a KCl(001) surface. 2011 , 84,	14
1406	van der Waals density functional study of energetic, structural, and vibrational properties of small water clusters and ice Ih. 2011 , 84,	42
1405	van der Waals interactions in the ground state of Mg(BH4)2 from density functional theory. 2011 , 83,	45

1404	FeP(Im)-AB Bonding Energies Evaluated with A Large Number of Density Functionals (P = porphine, Im = imidazole, AB = CO, NO, and O(2)). 2011 , 109, 2035-2048	11
1403	Cation binding to 15-TBA quadruplex DNA is a multiple-pathway cation-dependent process. 2011 , 39, 9789-802	64
1402	Achieving chiral resolution in self-assembled supramolecular structures through kinetic pathways. 2011 , 22, 275705	21
1401	Communication: The effect of dispersion corrections on the melting temperature of liquid water. 2011 , 134, 121105	135
1400	First-principles investigation of the adsorption of the 2,5-pyridine di-carboxylic acid onto the Cu(011) surface. 2011 , 134, 104708	6
1399	Theoretical investigations of candidate crystal structures for tarbonic acid. 2011, 134, 124511	11
1398	External coupled-cluster perturbation theory: description and application to weakly interaction dimers. Corrections to the random phase approximation. 2011 , 134, 184108	18
1397	Self-consistent meta-generalized gradient approximation study of adsorption of aromatic molecules on noble metal surfaces. 2011 , 135, 084704	34
1396	Communication: efficient counterpoise corrections by a perturbative approach. 2011 , 135, 081105	9
1395	The role of relativity and dispersion controlled inter-chain interaction on the band gap of thiophene, selenophene, and tellurophene oligomers. 2012 , 136, 094904	19
1394	Electronic and Structural Properties of Turbostratic Epitaxial Graphene on the 6H-SiC (000-1) Surface. 2012 , 717-720, 595-600	3
1393	Long-range corrected hybrid meta-generalized-gradient approximations with dispersion corrections. 2012 , 136, 154109	88
1392	Enzyme informatics. 2012 , 12, 1911-23	15
1391	Computational and Experimental Studies of Molecularly Imprinted Polymers for Organochlorine Pesticides Heptachlor and DDT. 2012 , 8, 562-568	13
1390	Dynamical screening of the van der Waals interaction between graphene layers. 2012 , 24, 424208	7
1389	Long-range correlation energies from frequency-dependent weighted exchange-hole dipole polarisabilities. 2012 , 136, 014104	15
1388	The electronic spectrum of CUONg4 (Ng = Ne, Ar, Kr, Xe): new insights in the interaction of the CUO molecule with noble gas matrices. 2012 , 137, 084308	23
1387	Water monomer interaction with gold nanoclusters from van der Waals density functional theory. 2012 , 136, 024702	14

1386	Electron correlation contribution to the physisorption of CO on MgF2(110). 2012 , 136, 124117	15
1385	Phase transition and chemical decomposition of shocked CO-N2 mixture. 2012 , 137, 054504	7
1384	Analysis of the basis set superposition error in molecular dynamics of hydrogen-bonded liquids: application to methanol. 2012 , 137, 104506	3
1383	Extension of local response dispersion method to excited-state calculation based on time-dependent density functional theory. 2012 , 137, 124106	16
1382	Second-order many-body perturbation study of ice lh. 2012 , 137, 204505	65
1381	Assessment of dispersion corrections in DFT calculations on large biological systems. 2012 , 110, 3061-3076	8
1380	Wave-packet approach to transport properties of carrier coupled with intermolecular and intramolecular vibrations of organic semiconductors. 2012 , 85,	43
1379	Potential energy surface of 4-hexyl-4?-cyanobiphenyl (6CB) on graphite surface: a DFT study with van der Waals corrections. 2012 , 38, 425-431	1
1378	Atomic-scale friction in graphene oxide: An interfacial interaction perspective from first-principles calculations. 2012 , 86,	75
1377	Infrared spectroscopy of hydrated naphthalene cluster anions. 2012 , 137, 104303	8
1376	A transferable ab initio based force field for aqueous ions. 2012 , 136, 114507	54
1375	Geometrical frustration of an argon monolayer adsorbed on the MgO (100) surface: An accurate periodic ab initio study. 2012 , 86,	30
1374	Novel C,N-chelate rhodium(III) and iridium(III) antitumor complexes incorporating a lipophilic steroidal conjugate and their interaction with DNA. 2012 , 41, 12847-56	74
1373	Nonequilibrium thermodynamics of interacting tunneling transport: variational grand potential, density functional formulation and nature of steady-state forces. 2012 , 24, 424219	10
1372	Structure and stability of weakly chemisorbed ethene adsorbed on low-index Cu surfaces: performance of density functionals with van der Waals interactions. 2012 , 24, 424217	18
1371	A COMPARATIVE STUDY ON INTERMOLECULAR HYDROGEN BOND INTERACTIONS IN MOLECULAR DIMERS USING DIFFERENT LEVELS OF COMPUTATIONAL METHODS. 2012 , 11, 1237-1259	7
1370	C8-linked bulky guanosine DNA adducts: experimental and computational insights into adduct conformational preferences and resulting mutagenicity. 2012 , 4, 1981-2007	22
1369	Fitting properties from density functional theory based molecular dynamics simulations to parameterize a rigid water force field. 2012 , 136, 054103	11

1368	Designing Fullerene Separation Materials: A Theoretical Study. 2012 , 20, 72-84	1
1367	Theoretische Chemie 2011. 2012 , 60, 323-331	
1366	Dispersion-corrected density functional theory calculations of the molecular binding of n-alkanes on Pd(111) and PdO(101). 2012 , 136, 054702	56
1365	A new DFT functional based on spin-states and SN2 barriers. 2012 ,	
1364	CO2 capture by metal-organic frameworks with van der Waals density functionals. 2012 , 116, 4957-64	86
1363	NMR solution structure of rat all-16): toward understanding the mechanism of rats' resistance to Alzheimer's disease. 2012 , 102, 136-43	45
1362	Synthesis, characterization and sorption properties of NH2-MIL-47. 2012 , 14, 15562-70	25
1361	TD-DFT Assessment of Functionals for Optical 0-0 Transitions in Solvated Dyes. 2012 , 8, 2359-72	342
1360	The Econjugated P-flowers C16(PH)8 and C16(PF)8 are potential materials for organic n-type semiconductors. 2012 , 14, 14832-41	21
1359	Quantum mechanical study of sulfuric acid hydration: atmospheric implications. 2012 , 116, 2209-24	95
1358	Ion pair recognition receptor based on an unsymmetrically 1,1'-disubstituted ferrocene-triazole derivative. 2012 , 77, 10083-92	48
1357	Long-time correlations and hydrophobe-modified hydrogen-bonding dynamics in hydrophobic hydration. 2012 , 134, 9362-8	51
1356	Mechanism for translocation of fluoroquinolones across lipid membranes. 2012 , 1818, 2563-71	60
1355	Random-phase approximation and its applications in computational chemistry and materials science. 2012 , 47, 7447-7471	389
1354	Lithium Storage on Graphdiyne Predicted by DFT Calculations. 2012 , 116, 26222-26226	153
1353	Absolute configuration of atropisomeric polychlorinated biphenyl 183 enantiomerically enriched in human samples. 2012 , 116, 9340-6	24
1352	van der Waals Interaction Energies of Small Fragments of P, As, Sb, S, Se, and Te: Comparison of Complete Basis Set Limit CCSD(T) and DFT with Approximate Dispersion. 2012 , 8, 2301-9	5
1351	Advanced Corrections of Hydrogen Bonding and Dispersion for Semiempirical Quantum Mechanical Methods. 2012 , 8, 141-51	336

1350	Quantum Modeling of Water and Oxygen Adsorption on Beryllium Surface. 2012, 116, 4662-4670	8
1349	On the polarity of buckminsterfullerene with a water molecule inside. 2012 , 116, 12184-8	35
1348	Interaction between anions and substituted molecular bowls. 2012, 14, 104-12	22
1347	Adsorption studies of C6H6 on Cu (111), Ag (111), and Au (111) within dispersion corrected density functional theory. 2012 , 137, 134703	36
1346	Binding of noble metal clusters with rare gas atoms: theoretical investigation. 2012 , 116, 12510-7	35
1345	Attenuating Away the Errors in Inter- and Intramolecular Interactions from Second-Order Mller-Plesset Calculations in the Small Aug-cc-pVDZ Basis Set. 2012 , 3, 3592-8	31
1344	Theoretical and experimental investigations of circular dichroism and absolute configuration determination of chiral anthracene photodimers. 2012 , 134, 4990-7	68
1343	Elastic and Vibrational Properties of ∃and ₱bO 2012 , 116, 21514-21522	35
1342	Solvent effects on hydrogen bonds in Watson Trick, mismatched, and modified DNA base pairs. 2012 , 998, 57-63	25
1341	Mechanistic investigation of the ruthenium-N-heterocyclic-carbene-catalyzed amidation of amines with alcohols. 2012 , 18, 15683-92	59
1340	Ferric complexes of 3-hydroxy-4-pyridinones characterized by density functional theory and Raman and UV-vis spectroscopies. 2012 , 51, 4473-81	18
1339	Theoretical studies of reactions of carbon dioxide mediated and catalysed by transition metal complexes. 2012 , 48, 10808-28	98
1338	N-O bond cleavage mechanism(s) in nitrous oxide reductase. 2012 , 17, 687-98	23
1337	Theory of Ferrocenyl Compounds. 2012 ,	
1336	Theoretical prediction of selectivity in kinetic resolution of secondary alcohols catalyzed by chiral DMAP derivatives. 2012 , 134, 9390-9	76
1335	Density Functional Theory Investigation of the Contributions of B tacking and Hydrogen-Bonding Interactions to the Aggregation of Model Asphaltene Compounds. 2012 , 26, 2727-2735	81
1334	The DNA and RNA sugar-phosphate backbone emerges as the key player. An overview of quantum-chemical, structural biology and simulation studies. 2012 , 14, 15257-77	68
1333	DFT-D studies of single porphyrin molecule on doped boron silicon surfaces. 2012 , 13, 3945-51	13

1332	Modeling van der Waals Interactions in Zeolites with Periodic DFT: Physisorption of n-Alkanes in ZSM-22. 2012 , 142, 1057-1060	57
1331	Contribution to the Understanding of Tribological Properties of Graphite Intercalation Compounds with Metal Chloride. 2012 , 47, 367-379	4
1330	On the Performance of Local Density Approximation in Describing the Adsorption of Electron Donating/Accepting Molecules on Graphene. 2012 , 406, 78-85	32
1329	Mechanistic insight into the cyclohexene epoxidation with VO(acac)2 and tert-butyl hydroperoxide. 2012 , 294, 1-18	34
1328	6,6-Dicyanopentafulvenes: electronic structure and regioselectivity in [2 + 2] cycloaddition-retroelectrocyclization reactions. 2012 , 134, 18139-46	45
1327	Differences in the Activation Processes of Phosphine-Containing and GrubbsHoveyda-Type Alkene Metathesis Catalysts. 2012 , 31, 4203-4215	77
1326	Prediction of CO2 Adsorption Properties in Zeolites Using Force Fields Derived from Periodic Dispersion-Corrected DFT Calculations. 2012 , 116, 10692-10701	107
1325	Poly-proline-based chiral stationary phases: a molecular dynamics study of triproline, tetraproline, pentaproline and hexaproline interfaces. 2012 , 1265, 70-87	13
1324	Assessment of the performance of MP2 and MP2 variants for the treatment of noncovalent interactions. 2012 , 116, 4159-69	101
1323	3D-RISM-KH molecular theory of solvation and density functional theory investigation of the role of water in the aggregation of model asphaltenes. 2012 , 14, 3922-34	33
1322	Mechanistic investigation of the iridium-catalysed alkylation of amines with alcohols. 2012 , 10, 2569-77	60
1321	Electrochemical properties of crystallized dilithium squarate: insight from dispersion-corrected density functional theory. 2012 , 14, 11398-412	22
1320	The stability of the acetic acid dimer in microhydrated environments and in aqueous solution. 2012 , 14, 4162-70	14
1319	Functionalized corannulene cations: a detailed theoretical survey. 2012 , 14, 3554-67	26
1318	Evaluating London Dispersion Interactions in DFT: A Nonlocal Anisotropic Buckingham-Hirshfeld Model. 2012 , 8, 125-34	17
1317	Ab initio calculation of the crystalline structure and IR spectrum of polymers: nylon 6 polymorphs. 2012 , 116, 8299-311	44
1316	Migration and chemical reaction of H+ in protonated 专家 alactose. 2012 , 14, 13522-6	3
1315	Interaction and reaction of the hydroxyl ion with �D-galactose and its hydrated complex: an ab initio molecular dynamics study. 2012 , 14, 12086-9	4

1314	DFT investigation of NH3 physisorption on CuSO4 impregnated SiO2. 2012 , 14, 6617-27	10
1313	Formation of a supramolecular chromophore: a spectroscopic and theoretical study. 2012 , 8, 66-69	57
1312	Deoxygenation of carbon dioxide by electrophilic terminal phosphinidene complexes. 2012 , 3, 3526	22
1311	The interaction of His337 with the Mn4Ca cluster of photosystem II. 2012 , 14, 4651-7	31
1310	The bulk and the gas phase of 1-ethyl-3-methylimidazolium ethylsulfate: dispersion interaction makes the difference. 2012 , 14, 12079-82	37
1309	Reaction dynamics at a metal surface; halogenation of Cu(110). 2012 , 157, 337-53; discussion 375-98	27
1308	New results for the formation of a muoniated radical in the Mu + Br2 system: a van der Waals complex or evidence for vibrational bonding in Br-Mu-Br?. 2012 , 14, 10953-66	17
1307	Oxygen activation in extradiol catecholate dioxygenases 🗈 density functional study. 2012 , 3, 1600	55
1306	Localized reaction at a smooth metal surface: p-diiodobenzene at Cu(110). 2012 , 134, 9320-6	37
1305	Buckyplates and buckybowls: examining the effects of curvature on Interactions. 2012, 116, 11920-6	56
1305	Buckyplates and buckybowls: examining the effects of curvature on Einteractions. 2012, 116, 11920-6 Structural and vibrational properties of EMoO3 from van der Waals corrected density functional theory calculations. 2012, 85,	56 4 ²
1304	Structural and vibrational properties of #MoO3 from van der Waals corrected density functional	
1304	Structural and vibrational properties of \(\frac{1}{2}MoO3 \) from van der Waals corrected density functional theory calculations. 2012 , 85,	42
1304	Structural and vibrational properties of EMoO3 from van der Waals corrected density functional theory calculations. 2012, 85, Theoretical and experimental studies on circular dichroism of carbo[n]helicenes. 2012, 116, 7372-85 Molecular Tweezers in Host@uest Complexes: A Computational Study through a DFT-D Approach.	4 ²
1304 1303 1302	Structural and vibrational properties of <code>BMoO3</code> from van der Waals corrected density functional theory calculations. 2012, 85, Theoretical and experimental studies on circular dichroism of carbo[n]helicenes. 2012, 116, 7372-85 Molecular Tweezers in Host@uest Complexes: A Computational Study through a DFT-D Approach. 2012, 116, 23067-23074 Accurate Intermolecular Interactions at Dramatically Reduced Cost: XPol+SAPT with Empirical	4 ² 175 7
1304 1303 1302	Structural and vibrational properties of £MoO3 from van der Waals corrected density functional theory calculations. 2012, 85, Theoretical and experimental studies on circular dichroism of carbo[n]helicenes. 2012, 116, 7372-85 Molecular Tweezers in Host@uest Complexes: A Computational Study through a DFT-D Approach. 2012, 116, 23067-23074 Accurate Intermolecular Interactions at Dramatically Reduced Cost: XPol+SAPT with Empirical Dispersion. 2012, 3, 3241-3248 Synthesis, Structural Characterization, and Sensing Properties of Clickable Unsymmetrical	4 ² 175 7 49
1304 1303 1302 1301	Structural and vibrational properties of EMoO3 from van der Waals corrected density functional theory calculations. 2012, 85, Theoretical and experimental studies on circular dichroism of carbo[n]helicenes. 2012, 116, 7372-85 Molecular Tweezers in Host@uest Complexes: A Computational Study through a DFT-D Approach. 2012, 116, 23067-23074 Accurate Intermolecular Interactions at Dramatically Reduced Cost: XPol+SAPT with Empirical Dispersion. 2012, 3, 3241-3248 Synthesis, Structural Characterization, and Sensing Properties of Clickable Unsymmetrical 1,1?-Disubstituted Ferrocene@riazole Derivatives. 2012, 31, 2085-2096 Efficient Approach for the Computational Study of Alcohol and Nitrile Adsorption in H-ZSM-5. 2012,	42 175 7 49 50

1296	A quantitative study of the clustering of polycyclic aromatic hydrocarbons at high temperatures. 2012 , 14, 4081-94	117
1295	Synthesis and Application of Strong Brlisted Acids Generated from the Lewis Acid Al(ORF)3 and an Alcohol. 2012 , 31, 7485-7491	34
1294	Supramolecular ordering of PTCDA molecules: the key role of dispersion forces in an unusual transition from physisorbed into chemisorbed state. 2012 , 6, 8536-45	45
1293	CF3 P h Reductive Elimination from [(Xantphos)Pd(CF3)(Ph)]. 2012 , 31, 1315-1328	79
1292	DFT study with inclusion of the Grimme potential on anatase TiO2: structure, electronic, and vibrational analyses. 2012 , 116, 11731-5	27
1291	A benchmark for non-covalent interactions in solids. 2012 , 137, 054103	260
1290	Study of Alkylthiolate Self-assembled Monolayers on Au(111) Using a Semilocal meta-GGA Density Functional. 2012 , 116, 7374-7379	41
1289	Absolute configuration of a cyclic dipeptide reflected in vibrational optical activity: ab initio and experimental investigation. 2012 , 116, 2554-63	24
1288	Far/Mid-Infrared Signatures of SolventBolute Interactions in a Microhydrated Model Peptide Chain. 2012 , 3, 3307-3311	22
1287	Physisorption of nucleobases on graphene: a comparative van der Waals study. 2012 , 24, 424210	72
1286	Bottom-up view of water network-mediated CO2 reduction using cryogenic cluster ion spectroscopy and direct dynamics simulations. 2012 , 116, 903-12	18
1285	Single electron transfer-mediated selective endo- and exocyclic bond cleavage processes in azaphosphiridine chromium(0) complexes: a computational study. 2012 , 51, 7250-6	22
1284	Solvent-driven reductive activation of carbon dioxide by gold anions. 2012 , 134, 18804-8	73
1283	Buildup and decay of the optical absorption in the ultrafast photo-generation and reaction of benzhydryl cations in solution. 2012 , 116, 11064-74	24
1282	Predicting the coordination number within copper chaperones: Atox1 as case study. 2012 , 116, 4425-32	5
1281	Modified corrections for London forces in solid-state density functional theory calculations of structure and lattice dynamics of molecular crystals. 2012 , 116, 6927-34	24
1280	Computed and experimental chemical shift parameters for rigid and flexible YAF peptides in the solid state. 2012 , 116, 1974-83	27
1279	Characterization of the dispersion interactions and an ab initio study of van der Waals potential energy parameters for coinage metal clusters. 2012 , 116, 11685-93	10

1278	Nanostructured diamine-fullerene derivatives: computational density functional theory study and experimental evidence for their formation via gas-phase functionalization. 2012 , 116, 1663-76	14
1277	Hydration of the bisulfate ion: atmospheric implications. 2012 , 116, 5151-63	55
1276	Experimental fingerprints for redox-active terpyridine in $[Cr(tpy)2](PF6)n$ (n = 3-0), and the remarkable electronic structure of $[Cr(tpy)2]1$ 2012 , 51, 3718-32	104
1275	Tail effect on trihydroxysilanes dimerization: A dispersion-corrected density functional theory study. 2012 , 606, 7-11	2
1274	NMR Analyses and Diffusion Coefficient Determination of Minor Constituents of Olive Oil: Combined Experimental and Theoretical Studies. 2012 , 57, 2619-2624	21
1273	Energy and geometry of cooperative hydrogen bonds in p-substituted calix[n]- and thiacalix[n]arenes: a quantum-chemical approach. 2012 , 116, 546-59	5
1272	Atomic C 6 dispersion coefficients: a four-component relativistic KohnBham study. 2012 , 110, 2535-2541	13
1271	Substituent effects on axle binding in amide pseudorotaxanes: comparison of NMR titration and ITC data with DFT calculations. 2012 , 10, 5954-64	22
1270	A Density Functional with Spherical Atom Dispersion Terms. 2012 , 8, 4989-5007	324
1269	Hydrogen-bonding networks from first-principles: exploring the guanidine crystal. 2012 , 116, 4551-9	29
1268	A benchmark comparison of Induction and Induction in the dimers of naphthalene and decalin, and coronene and perhydrocoronene. 2012 , 134, 17520-5	70
1267	Assessment of ten DFT methods in predicting structures of sheet silicates: importance of dispersion corrections. 2012 , 137, 114105	92
1266	Self-consistent addition of an atomic charge dependent hydrogen-bonding correction function. 2012 , 984, 9-12	3
1265	Thioformyl chloride dimer: An excellent model system for the assessment of new computational methods. 2012 , 983, 83-87	2
1264	Could 2,6-bis((E)-2-(furan-2-yl)vinyl)-1-methylpyridinium iodide and analog compounds intercalate DNA? A first principle prediction based on structural and electronic properties. 2012 , 985, 8-13	17
1263	Adsorption of methane on carbon models of coal surface studied by the density functional theory including dispersion correction (DFT-D3). 2012 , 992, 37-47	43
1262	Assessment of density functionals on intramolecular dispersion interaction in large normal alkanes. 2012 , 541, 7-11	17
1261	FTIR and DFT-D investigation of the structure of ruthenium pentacarbonyl in small alcohol solvents. 2012 , 543, 86-91	1

1260	Charge density studies on [(NO)Fe(S2C6H4)2][PPN] and [(NO)3Fe(S2C6H4)3] complexes. 2012 , 15, 237-249	7
1259	Substitution reactions in dinuclear Ru-Hbpp complexes: an evaluation of through-space interactions. 2012 , 51, 1889-901	21
1258	Perspective: Advances and challenges in treating van der Waals dispersion forces in density functional theory. 2012 , 137, 120901	813
1257	Exocyclic bond cleavage in oxaphosphirane complexes?. 2012 , 18, 13405-11	16
1256	Accurate Hydrogen Positions in Organic Crystals: Assessing a Quantum-Chemical Aide. 2012 , 12, 1014-1021	66
1255	A high level computational study of the CH4/CF4 dimer: how does it compare with the CH4/CH4 and CF4/CF4 dimers?. 2012 , 110, 377-387	18
1254	The accuracy of DFT-optimized geometries of functional transition metal compounds: a validation study of catalysts for olefin metathesis and other reactions in the homogeneous phase. 2012 , 41, 5526-41	346
1253	Water structure and charge transfer phenomena at the liquid-graphene interface. 2012 , 14, 14605-10	17
1252	Detection of mercury-TpT dinucleotide binding by Raman spectra: a computational study. 2012 , 116, 8313-20	17
1251	Theoretical Approaches to Ionic Liquids: From Past History to Future Directions. 2012 , 181-230	2
1250	A qualitative failure of B3LYP for textbook organic reactions. 2012 , 14, 7170-5	52
1249	Pentacoordinated Organoaluminum Complexes: A Computational Insight. 2012 , 31, 8498-8504	12
1248	Optical isotropy in structurally anisotropic halide scintillators: Ab initio study. 2012 , 86,	23
1247	ArylBurface Bonding: A Density Functional Theory (DFT) Simulation Approach. 2012, 37-52	2
1246	Carbon Nanotube Container: Complexes of C50H10 with Small Molecules. 2012 , 8, 4546-55	15
1245	Highly selective mercury(II) cations detection in mixed-aqueous media by a ferrocene-based fluorescent receptor. 2012 , 41, 4437-44	27
1244	Improved description of soft layered materials with van der Waals density functional theory. 2012 , 24, 424216	134
1243	Theoretical Methods for Supramolecular Chemistry. 2012 , 743-793	

1242	Density functional theory with fractional orbital occupations. 2012 , 136, 154104	99
1241	Combined theoretical and computational study of interstrand DNA guanine-guanine cross-linking by trans-[Pt(pyridine)2] derived from the photoactivated prodrug trans,trans,trans-[Pt(N3)2(OH)2(pyridine)2]. 2012 , 51, 6830-41	39
1240	Correction to DFT interaction energies by an empirical dispersion term valid for a range of intermolecular distances. 2012 , 14, 3414-24	8
1239	Stepwise Diels-Alder: more than just an oddity? A computational mechanistic study. 2012 , 77, 6563-73	45
1238	Quantum Chemistry Methods. 2012 , 1119-1145	2
1237	Exploring structural and optical properties of fluorescent proteins by squeezing: modeling high-pressure effects on the mStrawberry and mCherry red fluorescent proteins. 2012 , 116, 12426-40	26
1236	Can Aromatic Eclouds Complex Divalent Germanium and Tin Compounds? A DFT Study. 2012, 31, 1605-1617	24
1235	Ab initio molecular dynamics study of water at constant pressure using converged basis sets and empirical dispersion corrections. 2012 , 137, 044506	73
1234	The performance of density functional based methods in the description of selected biological systems and processes. 2012 , 14, 14943-53	27
1233	Structural, electronic and ferroelectric properties of croconic acid crystal: a DFT study. 2012 , 14, 14673-81	35
1233	Structural, electronic and ferroelectric properties of croconic acid crystal: a DFT study. 2012 , 14, 14673-81 Hybrid dynamics simulation engine for metalloproteins. 2012 , 103, 767-76	22
1232	Hybrid dynamics simulation engine for metalloproteins. 2012 , 103, 767-76 COSMO-DFTr study of cellulose fragments: Structural features, relative energy, and hydration	22
1232	Hybrid dynamics simulation engine for metalloproteins. 2012 , 103, 767-76 COSMO-DFTr study of cellulose fragments: Structural features, relative energy, and hydration energies. 2012 , 999, 138-151 2,4-Diazido-5-iodo-pyrimidine crystal under high pressure: A comparison of DFT and DFT-D studies.	22
1232 1231 1230	Hybrid dynamics simulation engine for metalloproteins. 2012 , 103, 767-76 COSMO-DFTr study of cellulose fragments: Structural features, relative energy, and hydration energies. 2012 , 999, 138-151 2,4-Diazido-5-iodo-pyrimidine crystal under high pressure: A comparison of DFT and DFT-D studies. 2012 , 1000, 60-69 Density functional investigation of the electronic properties of B80 fullerene exposed to	7 8
1232 1231 1230	Hybrid dynamics simulation engine for metalloproteins. 2012, 103, 767-76 COSMO-DFTr study of cellulose fragments: Structural features, relative energy, and hydration energies. 2012, 999, 138-151 2,4-Diazido-5-iodo-pyrimidine crystal under high pressure: A comparison of DFT and DFT-D studies. 2012, 1000, 60-69 Density functional investigation of the electronic properties of B80 fullerene exposed to regioselective chemisorption of nucleophiles NH3, PH3 and AsH3. 2012, 52, 861-871 Physisorption, Diffusion, and Chemisorption Pathways of H2 Molecule on Graphene and on (2,2)	22 7 8
1232 1231 1230 1229	Hybrid dynamics simulation engine for metalloproteins. 2012, 103, 767-76 COSMO-DFTr study of cellulose fragments: Structural features, relative energy, and hydration energies. 2012, 999, 138-151 2,4-Diazido-5-iodo-pyrimidine crystal under high pressure: A comparison of DFT and DFT-D studies. 2012, 1000, 60-69 Density functional investigation of the electronic properties of B80 fullerene exposed to regioselective chemisorption of nucleophiles NH3, PH3 and AsH3. 2012, 52, 861-871 Physisorption, Diffusion, and Chemisorption Pathways of H2 Molecule on Graphene and on (2,2) Carbon Nanotube by First Principles Calculations. 2012, 8, 1288-94 Metal ion binding with carbon nanotubes and graphene: Effect of chirality and curvature. 2012,	22 7 8 8

1224	The significance of the alkene size and the nature of the metal ion in metal-alkene complexes: a theoretical study. 2012 , 41, 4965-75	38
1223	Uncovering molecular secrets of ionic liquids. 1-24	9
1222	Van der Waals interactions in solids using the exchange-hole dipole moment model. 2012 , 136, 174109	154
1221	Highlights on Anthocyanin Pigmentation and Copigmentation: A Matter of Flavonoid Estacking Complexation To Be Described by DFT-D. 2012 , 8, 2034-43	58
122 0	Predictions of Gibbs free energies for the adsorption of polyaromatic and nitroaromatic environmental contaminants on carbonaceous materials: efficient computational approach. 2012 , 28, 13307-17	18
1219	How Many Ligands Can Be Bound by Magnesium-Porphyrin? A Symmetry-Adapted Perturbation Theory Study. 2012 , 8, 2972-82	17
1218	The effect of side-chain length on the solid-state structure and optoelectronic properties of fluorene-alt-benzothiadiazole based conjugated polymersa DFT study. 2012 , 116, 10597-606	18
1217	Structural evolution of amino acid crystals under stress from a non-empirical density functional. 2012 , 24, 424209	48
1216	Combined Density Functional Theory and Monte Carlo Analysis of Monomolecular Cracking of Light Alkanes Over H-ZSM-5. 2012 , 116, 23408-23417	50
1215	Influence of Acid Strength and Confinement Effect on the Ethylene Dimerization Reaction over Solid Acid Catalysts: A Theoretical Calculation Study. 2012 , 116, 12687-12695	79
1214	Multichannel recognition of hydrogen sulphate anion by a Zn(II)EriazoleByridine complex bearing a ferrocenyl pendant. 2012 , 24, 826-832	7
1213	Shock Hugoniot calculations of polymers using quantum mechanics and molecular dynamics. 2012 , 137, 204901	30
1212	A Multilevel Strategy for the Exploration of the Conformational Flexibility of Small Molecules. 2012 , 8, 1808-19	32
1211	Oxo vs Imido Alkylidene d0-Metal Species: How and Why Do They Differ in Structure, Activity, and Efficiency in Alkene Metathesis?. 2012 , 31, 6812-6822	77
121 0	MOLECULAR BIOLOGY AT THE QUANTUM LEVEL: CAN MODERN DENSITY FUNCTIONAL THEORY FORGE THE PATH?. 2012 , 02, 1230006	7
1209	Wetting and interfacial properties of water nanodroplets in contact with graphene and monolayer boron-nitride sheets. 2012 , 6, 2401-9	193
1208	Computational studies of protonated �D-galactose and its hydrated complex: structures, interactions, proton transfer dynamics, and spectroscopy. 2012 , 116, 4851-9	15
1207	Bridging Static and Dynamical Descriptions of Chemical Reactions: An ab Initio Study of CO2 Interacting with Water Molecules. 2012 , 8, 4029-39	39

(2012-2012)

1206	Density Functional Theory of Bose E linstein Condensation: Road to Chemical Bonding Quantum Condensate. 2012 , 1-49	13
1205	The Cobalt-Methyl Bond Dissociation in Methylcobalamin: New Benchmark Analysis Based on Density Functional Theory and Completely Renormalized Coupled-Cluster Calculations. 2012 , 8, 1870-94	78
1204	A Hierarchy of Methods for the Energetically Accurate Modeling of Isomerism in Monosaccharides. 2012 , 8, 2630-45	49
1203	Wavefunction-based electron correlation methods for solids. 2012 , 14, 7605-14	7 2
1202	Multiscale Molecular Methods in Applied Chemistry. 2012,	33
1201	A first principles molecular dynamics study of the solvation structure and migration kinetics of an excess proton and a hydroxide ion in binary water-ammonia mixtures. 2012 , 136, 114509	6
1200	Investigating inclusion complexes using quantum chemical methods. 2012, 41, 3119-28	58
1199	Feasibility of Single-Walled Carbon Nanotubes as Materials for CO2 Adsorption: A DFT Study. 2012 , 116, 21083-21092	26
1198	Theoretical study on steric effects of DNA phosphorothioation: B-helical destabilization in Rp-phosphorothioated DNA. 2012 , 116, 10639-48	15
1197	An Efficient Method to Evaluate Intermolecular Interaction Energies in Large Systems Using Overlapping Multicenter ONIOM and the Fragment Molecular Orbital Method. 2012 , 3, 2604-2610	19
1196	Advancing Understanding and Design of Functional Materials Through Theoretical and Computational Chemical Physics. 2012 , 209-278	3
1195	Rationale for switching to nonlocal functionals in density functional theory. 2012 , 24, 424215	15
1194	Practical Aspects of Computational Chemistry II. 2012,	2
1193	Why urease is a di-nickel enzyme whereas the CcrA ∄actamase is a di-zinc enzyme. 2012 , 116, 10649-56	25
1192	Guanidinium in aqueous solution studied by quantum mechanical charge field-molecular dynamics (QMCF-MD). 2012 , 14, 7012-27	17
1191	Noncovalent Interactions in SIESTA Using the vdW-DF Functional: S22 Benchmark and Macrocyclic Structures. 2012 , 8, 281-9	25
1190	Quantum and classical dynamics simulations of ATP hydrolysis in solution. 2012 , 8, 2328-2335	39
1189	Controlling the local arrangements of Estacked polycyclic aromatic hydrocarbons through substituent effects. 2012 , 14, 6140	22

1188	First-principles kinetic modeling in heterogeneous catalysis: an industrial perspective on best-practice, gaps and needs. 2012 , 2, 2010	124
1187	In Silico Nanocatalysis with Transition Metal Particles: Where Are We Now?. 2012, 443-481	O
1186	Theoretical design of the biradical character in 1,3-diphosphacyclobutanediyl and homologous structures. 2012 , 14, 2015-23	22
1185	Van der Waals interactions between hydrocarbon molecules and zeolites: periodic calculations at different levels of theory, from density functional theory to the random phase approximation and Mller-Plesset perturbation theory. 2012 , 137, 114111	108
1184	Progress in modeling of ion effects at the vapor/water interface. 2012 , 63, 401-18	108
1183	Folded graphene nanoribbons with single and double closed edges. 2012 , 85,	13
1182	Stacking interactions between carbohydrate and protein quantified by combination of theoretical and experimental methods. 2012 , 7, e46032	45
1181	Extensions of DFTB to investigate molecular complexes and clusters. 2012 , 249, 245-258	29
1180	Properties of crystalline coronene: Dispersion forces leading to a larger van der Waals radius for carbon. 2012 , 249, 1438-1444	26
1179	Energy decomposition analysis. 2012 , 2, 43-62	499
1179 1178	Energy decomposition analysis. 2012, 2, 43-62 Can computational approaches aid in untangling the inherent complexity of practical organic photovoltaic systems?. 2012, 50, 1071-1089	499
• •	Can computational approaches aid in untangling the inherent complexity of practical organic	
1178	Can computational approaches aid in untangling the inherent complexity of practical organic photovoltaic systems?. 2012, 50, 1071-1089 Estimating stacking interaction energy using atom in molecules properties: Homodimers of benzene and pyridine. 2012, 112, 3008-3017 DFT modeling of band shifts and widths in the absorption spectrum of a	
1178	Can computational approaches aid in untangling the inherent complexity of practical organic photovoltaic systems?. 2012, 50, 1071-1089 Estimating stacking interaction energy using atom in molecules properties: Homodimers of benzene and pyridine. 2012, 112, 3008-3017 DFT modeling of band shifts and widths in the absorption spectrum of a 9-(diphenylamino)acridine/silica receptor center upon its interaction with gas-phase NH3, C2H5OH,	28
1178 1177 1176	Can computational approaches aid in untangling the inherent complexity of practical organic photovoltaic systems?. 2012, 50, 1071-1089 Estimating stacking interaction energy using atom in molecules properties: Homodimers of benzene and pyridine. 2012, 112, 3008-3017 DFT modeling of band shifts and widths in the absorption spectrum of a 9-(diphenylamino)acridine/silica receptor center upon its interaction with gas-phase NH3, C2H5OH, and (CH3)2CO molecules. 2012, 112, 3110-3118 Theoretical investigation of the Anti-Parkinson drug rasagiline and its salts: conformations and	28 7 2
1178 1177 1176 1175	Can computational approaches aid in untangling the inherent complexity of practical organic photovoltaic systems?. 2012, 50, 1071-1089 Estimating stacking interaction energy using atom in molecules properties: Homodimers of benzene and pyridine. 2012, 112, 3008-3017 DFT modeling of band shifts and widths in the absorption spectrum of a 9-(diphenylamino)acridine/silica receptor center upon its interaction with gas-phase NH3, C2H5OH, and (CH3)2CO molecules. 2012, 112, 3110-3118 Theoretical investigation of the Anti-Parkinson drug rasagiline and its salts: conformations and infrared spectra. 2012, 10, 395-406	28 7 2
1178 1177 1176 1175	Can computational approaches aid in untangling the inherent complexity of practical organic photovoltaic systems?. 2012, 50, 1071-1089 Estimating stacking interaction energy using atom in molecules properties: Homodimers of benzene and pyridine. 2012, 112, 3008-3017 DFT modeling of band shifts and widths in the absorption spectrum of a 9-(diphenylamino)acridine/silica receptor center upon its interaction with gas-phase NH3, C2H5OH, and (CH3)2CO molecules. 2012, 112, 3110-3118 Theoretical investigation of the Anti-Parkinson drug rasagiline and its salts: conformations and infrared spectra. 2012, 10, 395-406 Computational modelling of inorganic solids. 2012, 108, 449	28 7 2 1

1170	Molecular Tailoring: Reaction Path Control with Bulky Substituents. 2012 , 31, 3207-3212		26
1169	Amino acid analogues bind to carbon nanotube via Einteractions: comparison of molecular mechanical and quantum mechanical calculations. 2012 , 136, 025103		82
1168	Chapter 2:Transition Metal Systems. 2012 , 27-55		1
1167	Bonds or not bonds? Pancake bonding in 1,2,3,5-dithiadiazolyl and 1,2,3,5-diselenadiazolyl radical dimers and their derivatives. 2012 , 14, 10713-25		68
1166	Dispersion-Corrected Density Functional Theory and Classical Force Field Calculations of Water Loading on a Pyrophyllite(001) Surface. 2012 , 116, 17134-17141		36
1165	Revealing the true crystal structure of L-phenylalanine using solid-state density functional theory. 2012 , 14, 1113-6		28
1164	Including many-body effects in models for ionic liquids. 2012 , 131, 1		97
1163	Geometry, Electronic Structure, and Bonding in CuMCh2(M = Sb, Bi; Ch = S, Se): Alternative Solar Cell Absorber Materials?. 2012 , 116, 7334-7340		87
1162	Comparison of the electronic structure of different perylene-based dye-aggregates. <i>Journal of Computational Chemistry</i> , 2012 , 33, 1544-53	3.5	52
1161	Empirical van der Waals corrections to solid-state density functional theory: Iodine and phosphorous containing molecular crystals. <i>Journal of Computational Chemistry</i> , 2012 , 33, 1615-22	3.5	4
1160	Implementation of empirical dispersion corrections to density functional theory for periodic systems. <i>Journal of Computational Chemistry</i> , 2012 , 33, 2023-31	3.5	107
1159	Binding energies of five molecular pincers calculated by explicit and implicit solvent models. Journal of Computational Chemistry, 2012 , 33, 2310-7	3.5	12
1158	Accurate Computation of Structures and Strain Energies of Cyclophanes with Modern DFT Methods. 2012 , 52, 180-192		32
1157	Thermodynamics of chemical reactions with COSMO-RS: the extreme case of charge separation or recombination. <i>Journal of Computational Chemistry</i> , 2012 , 33, 1304-20	3.5	23
1156	Van der Waals interaction between P4 molecules: Density functional theory calculations with dispersion correction. 2012 , 60, 410-414		2
1155	Structural and electronic properties of bilayer and trilayer graphdiyne. 2012 , 4, 3990-6		114
1154	Universal Correction of Density Functional Theory to Include London Dispersion (up to Lr, Element 103). 2012 , 3, 360-3		41
1153	Origin of regioselectivity in \text{\text{\text{Humulene functionalization.}}} 2012, 77, 2865-9		18

1152	Water at hydrophobic interfaces delays proton surface-to-bulk transfer and provides a pathway for lateral proton diffusion. 2012 , 109, 9744-9	80
1151	Nanodiamonds in sugar rings: an experimental and theoretical investigation of cyclodextrin-nanodiamond inclusion complexes. 2012 , 10, 4524-30	42
1150	Development of Accurate DFT Methods for Computing Redox Potentials of Transition Metal Complexes: Results for Model Complexes and Application to Cytochrome P450. 2012 , 8, 442-59	58
1149	Comparing van der Waals Density Functionals for CO2 Adsorption in Metal Organic Frameworks. 2012 , 116, 16957-16968	63
1148	H2O-Aktivierung filden Wasserstoffatom-Transfer: korrekte Strukturen, revidierte Mechanismen. 2012 , 124, 3320-3324	22
1147	Experimentelle und theoretische Untersuchungen der Synthesen, spektroskopischen Daten und Reaktionen des Formylazids. 2012 , 124, 4796-4800	8
1146	H2O activation for hydrogen-atom transfer: correct structures and revised mechanisms. 2012 , 51, 3266-70	55
1145	Experimental and theoretical studies on the synthesis, spectroscopic data, and reactions of formyl azide. 2012 , 51, 4718-21	33
1144	Experimental and Computational Investigations of the Deactivation of H-ZSM-5 Zeolite by Coking in the Conversion of Ethanol into Hydrocarbons. 2012 , 4, 802-814	17
1143	Structure of sodiated polyglycines. 2012 , 18, 4583-92	22
1143	Structure of sodiated polyglycines. 2012 , 18, 4583-92 The role of pendant amines in the breaking and forming of molecular hydrogen catalyzed by nickel complexes. 2012 , 18, 6493-506	22 98
	The role of pendant amines in the breaking and forming of molecular hydrogen catalyzed by nickel	
1142	The role of pendant amines in the breaking and forming of molecular hydrogen catalyzed by nickel complexes. 2012 , 18, 6493-506 How is methane formed and oxidized reversibly when catalyzed by Ni-containing methyl-coenzyme	98
1142	The role of pendant amines in the breaking and forming of molecular hydrogen catalyzed by nickel complexes. 2012 , 18, 6493-506 How is methane formed and oxidized reversibly when catalyzed by Ni-containing methyl-coenzyme M reductase?. 2012 , 18, 6309-15 Silver and gold complexes with a new 1,10-phenanthroline analogue N-heterocyclic carbene: a	98
1142 1141 1140	The role of pendant amines in the breaking and forming of molecular hydrogen catalyzed by nickel complexes. 2012, 18, 6493-506 How is methane formed and oxidized reversibly when catalyzed by Ni-containing methyl-coenzyme M reductase?. 2012, 18, 6309-15 Silver and gold complexes with a new 1,10-phenanthroline analogue N-heterocyclic carbene: a combined structural, theoretical, and photophysical study. 2012, 18, 5506-9 Mechanism of the cycloaddition of carbon dioxide and epoxides catalyzed by cobalt-substituted	98 40 47
1142 1141 1140	The role of pendant amines in the breaking and forming of molecular hydrogen catalyzed by nickel complexes. 2012, 18, 6493-506 How is methane formed and oxidized reversibly when catalyzed by Ni-containing methyl-coenzyme M reductase?. 2012, 18, 6309-15 Silver and gold complexes with a new 1,10-phenanthroline analogue N-heterocyclic carbene: a combined structural, theoretical, and photophysical study. 2012, 18, 5506-9 Mechanism of the cycloaddition of carbon dioxide and epoxides catalyzed by cobalt-substituted 12-tungstenphosphate. 2012, 18, 9870-6 Synthesis, coupling, and condensation reactions of 1,2-diborylated benzenes: an experimental and	98 40 47 55
1142 1141 1140 1139 1138	The role of pendant amines in the breaking and forming of molecular hydrogen catalyzed by nickel complexes. 2012, 18, 6493-506 How is methane formed and oxidized reversibly when catalyzed by Ni-containing methyl-coenzyme M reductase?. 2012, 18, 6309-15 Silver and gold complexes with a new 1,10-phenanthroline analogue N-heterocyclic carbene: a combined structural, theoretical, and photophysical study. 2012, 18, 5506-9 Mechanism of the cycloaddition of carbon dioxide and epoxides catalyzed by cobalt-substituted 12-tungstenphosphate. 2012, 18, 9870-6 Synthesis, coupling, and condensation reactions of 1,2-diborylated benzenes: an experimental and quantum-chemical study. 2012, 18, 11284-95	98 40 47 55 45

1134	Force fields for studying the structure and dynamics of ionic liquids: a critical review of recent developments. 2012 , 13, 1625-37	218
1133	Intermolecular interactions in weak donor-acceptor complexes from symmetry-adapted perturbation and coupled-cluster theory: tetracyanoethylene-benzene and tetracyanoethylene-p-xylene. 2012 , 13, 2769-76	10
1132	Three types of induced tryptophan optical activity compared in model dipeptides: theory and experiment. 2012 , 13, 2748-60	15
1131	Counterion-Induced Inversion of Conformer Stability of a [5]Helquat Dication. 2012 , 77, 624-635	8
1130	Density Functional Theory Study of the Interaction of Hydrogen with Li6C60. 2012 , 3, 1084-8	46
1129	Vibrational Davydov Splittings and Collective Mode Polarizations in Oriented Organic Semiconductor Crystals. 2012 , 116, 14491-14503	22
1128	Intermolecular Interactions. 2012 , 157-193	5
1127	Weak Intermolecular Interactions: A Supermolecular Approach. 2012 , 443-466	9
1126	Computational Modeling of DNA and RNA Fragments. 2012 , 1257-1275	
1125	Assessment of density functional theory to calculate the phase transition pressure of ice. 2012 , 14, 11484-90	20
1124	Communication: Density functional theory overcomes the failure of predicting intermolecular interaction energies. 2012 , 136, 161102	56
1123	Structural and Energetic Landscape of Fluorinated 1,4-Phenylenediboronic Acids. 2012 , 12, 3720-3734	51
1122	Impact of neighboring chains on torsional defects in oligothiophenes. 2012 , 116, 2997-3003	23
1121	Noncovalent bicomponent self-assemblies on a silicon surface. 2012 , 6, 6905-11	42
1120	A (Nearly) Universally Applicable Method for Modeling Noncovalent Interactions Using B3LYP. 2012 , 3, 1738-44	99
1119	Atomistic theory and simulation of the morphology and structure of ionic nanoparticles. 2012 , 4, 1051-67	14
1118	Impact of DFT functionals on the predicted magnesium DNA interaction: an ONIOM study. 2012 , 131, 1	23
1117	Adsorption of successive layers of H2 molecules on a model copper surface: performances of second- to fifth-rung exchange-correlation functionals. 2012 , 131, 1	3

1116	Reductive activation of the heme iron-nitrosyl intermediate in the reaction mechanism of cytochrome c nitrite reductase: a theoretical study. 2012 , 17, 741-60		34
1115	Intermolecular potentials for simulations of collisions of SiNCS+ and (CH3)2SiNCS+ ions with fluorinated self-assembled monolayers. 2012 , 399, 193-204		7
1114	Physisorption of helium on a TiO2(110) surface: Periodic and finite cluster approaches. 2012 , 399, 272-2	180	10
1113	A first principles simulation study of fluctuations of hydrogen bonds and vibrational frequencies of water at liquidNapor interface. 2012 , 392, 96-104		34
1112	Wannier functions approach to van der Waals interactions in ABINIT. 2012 , 183, 480-485		5
1111	A DFT-D evaluation of the complexation of a molecular tweezer with small aromatic molecules. 2012 , 522, 11-16		16
1110	Seeking for reliable double-hybrid density functionals without fitting parameters: The PBE0-2 functional. 2012 , 538, 121-125		92
1109	A periodic hybrid DFT approach (including dispersion) to MgCl2-supported ZieglerNatta catalysts [] 1: TiCl4 adsorption on MgCl2 crystal surfaces. 2012 , 286, 103-110		90
1108	The chemical tuning of a weak zinc binding motif for histone deacetylase using electronic effects. 2012 , 80, 203-14		6
1107	Theoretical insight into the minor role of paring mechanism in the methanol-to-olefins conversion within HSAPO-34 catalyst. 2012 , 158, 264-271		41
1106	Li and Na Co-decorated carbon nitride nanotubes as promising new hydrogen storage media. 2012 , 376, 631-636		18
1105	Self assembly and chirality transfer in D-Alaninol on the Cu(100) surface. 2012 , 66, 1		2
1104	Assessment of a variety of dispersion-corrected density functional theory calculations used in molecular crystal structure prediction. 2012 , 4,		0
1103	Carboxylation of arene C-H bonds with CO2: a DFT-based approach to catalyst design. 2012 , 18, 170-7		55
1102	Interaction and protection mechanism between Li@C(60) and nucleic acid bases (NABs): performance of PM6-DH2 on noncovalent interaction of NABs-Li@C60. <i>Journal of Computational Chemistry</i> , 2012 , 33, 490-501	3.5	9
1101	Lennard-Jones parameters for small diameter carbon nanotubes and water for molecular mechanics simulations from van der Waals density functional calculations. <i>Journal of Computational Chemistry</i> , 2012 , 33, 652-8	3.5	28
1100	Dispersive interactions in water bilayers at metallic surfaces: a comparison of the PBE and RPBE functional including semiempirical dispersion corrections. <i>Journal of Computational Chemistry</i> , 2012 , 33, 695-701	3.5	119
1099	An automated approach for the parameterization of accurate intermolecular force-fields: pyridine as a case study. <i>Journal of Computational Chemistry</i> , 2012 , 33, 1055-67	3.5	39

1098 A DFT study of the interaction between microhydrated anions and naphthalendiimides. 2012 , 13, 570)-7 7
On the accuracy of DFT methods in reproducing ligand substitution energies for transition metal complexes in solution: the role of dispersive interactions. 2012 , 13, 562-9	53
Prediction of binding bond energy between phosphorous-based ionic liquids and CO2. Assessment of the CO2linion interactions. 2012 , 18, 143-150	12
1095 Electron correlation methods based on the random phase approximation. 2012 , 131, 1	315
1094 Intermolecular interactions in nitrogen-containing aromatic systems. 2012 , 131, 1	13
An improved theoretical approach to the empirical corrections of density functional theory. 2012 , 26, 199-213	2
Microsolvation effect and hydrogen-bonding pattern of taurine-water TA-(H2O)n (n = 1-3) complexes. 2012 , 18, 265-74	6
1091 Aromatic interactions as control elements in stereoselective organic reactions. 2013 , 46, 979-89	183
1090 Understanding substituent effects in noncovalent interactions involving aromatic rings. 2013 , 46, 102	29-38 383
Self-consistent field treatment and analytical energy gradient of local response dispersion method. 2013 , 113, 257-262	16
1088 A quantum chemistry study of DsPa unnatural DNA base pair. 2013, 113, 504-509	1
1087 The multiple roles of histidine in protein interactions. 2013 , 7, 44	230
1086 Improved DFT-based interpretation of ESI-MS of aqueous metal cations. 2013 , 24, 926-31	4
1085 Polymerization of polyanthrylene on a titanium dioxide (011)-(211) surface. 2013 , 52, 10300-3	48
1084 Hexagonal boron nitride on transition metal surfaces. 2013 , 132, 1	85
1083 Dispersion-corrected Rung 3.5 density functionals. 2013 , 132, 1	1
1082 Theoretical Insights into the Nature of Divalent Lanthanidelligand Interactions. 2013 , 32, 1265-1271	28
Theoretical Design of Econjugated Heteropolycyclic Compounds Containing a Tricoordinated Boron Center. 2013 , 117, 14999-15008	11

1080	Theoretical study of the oxidation of phenolates by the [Cu2O2(N,N'-di-tert-butylethylenediamine)2]2+ complex. 2013 , 19, 1942-54	18
1079	Characterization of graphenefullerene interactions: Insights from density functional theory. 2013 , 582, 115-118	20
1078	Effects of metal coordination on the Esystem of the 2,5-bis-{(pyrrolidino)-methyl}-pyrrole pincer ligand. 2013 , 52, 9539-48	22
1077	Evaluation of the Role of Water in the H2 Bond Formation by Ni(II)-Based Electrocatalysts. 2013 , 9, 3505-14	7
1076	Supramolecular ring structures of 7-methylguanine: a computational study of its self-assembly and anion binding. 2012 , 18, 225-35	3
1075	Error estimates for (semi-)empirical dispersion terms and large biomacromolecules. 2013, 11, 6515-9	8
1074	Effects of aromatic trifluoromethylation, fluorination, and methylation on intermolecular \blacksquare interactions. 2013 , 117, 7970-9	21
1073	Diferrocenylpyrylium salts and electron rich bispyran from oxidative coupling of ferrocenylpyran. Example of redox systems switched by proton transfer. 2013 , 37, 2066	11
1072	Many-body dispersion interactions from the exchange-hole dipole moment model. 2013 , 138, 054103	59
1071	LONG-RANGE VAN DER WAALS INTERACTION. 2013 , 27, 1330011	14
1070	The structures of two aldazines: [1,1'-(1E,1'E)-hydrazine-1,2-diylidenebis(methan-1-yl-1-ylidene)dinaphthalen-2-ol] (Lumogen) and 2,2'-(1E,1'E)-hydrazine-1,2-diylidenebis(methan-1-yl-1-ylidene)diphenol (salicylaldazine) in the solid	5
1069	Density-Functional Theory with Dispersion-Correcting Potentials for Methane: Bridging the Efficiency and Accuracy Gap between High-Level Wave Function and Classical Molecular Mechanics Methods. 2013 , 9, 3342-9	9
1068	Mechanistic investigation of the one-pot formation of amides by oxidative coupling of alcohols with amines in methanol. 2013 , 203, 211-216	16
1067	Supramolecular Cl???H and O???H interactions in self-assembled 1,5-dichloroanthraquinone layers on Au(111). 2013 , 14, 1177-81	18
		18
1066	on Au(111). 2013 , 14, 1177-81	
1066	on Au(111). 2013, 14, 1177-81 Analysis of supramolecular complex energetics in artificial replicators. 2013, 4, 3591	6

(2013-2013)

1062	Nonlocal van der Waals Approach Merged with Double-Hybrid Density Functionals: Toward the Accurate Treatment of Noncovalent Interactions. 2013 , 9, 3437-43	46
1061	Recent Progress in Density Functional Methodology for Biomolecular Modeling. 2013, 1-64	7
1060	Qualitative change of character of dispersive interaction with intermolecular distance. 2013 , 139, 044103	2
1059	Dynamics of supercritical methanol of varying density from first principles simulations: hydrogen bond fluctuations, vibrational spectral diffusion, and orientational relaxation. 2013 , 138, 224501	13
1058	From hydrogen bond donor to acceptor: the effect of ethanol fluorination on the first solvating water molecule. 2013 , 15, 16065-73	42
1057	A successive layer-by-layer assembly of supramolecular frameworks driven by a novel type of face-to-face III interactions. 2013 , 15, 7879	106
1056	Ultraviolet and infrared spectroscopy of neutral and ionic non-covalent diastereomeric complexes in the gas phase. 2013 , 24, 259-267	5
1055	Porous Graphene and Nanomeshes. 2013 , 129-151	1
1054	The study of performance of DFT functional for van der Waals interactions. 2013, 1004, 56-60	3
1053	Surface Functionalization of Graphene. 2013 , 233-253	2
1052	Thermal accommodation coefficients for laser-induced incandescence sizing of metal nanoparticles in monatomic gases. 2013 , 112, 409-420	26
1051	Ab initio prediction of proton NMR chemical shifts in imidazolium ionic liquids. 2013 , 117, 3186-97	54
1050	DFT study of the ExBox[aromatic hydrocarbon host-guest complex. 2013, 117, 8484-91	30
1049	Understanding the reactivity of Pd(0)/PR3-catalyzed intermolecular C(sp(3))-H bond arylation. 2013 , 135, 14206-14	71
1048	Ferrocenoyl phenylalanine: a new strategy toward supramolecular hydrogels with multistimuli responsive properties. 2013 , 135, 13379-86	175
1047	Theoretical Toolkits for Inorganic and Bioinorganic Complexes: Their Applications and Insights. 2013 , 1-57	1
1046	Adsorption in Metal-Organic Frameworks. 2013 , 989-1006	3
1045	Weak Hydrogen Bonding. 2013 , 341-357	

1044	Thorough theoretical search of conformations of neutral, protonated and deprotonated glutamine in gas phase. 2013 , 1020, 14-21		10
1043	Effects of local protein environment on the binding of diatomic molecules to heme in myoglobins. DFT and dispersion-corrected DFT studies. 2013 , 19, 3307-23		6
1042	Optically pure heterobimetallic helicates from self-assembly and click strategies. 2013 , 42, 14967-81		9
1041	Spin-component-scaled double hybrids: An extensive search for the best fifth-rung functionals blending DFT and perturbation theory. <i>Journal of Computational Chemistry</i> , 2013 , 34, 2327-44	3.5	200
1040	Quantum chemical studies on adsorption of CO2 on nitrogen-containing molecular segment models of coal. 2013 , 616, 85-92		28
1039	Concurrent loss of aromaticity and onset of superexchange in Mg3Na2 with an increasing NaMg3 distance. 2013 , 132, 1		5
1038	Contribution of van der Waals interactions to the adsorption energy of C2H2, C2H4, and C6H6 on Si(100). 2013 , 557, 159-162		10
1037	Dynamics of hydrogen bonds and vibrational spectral diffusion in liquid methanol from first principles simulations with dispersion corrected density functional. 2013 , 415, 1-7		15
1036	CO2 Adsorption on Cu2O(111): A DFT+U and DFT-D Study. 2013 , 117, 26048-26059		116
1035	Nicotinamide phosphoribosyltransferase inhibitors, design, preparation, and structure-activity relationship. 2013 , 56, 9071-88		26
1034	On the acceptor properties of a Al-Nacnac carbene analogue, a density functional investigation. 2013 , 744, 172-177		9
1033	Fast and accurate computational modeling of adsorption on graphene: a dispersion interaction challenge. 2013 , 15, 18815-21		56
1032	Theoretical study of the binding strength and magnetical response properties involved in the formation of the Edonor/Exceptor [TTFIBPQT]4+ hostiguest system. 2013 , 54, 119-122		4
1031	Structure and intermolecular vibrations of perylenel trans-1,2-dichloroethene, a weak charge-transfer complex. 2013 , 117, 10702-13		10
1030	Oxazoline-based organocatalyst for enantioselective strecker reactions: a protocol for the synthesis of levamisole. 2013 , 19, 14224-32		16
1029	Crystal structure and charge transport properties of poly(arylene-ethynylene) derivatives: a DFT approach. 2013 , 138, 154902		13
1028	Importance of dispersion in density functional calculations of cesium chloride and its related halides. 2013 , 88,		26
1027	Relationship between conformational dynamics and electron transfer in a desolvated peptide. Part I. Structures. 2013 , 117, 1746-55		5

(2013-2013)

1026	Ultraviolet degradation of procymidonestructural characterization by gas chromatography coupled with mass spectrometry and potential toxicity of photoproducts using in silico tests. 2013 , 27, 1505-16	12
1025	Incrementally Corrected Periodic Local MP2 Calculations: I. The Cohesive Energy of Molecular Crystals. 2013 , 9, 5590-8	40
1024	Bulk Liquid Water at Ambient Temperature and Pressure from MP2 Theory. 2013 , 4, 3753-3759	117
1023	A simple monomer-based model-Hamiltonian approach to combine excitonic coupling and Jahn-Teller theory. 2013 , 139, 174101	3
1022	Metal-dependent activity of Fe and Ni acireductone dioxygenases: how two electrons reroute the catalytic pathway. 2013 , 425, 3007-18	30
1021	Interaction of Pyridine Derivatives with a Gold (111) Surface as a Model for Adsorption to Large Nanoparticles. 2013 , 117, 4470-4479	36
1020	Adsorption of carbon dioxide on Al12X clusters studied by density functional theory: effect of charge and doping. 2013 , 117, 12519-28	9
1019	Structural and electronic properties of perylene from first principles calculations. 2013 , 138, 094509	30
1018	Easy methods to study the smart energetic TNT/CL-20 co-crystal. 2013 , 19, 4909-17	51
1017	A quantum chemical perspective on (6-4) photolesion repair by photolyases. 2013 , 15, 19957-69	22
1016	Binding of O2 and NO to heme in heme-nitric oxide/oxygen-binding (H-NOX) proteins. A theoretical study. 2013 , 117, 10103-14	16
1015	Hexamers and witchamers: Which hex do you choose?. 2013 , 1021, 70-83	13
1014	5-Aminotetrazole induces spin crossover in iron(III) pentadentate Schiff base complexes: experimental and theoretical investigations. 2013 , 42, 16279-88	13
1013	Liquid Methanol from DFT and DFT/MM Molecular Dynamics Simulations. 2013 , 9, 106-18	44
1012	DFT Study on the NMR Chemical Shifts of Molecules Confined in Carbon Nanotubes. 2013 , 117, 23418-23424	13
1011	IR spectroscopy of crystalline polymers from ab initio calculations: Nylon 6,6. 2013 , 66, 83-92	25
1010	Antioxidant properties of phenolic Schiff bases: structure-activity relationship and mechanism of action. 2013 , 27, 951-64	63
1009	Metaphenylene-based nitroxide diradicals: a protocol to calculate intermolecular coupling constant in a one-dimensional chain. 2013 , 117, 13151-60	8

1008 Understanding the defect chemistry of tin monoxide. 2013, 1, 8194

59

1007	Catalyzed Surface-Aligned Reaction, H(ad) + H2(ad) = H2(g) + H(ad) on Coinage Metals. 2013 , 13072200030300	01
1006	Placing Ag+ ion inside penta-indenocorannulene bowl. 2013 , 58, 47-52	7
1005	Ab initio study of elastic properties of super hard and graphitic structures of C3N4. 2013 , 69, 299-303	26
1004	Copper-chaperones with dicoordinated Cu(I)unique protection mechanism. 2013, 81, 1411-9	2
1003	First principles prediction of an insensitive high energy density material. 2013 , 15, 17681-8	16
1002	Vibrationally induced charge transfer in a bimolecular model complex in vacuo. 2013 , 138, 224301	2
1001	Computational Techniques. 2013 , 1-28	3
1000	Endohedral and exohedral complexes of substituted benzenes with carbon nanotubes and graphene. 2013 , 139, 094703	19
999	Temperature-dependent self-assembly of adenine derivative on HOPG. 2013 , 29, 10737-43	15
998	Improved Density Dependent Correction for the Description of London Dispersion Forces. 2013 , 9, 4293-9	138
997	A QM/MM refinement of an experimental DNA structure with metal-mediated base pairs. 2013 , 127, 203-10	63
996	Spin Crossover during ∰Hydride Elimination in High-Spin Iron(II) ဩnd Cobalt(II) ဩlkyl Complexes. 2013 , 32, 4741-4751	55
995	Quantum chemical challenges for the binding of simple alkanes to supramolecular hosts. 2013 , 117, 13409-17	23
994	Role of the Membrane Dipole Potential for Proton Transport in Gramicidin A Embedded in a DMPC Bilayer. 2013 , 9, 3826-31	12
993	Electronic structures of homoleptic [tris(2,2'-bipyridine)M]n complexes of the early transition metals ($M = Sc, Y, Ti, Zr, Hf, V, Nb, Ta; n = 1+, 0, 1-, 2-, 3-)$: an experimental and density functional theoretical study. 2013 , 52, 2242-56	47
992	Structures, stability, and growth sequence patterns of small homoclusters of naphthalene, anthracene, phenanthrene, phenalene, naphthacene, and pyrene. 2013 , 1021, 84-90	27
991	Contribution of the empirical dispersion correction on the conformation of short alanine peptides obtained by gas-phase QM calculations. 2013 , 91, 859-865	9

990	Predicting anisotropic displacement parameters using molecular dynamics: density functional theory plus dispersion modelling of thermal motion in benzophenone. 2013 , 46, 656-662	13
989	Bisactinyl halogenated complexes: relativistic density functional theory calculation and experimental synthesis. 2013 , 3, 1572-1582	8
988	Zigzag graphene nanoribbons with curved edges. 2013 , 3, 10014	6
987	Examining the formation of specific interactions between poly(3,4-ethylenedioxythiophene) and nucleotide bases. 2013 , 3, 2639	5
986	Effect of Geometry Optimizations on QM-Cluster and QM/MM Studies of Reaction Energies in Proteins. 2013 , 9, 4205-14	61
985	On the method-dependence of transition state asynchronicity in Diels-Alder reactions. 2013 , 15, 5108-14	67
984	Assessment of Kohn-Sham density functional theory and Mller-Plesset perturbation theory for ionic liquids. 2013 , 15, 13664-75	85
983	Synthesis and structures of tridentate	21
982	Weakly bound PTCDI and PTCDA dimers studied by using MP2 and DFT methods with dispersion correction. 2013 , 15, 13978-90	5
981	Electronic excitation and structural relaxation of the adenine dinucleotide in gas phase and solution. 2013 , 12, 1440-52	43
980	Theoretical study of amino derivatives and anticancer platinum drug grafted on various carbon nanostructures. 2013 , 139, 174704	11
979	Consistent descriptions of metalligand bonds and spin-crossover in inorganic chemistry. 2013 , 257, 196-209	153
978	A systematic approach to identify cooperatively bound homotrimers. 2013 , 117, 174-82	15
977	Aromatic Excimers: Ab Initio and TD-DFT Study. 2013 , 9, 847-56	45
976	IR, Raman and SERS spectra of propantheline bromide. 2013 , 103, 1-10	4
975	Triazolyl donor/acceptor chromophore decorated unnatural nucleosides and oligonucleotides with duplex stability comparable to that of a natural adenine/thymine pair. 2013 , 78, 278-91	25
974	Principles and applications of halogen bonding in medicinal chemistry and chemical biology. 2013 , 56, 1363-88	792
973	Analysis of the performance of DFT-D, M05-2X and M06-2X functionals for studying 🗹 interactions. 2013 , 557, 170-175	59

972	Hydration structure of salt solutions from ab initio molecular dynamics. 2013 , 138, 014501	128
971	The Fate of a Zwitterion in Water from ab Initio Molecular Dynamics: Monoethanolamine (MEA)-CO2. 2013 , 9, 28-32	43
970	Exo/endo Selectivity of the Ring-Closing Enyne Methathesis Catalyzed by Second Generation Ru-Based Catalysts. Influence of Reactant Substituents. 2013 , 3, 206-218	28
969	Self-assembly of N3-substituted xanthines in the solid state and at the solid-liquid interface. 2013 , 29, 7283-90	9
968	The application of quantum mechanics in structure-based drug design. 2013, 8, 263-76	53
967	The role of van der Waals forces in water adsorption on metals. 2013 , 138, 024708	155
966	Topology switching in [32]heptaphyrins controlled by solvent, protonation, and meso substituents. 2013 , 19, 1617-28	45
965	Polarized Molecular Orbital Model Chemistry 3. The PMO Method Extended to Organic Chemistry. 2013 , 9, 33-45	16
964	A Critical Assessment of Two-Body and Three-Body Interactions in Water. 2013 , 9, 1103-14	111
963	Zwitterions are the most stable form for neutral arginylglycine in gas phase: Clear theoretical evidence. 2013 , 1008, 96-102	9
962	New V(IV)-based metal-organic framework having framework flexibility and high CO2 adsorption capacity. 2013 , 52, 113-20	63
961	Intricacies of Describing Weak Interactions Involving Halogen Atoms within Density Functional Theory. 2013 , 9, 955-64	21
960	Formation of a Ph2PCH(BH3)P(BH3)Ph2 ligand via formal 1,2-borane migration. 2013, 49, 1121-3	12
959	Inelastic neutron scattering, Raman and DFT investigations of the adsorption of phenanthrenequinone on onion-like carbon. 2013 , 52, 150-157	12
958	Assessment of a Nonlocal Correction Scheme to Semilocal Density Functional Theory Methods. 2013 , 9, 273-83	24
957	Long-Range Corrected Hybrid Density Functionals with Improved Dispersion Corrections. 2013, 9, 263-72	321
956	Insight on the interaction of polychlorobiphenyl with nucleic acid-base. 2013 , 19, 581-8	3
955	Mechanism of AlcohollWater Separation in MetallDrganic Frameworks. 2013 , 117, 4124-4130	28

954	Spin-polarized semiconductors: tuning the electronic structure of graphene by introducing a regular pattern of sp3 carbons on the graphene plane. 2013 , 9, 306-11	9
953	Rhodium catalyzed hydroamination of C2H4 with NH3 with pincer derived PE(CH2CH2X)P ligands [] Fighting the energy span. 2013 , 748, 13-20	7
952	Supramolecular interactions of anthraquinone networks on Au(111): Hydrogen bonds and van der Waals interactions. 2013 , 268, 432-435	9
951	Fragmentation reactions of Si2Cl6+ in the gas phase quantum-chemical and mass-spectrometric assessment. 2013 , 354-355, 378-390	5
950	Silyl group migration in a P-silylated phosphonium ylide derived from dppm IA combined experimental and theoretical study. 2013 , 32, 28-31	6
949	Incipient chemical bond formation of Xe to a cationic silicon cluster: Vibrational spectroscopy and structure of the Si4Xe+ complex. 2013 , 557, 49-52	10
948	Modeling materials and processes in dye-sensitized solar cells: understanding the mechanism, improving the efficiency. 2014 , 352, 151-236	18
947	Adsorption of a single Pt atom on polyaromatic hydrocarbons from first-principle calculations. 2013 , 575, 76-80	8
946	Wogonin hosted @ tyclodextrin: Structural, electronic and nuclear studies. 2013, 188, 13-21	6
945	Photoelectrochemical properties of the CT1 dye: A DFT study. 2013 , 1046, 116-123	17
945	Photoelectrochemical properties of the CT1 dye: A DFT study. 2013, 1046, 116-123 Frequency dependence of the reorientational motion of OD bonds of deuterated methanol in liquid phase: A first principles molecular dynamics study. 2013, 182, 43-47	3
	Frequency dependence of the reorientational motion of OD bonds of deuterated methanol in	
944	Frequency dependence of the reorientational motion of OD bonds of deuterated methanol in liquid phase: A first principles molecular dynamics study. 2013 , 182, 43-47 Benchmark Study for the Cysteine-Histidine Proton Transfer Reaction in a Protein Environment:	3
944	Frequency dependence of the reorientational motion of OD bonds of deuterated methanol in liquid phase: A first principles molecular dynamics study. 2013 , 182, 43-47 Benchmark Study for the Cysteine-Histidine Proton Transfer Reaction in a Protein Environment: Gas Phase, COSMO, QM/MM Approaches. 2013 , 9, 1765-77 Zipping and unzipping of a paddlewheel metal-organic framework to enable two-step synthetic and	3
944 943 942	Frequency dependence of the reorientational motion of OD bonds of deuterated methanol in liquid phase: A first principles molecular dynamics study. 2013, 182, 43-47 Benchmark Study for the Cysteine-Histidine Proton Transfer Reaction in a Protein Environment: Gas Phase, COSMO, QM/MM Approaches. 2013, 9, 1765-77 Zipping and unzipping of a paddlewheel metal-organic framework to enable two-step synthetic and structural transformation. 2013, 19, 3552-7 Angular Distortions at Benzylic Carbons Due to Intramolecular Polarization-Induced Metal&rene	3 33 24
944 943 942 941	Frequency dependence of the reorientational motion of OD bonds of deuterated methanol in liquid phase: A first principles molecular dynamics study. 2013, 182, 43-47 Benchmark Study for the Cysteine-Histidine Proton Transfer Reaction in a Protein Environment: Gas Phase, COSMO, QM/MM Approaches. 2013, 9, 1765-77 Zipping and unzipping of a paddlewheel metal-organic framework to enable two-step synthetic and structural transformation. 2013, 19, 3552-7 Angular Distortions at Benzylic Carbons Due to Intramolecular Polarization-Induced Metal Arene Interactions: A Case Study with Open-Shell Chromium(II) NHC Complexes. 2013, 32, 1842-1850	3 33 24
944943942941940	Frequency dependence of the reorientational motion of OD bonds of deuterated methanol in liquid phase: A first principles molecular dynamics study. 2013, 182, 43-47 Benchmark Study for the Cysteine-Histidine Proton Transfer Reaction in a Protein Environment: Gas Phase, COSMO, QM/MM Approaches. 2013, 9, 1765-77 Zipping and unzipping of a paddlewheel metal-organic framework to enable two-step synthetic and structural transformation. 2013, 19, 3552-7 Angular Distortions at Benzylic Carbons Due to Intramolecular Polarization-Induced Metal Arene Interactions: A Case Study with Open-Shell Chromium(II) NHC Complexes. 2013, 32, 1842-1850 Density Functional Theory and Molecular Interactions: Dispersion Interactions. 2013, 65-96	3 33 24 13

936	Ab initio calculation of the IR spectrum of PTFE: helical symmetry and defects. 2013, 117, 706-18	53
935	Determination of absolute configuration and conformation of a cyclic dipeptide by NMR and chiral spectroscopic methods. 2013 , 117, 1721-36	47
934	Reliable approach for prediction of heats of formation of polycyclic saturated hydrocarbons using recently developed density functionals. 2013 , 1011, 30-36	17
933	Molecular architecture using novel types of non-covalent Enteractions involving aromatic neutrals, aromatic cations and Eanions. 2013 , 15, 1285	117
932	Insights into the reaction mechanism of methanol-to-olefins conversion in HSAPO-34 from first principles: Are olefins themselves the dominating hydrocarbon pool species?. 2013 , 301, 8-19	112
931	Photophysical properties of azaboradibenzo[6]helicene derivatives. 2013 , 1, 2354	22
930	Hydrogen-bonding effects on the reactivity of [X-Fe(III)-O-Fe(IV)?O] (X = OH, F) complexes toward C-H bond cleavage. 2013 , 52, 3976-84	28
929	Optimization of Crystal Structures of Archetypical Pharmaceutical Compounds: A Plane-Wave DFT-D Study Using Quantum Espresso. 2013 , 13, 2181-2189	20
928	Prediction of Water Adsorption in Copper-Based Metal Drganic Frameworks Using Force Fields Derived from Dispersion-Corrected DFT Calculations. 2013 , 117, 7519-7525	46
927	Intermolecular Interactions in Dye-Sensitized Solar Cells: A Computational Modeling Perspective. 2013 , 4, 956-74	71
926	Interactions of aromatic radicals with water. 2013 , 14, 805-11	18
925	Free radical scavenging by natural polyphenols: atom versus electron transfer. 2013 , 117, 2082-92	172
924	An ab initio approach to understanding the specific ion effect. 2013 , 160, 89-101; discussion 103-20	43
923	Torsional barriers of substituted biphenyls calculated using density functional theory: a benchmarking study. 2013 , 11, 2859-71	47
922	Silica surface features and their role in the adsorption of biomolecules: computational modeling and experiments. 2013 , 113, 4216-313	414
921	Hybrid improper ferroelectricity in a multiferroic and magnetoelectric metal-organic framework. 2013 , 25, 2284-90	246
920	On polymorphism of 2-(4-fluorophenylamino)-5-(2,4-dihydroxybenzeno)-1,3,4-thiadiazole (FABT) DMSO solvates. 2013 , 15, 1978	27
919	Toward a physically based quantitative modeling of impact sensitivities. 2013 , 117, 2253-9	36

918	Absorption of CO2 and CS2 into the Hofmann-type porous coordination polymer: electrostatic versus dispersion interactions. 2013 , 135, 4840-9	63
917	Halogen Bonds: Benchmarks and Theoretical Analysis. 2013 , 9, 1918-31	357
916	Theoretical Prediction of Spin-Crossover at the Molecular Level. 2013 , 443-454	5
915	Effective fragment potential method in Q-CHEM: a guide for users and developers. <i>Journal of Computational Chemistry</i> , 2013 , 34, 1060-70	44
914	Steric control in the Edimerization of oligothiophene radical cations annelated with bicyclo[2.2.2]octene units. 2013 , 19, 5457-67	36
913	New parameterization scheme of DFT-D for graphitic materials. 2013 , 117, 2844-53	12
912	Cross- versus homo-photocyclodimerization of anthracene and 2-anthracenecarboxylic acid mediated by a chiral hydrogen-bonding template. Factors controlling the cross-/homo-selectivity and enantioselectivity. 2013 , 78, 3073-85	17
911	Urea in aqueous solution studied by quantum mechanical charge field-molecular dynamics (QMCF-MD). 2013 , 9, 1864-76	9
910	Single-electron induces double-reaction by charge delocalization. 2013 , 135, 6220-5	33
909	New Cu(I)-ethylene complexes based on tridentate imine ligands: synthesis and structure. 2013 , 52, 3765-71	9
908	Regio- and stereocontrolled synthesis of oligostilbenoids: theoretical highlights at the supramolecular level. 2013 , 76, 538-46	13
907	A dispersion-corrected density-functional theory study of small molecules adsorbed in alkali-exchanged chabazites. 2013 , 228, 124-133	11
906	Assessment of density functionals for van der Waals complexes of sodium and benzene. 2013 , 111, 1211-1218	8 5
905	Q-Chem: an engine for innovation. 2013 , 3, 317-326	257
904	A molecular study of tetrakis(p-methoxyphenyl)porphyrin and its Zn(II) complex as discotic liquid crystals. 2013 , 113, 2287-2294	5
903	Noncovalent interactions of metal cations and arenes probed with thallium(I) complexes. 2013 , 52, 5749-56	14
903	Noncovalent interactions of metal cations and arenes probed with thallium(I) complexes. 2013 , 52, 5749-56 Bond energy decomposition analysis for subsystem density functional theory. 2013 , 138, 094113	14

900	A density-functional theory-based neural network potential for water clusters including van der Waals corrections. 2013 , 117, 7356-66	128
899	Liquid Structure and Cluster Formation in Ionic Liquid/Water Mixtures (An Extensive ab initio Molecular Dynamics Study on 1-Ethyl-3-Methylimidazolium Acetate/Water Mixtures (Part. 2013 , 227, 177-204	36
898	Conformational control in [22]- and [24]pentaphyrins(1.1.1.1.1) by meso substituents and their N-fusion reaction. 2013 , 78, 4419-31	25
897	Similarities and differences in the optical response of perylene-based hetero-bichromophores and their monomeric units. 2013 , 14, 1413-22	7
896	A relativistic DFT methodology for calculating the structures and NMR chemical shifts of octahedral platinum and iridium complexes. 2013 , 15, 7740-54	69
895	Theoretical and experimental study of lone pair interactions in THF/chloranilic acid system. 2013 , 24, 215-222	8
894	Benchmark quantum-chemical calculations on a complete set of rotameric families of the DNA sugar-phosphate backbone and their comparison with modern density functional theory. 2013 , 15, 7295-310	25
893	Performance of dispersion-corrected double hybrid density functional theory: a computational study of OCS-hydrocarbon van der Waals complexes. 2013 , 138, 164319	20
892	Short Estacking in N-Rich Ionic Aromatic Compounds. 2013, 13, 3255-3260	15
891	Accounting for van der Waals interactions between adsorbates and surfaces in density functional theory based calculations: selected examples. 2013 , 3, 13085	120
891 890		120 61
	theory based calculations: selected examples. 2013, 3, 13085 Efficient Methods for the Quantum Chemical Treatment of Protein Structures: The Effects of London-Dispersion and Basis-Set Incompleteness on Peptide and Water-Cluster Geometries. 2013,	
890	theory based calculations: selected examples. 2013, 3, 13085 Efficient Methods for the Quantum Chemical Treatment of Protein Structures: The Effects of London-Dispersion and Basis-Set Incompleteness on Peptide and Water-Cluster Geometries. 2013, 9, 3240-51	61
890 889	theory based calculations: selected examples. 2013, 3, 13085 Efficient Methods for the Quantum Chemical Treatment of Protein Structures: The Effects of London-Dispersion and Basis-Set Incompleteness on Peptide and Water-Cluster Geometries. 2013, 9, 3240-51 Polymorphism in cisplatin anticancer drug. 2013, 117, 6421-9 Complexes of 4-substituted phenolates with HF and HCN: energy decomposition and electronic	61
890 889 888	theory based calculations: selected examples. 2013, 3, 13085 Efficient Methods for the Quantum Chemical Treatment of Protein Structures: The Effects of London-Dispersion and Basis-Set Incompleteness on Peptide and Water-Cluster Geometries. 2013, 9, 3240-51 Polymorphism in cisplatin anticancer drug. 2013, 117, 6421-9 Complexes of 4-substituted phenolates with HF and HCN: energy decomposition and electronic structure analyses of hydrogen bonding. <i>Journal of Computational Chemistry</i> , 2013, 34, 696-705 Vibrational spectroscopy of bisulfate/sulfuric acid/water clusters: structure, stability, and infrared	61 27 8
890 889 888 887	Efficient Methods for the Quantum Chemical Treatment of Protein Structures: The Effects of London-Dispersion and Basis-Set Incompleteness on Peptide and Water-Cluster Geometries. 2013, 9, 3240-51 Polymorphism in cisplatin anticancer drug. 2013, 117, 6421-9 Complexes of 4-substituted phenolates with HF and HCN: energy decomposition and electronic structure analyses of hydrogen bonding. Journal of Computational Chemistry, 2013, 34, 696-705 Vibrational spectroscopy of bisulfate/sulfuric acid/water clusters: structure, stability, and infrared multiple-photon dissociation intensities. 2013, 117, 7081-90	61 27 8 49
890 889 888 887	Efficient Methods for the Quantum Chemical Treatment of Protein Structures: The Effects of London-Dispersion and Basis-Set Incompleteness on Peptide and Water-Cluster Geometries. 2013, 9, 3240-51 Polymorphism in cisplatin anticancer drug. 2013, 117, 6421-9 Complexes of 4-substituted phenolates with HF and HCN: energy decomposition and electronic structure analyses of hydrogen bonding. <i>Journal of Computational Chemistry</i> , 2013, 34, 696-705 Vibrational spectroscopy of bisulfate/sulfuric acid/water clusters: structure, stability, and infrared multiple-photon dissociation intensities. 2013, 117, 7081-90 Nonlocal van der Waals functionals: the case of rare-gas dimers and solids. 2013, 138, 204103 Analysis of an alternative to the H-atom abstraction mechanism in methane C-H bond activation by	61 27 8 49 37

882	Electronic Control of the Tip-Induced Hopping of an Hexaphenyl-Benzene Molecule Physisorbed on a Bare Si(100) Surface at 9 K. 2013 , 117, 13663-13675	13
881	Sampling of Transition States for Predicting Diastereoselectivity Using Automated Search Method-Aqueous Lanthanide-Catalyzed Mukaiyama Aldol Reaction. 2013 , 9, 2882-6	43
880	How to understand quantum chemical computations on DNA and RNA systems? A practical guide for non-specialists. 2013 , 64, 3-11	37
879	Crystal Structures and Density Functional Theory Calculations of o- and p-Nitroaniline Derivatives: Combined Effect of Hydrogen Bonding and Aromatic Interactions on Dimerization Energy. 2013 , 13, 3603-3612	15
878	Ab initio and classical molecular dynamics studies of the structural and dynamical behavior of water near a hydrophobic graphene sheet. 2013 , 138, 204702	53
877	Influence of Interface Structure on the Properties of ZnO/Graphene Composites: A Theoretical Study by Density Functional Theory Calculations. 2013 , 117, 10536-10544	66
876	Accurate metalligand bond energies in the IP-C2H4 and IP-C60 complexes of Pt(PH3)2, with application to their Bis(triphenylphosphine) analogues. 2013 , 111, 1599-1611	7
875	Interplay between Supramolecularity and Substrate Symmetry in the Dehydrogenation of d-Alaninol on Cu(100) and Cu(110) Surfaces. 2013 , 117, 10545-10551	6
874	Estacking effects on the EPR parameters of a prototypical DNA spin label. 2013, 15, 10466-71	2
873	Mechanistic dichotomy in the asymmetric allylation of aldehydes with allyltrichlorosilanes catalyzed by chiral pyridine N-oxides. 2013 , 19, 9167-85	29
872	The effects of PII changes on intermolecular interactions in crystal structure of iodoform. 2013 , 1041, 106-112	9
871	DFT studies of structure and vibrational spectra of 4-benzylidene-1-phenyl-2-selenomorpholino-1H-imidazol-5(4H)-one and its derivatives. 2013 , 110, 333-42	6
870	Pore Selectivity for Olefin Protonation Reactions Confined inside Mordenite Zeolite: A Theoretical Calculation Study. 2013 , 117, 2194-2202	35
869	Towards an understanding of the vibrational spectrum of the neutral Au7 cluster. 2013 , 15, 1929-43	9
868	A DFT study of gas molecules adsorption on the anatase (001) nanotube arrays. 2013, 67, 174-181	35
867	Factors that distort the heme structure in Heme-Nitric Oxide/OXygen-Binding (H-NOX) protein domains. A theoretical study. 2013 , 118, 28-38	3
866	Predicting the impact of functionalized ligands on CO2 adsorption in MOFs: A combined DFT and Grand Canonical Monte Carlo study. 2013 , 168, 225-238	40
865	Comparative study of friction properties for hydrogen- and fluorine-modified diamond surfaces: A first-principles investigation. 2013 , 608, 74-79	24

864	Carbon monoxide adsorption on beryllium surfaces. 2013 , 608, 265-274	3
863	Evaluation of Approximate Exchange-Correlation Functionals in Predicting One-Bond (31)P-(1)H NMR Indirect Spin-Spin Coupling Constants. 2013 , 9, 1443-51	11
862	Theoretical study of structural, spectroscopic and reaction properties of trans-bis(imido) uranium(VI) complexes. 2013 , 52, 9143-52	9
861	Molecular Multistate Systems Formed in Two-Dimensional Porous Networks on Ag(111). 2013 , 117, 302-306	27
860	Binding interactions in dimers of phenalenyl and closed-shell analogues. 2013 , 117, 3642-9	33
859	Dispersion corrected double high-hybrid and gradient-corrected density functional theory study of light cation dihydrogen (M+ \mathbb{H} 2, where M = Li, Na, B and Al) van der Waals complexes. 2013 , 24, 549-558	13
858	Obtaining the lattice energy of the anthracene crystal by modern yet affordable first-principles methods. 2013 , 138, 204304	17
857	Stacking and hydrogen bond interactions between adenine and gallic acid. 2013 , 19, 5293-9	4
856	Water Adsorption at the Tetrahedral Titania Surface Layer of SrTiO(110)-(4 🗈). 2013 , 117, 26060-26069	29
855	Hydrostatic and [001] Uniaxial Pressure on Anatase TiO2 by Periodic B3LYP-D* Calculations. 2013 , 117, 7050-7061	19
854	Stochastic Search of Molecular Cluster Interaction Energy Surfaces with Coupled Cluster Quality Prediction. The Phenylacetylene Dimer. 2013 , 9, 3848-54	2
853	Enabling forbidden processes: quantum and solvation enhancement of nitrate anion UV absorption. 2013 , 117, 12868-77	27
852	Atom-Scale Reaction Pathways and Free-Energy Landscapes in Oxygen Plasma Etching of Graphene. 2013 , 4, 1592-6	27
851	Supramolecular organization of heptapyrenotide oligomersan in depth investigation by molecular dynamics simulations. 2013 , 117, 2576-85	8
850	Hierarchical simulations of hybrid polymerBolid materials. 2013 , 9, 6696	56
849	Molecular-level computational studies of single wall carbon nanotubepolyethylene composites. 2013 , 69, 443-454	40
848	The Importance of Electron Correlation on Stacking Interaction of Adenine-Thymine Base-Pair Step in B-DNA: A Quantum Monte Carlo Study. 2013 , 9, 1081-6	24
847	The Performance of Density Functionals for Sulfate-Water Clusters. 2013 , 9, 1368-80	61

846	Conformational heterogeneity of methyl 4-hydroxycinnamate: a gas-phase UV-IR spectroscopic study. 2013 , 117, 4798-805	15
845	First-principles molecular dynamics simulation of atmospherically relevant anion solvation in supercooled water droplet. 2013 , 135, 15549-58	29
844	Examining the Accuracy of Density Functional Theory for Predicting the Thermodynamics of Water Incorporation into Minerals: The Hydrates of Calcium Carbonate. 2013 , 117, 17814-17823	33
843	Extension of the B3LYPdispersion-correcting potential approach to the accurate treatment of both inter- and intra-molecular interactions. 2013 , 132, 1	34
842	Linear and Hexagonal Porous Structures of an Organic Charge Acceptor Hexaaza-triphenylene-hexacarbonitrile on Au(111) with CNICN Dipolar Interactions. 2013 , 117, 21371-21375	5
841	DFT Studies of Pristine Hexagonal Ge1Sb2Te4(0001), Ge2Sb2Te5(0001), and Ge1Sb4Te7(0001) Surfaces. 2013 , 117, 15075-15089	27
840	Analysis of van der Waals density functional components: Binding and corrugation of benzene and C60 on boron nitride and graphene. 2013 , 87,	87
839	Atypical water lattices and their possible relevance to the amorphous ices: A density functional study. 2013 , 3, 042119	5
838	STM imagery and density functional calculations of C60 fullerene adsorption on the 6H-SiC(0001)-3B surface. 2013 , 87,	9
837	Shortcomings of the standard Lennard-Jones dispersion term in water models, studied with force matching. 2013 , 139, 184111	8
836	Full DFT-D description of a nanoporous supramolecular network on a silicon surface. 2013 , 138, 084704	11
835	Structure and energetics of benzene adsorbed on transition-metal surfaces: density-functional theory with van der Waals interactions including collective substrate response. 2013 , 15, 053046	129
834	Methanol Adsorption on Graphene. 2013 , 2013, 1-6	28
833	Exploring the Interaction between Lithium Ion and Defective Graphene Surface Using Dispersion Corrected DFT Studies. 2013 , 53, 23-32	6
832	Identification of intermediates in zeolite-catalyzed reactions by in situ UV/Vis microspectroscopy and a complementary set of molecular simulations. 2013 , 19, 16595-606	59
831	Dispersion corrections in graphenic systems: a simple and effective model of binding. 2013 , 25, 445010	27
830	Water dynamics: relation between hydrogen bond bifurcations, molecular jumps, local density & hydrophobicity. 2013 , 3, 2991	29
829	Theoretical aspects of hydrolysis of peptide bonds by zinc metalloenzymes. 2013 , 19, 16634-45	9

828	Theoretical study of the electronic excitations of free-base porphyrin-Ar2 van der Waals complexes. 2013 , 139, 074303	3
827	Strong anisotropy of momentum-relaxation time induced by intermolecular vibrations of single-crystal organic semiconductors. 2013 , 88,	25
826	Effects of a remote binding partner on the electric field and electric field gradient at an atom in a weakly bound trimer. 2013 , 139, 034320	3
825	Transport properties of individual C60-molecules. 2013 , 139, 234701	26
824	Systematic theoretical investigation of the phthalocyanine based dimer: MnPc⊞/F16CoPc□ 2013 , 87,	8
823	Electron-doped organics: Charge-disproportionate insulators and Hubbard-Frfilich metals. 2013 , 88,	15
822	B-DNA Structure and Stability as Function of Nucleic Acid Composition: Dispersion-Corrected DFT Study of Dinucleoside Monophosphate Single and Double Strands. 2013 , 2, 186-93	26
821	Harris-type van der Waals density functional scheme. 2013 , 88,	6
820	Edge and substrate-induced bandgap in zigzag graphene nanoribbons on the hexagonal nitride boron 8-ZGNR/h-BN(0001). 2013 , 3, 092105	18
819	Insights into the dynamics of evaporation and proton migration in protonated water clusters from large-scale Born-Oppenheimer direct dynamics. <i>Journal of Computational Chemistry</i> , 2013 , 34, 533-44	7
818	Molecular dynamics study of the pressure-dependent terahertz infrared absorption spectrum of \oplus and \oplus RDX. 2013 , 139, 044108	16
817	Density functional theory study of the interaction of vinyl radical, ethyne, and ethene with benzene, aimed to define an affordable computational level to investigate stability trends in large van der Waals complexes. 2013 , 139, 244306	8
816	The atomic scale structure of CXV carbon: wide-angle x-ray scattering and modeling studies. 2013 , 25, 454203	7
815	DFT study on the recovery of Hoveyda-grubbs-type catalyst precursors in enyne and diene ring-closing metathesis. 2013 , 19, 14553-65	25
814	Interaction of platinum nanoparticles with graphitic carbon structures: a computational study. 2013 , 14, 2984-9	33
813	Tuning of the Dienophilic Reactivity of Imidazo[1,2-a]pyridine: A Comparison of DFT and Dispersion-Corrected DFT Calculations. 2013 , 86, 57-66	1
812	Polymerization of Polyanthrylene on a Titanium Dioxide (011)-(21) Surface. 2013, 125, 10490-10493	12
811	Density Functional Theory with Modified Dispersion Correction for Metals Applied to Self-Assembled Monolayers of Thiols on Au(111). 2013 , 2013, 1-9	33

810	Stability Analysis and Frontier Orbital Study of Different Glycol and Water Complex. 2013, 2013, 1-16	12
809	Chemical Dynamics Simulations of the Hydroxyl Radical Reaction with Ethene. 2013, 26, 765-773	4
808	Theoretical study of the adsorption of benzene on coinage metals. 2014 , 10, 1775-84	46
807	Theoretical Simulations of Reactive and Nonreactive Scattering of Light Diatomic Molecules from Metal Surfaces: Past, Present, and Future. 2014 , 2014, 1-21	
806	Platinum(II) oxalato complexes involving adenosine-based N-donor ligands: synthesis, characterization and cytotoxicity evaluation. 2014 , 19, 3832-47	9
805	Computer Simulations of Prebiotic Systems. 2014,	5
804	. 2014,	4
803	Physical Nature of Fatty Acid Amide Hydrolase Interactions with Its Inhibitors: Testing a Simple Nonempirical Scoring Model. 2014 , 118, 14727-36	8
802	Promoting alkali and alkaline-earth metals on MgO for enhancing CO2 capture by first-principles calculations. 2014 , 16, 24818-23	28
801	DFT investigation on hydrogen bonding in cyclohexane-1,2,3,4,5-pentol crystal structure. 2014 , 55, 1596-1600	5 1
800	INTERLAYER INTERACTION AND SCREENING IN MoS2. 2014 , 21, 1450039	11
799	Role of size and shape selectivity in interaction between gold nanoclusters and imidazole: a theoretical study. 2014 , 20, 2534	17
798	Chalcogenide-Based Nanodevices for Renewable Energy. 2014 , 269-287	
797	Nature of Sigma-Type Lithium Bonding Interaction in Nanoscale. 2014 , 04, 1441020	
796	Graphene on Rh(111): Combined DFT, STM, and NC-AFM Studies. 2014, 93, 8-16	7
795	Functionalization of the pristine and stone-wales defected BC3 graphenes with pyrene. 2014 , 20, 2539	17
794	Analysis of SnS2 hyperdoped with V proposed as efficient absorber material. 2014 , 26, 395501	5
793	Color Tuning and Noteworthy Photoluminescence Quantum Yields in Crystalline Mono-/Dinuclear ZnII Complexes. 2014 , 2014, 5916-5924	27

792	Intermolecular Mand H/Interactions in dimers researched by different computational methods. 2014 , 13, 1450057	2
791	Contribution of phenylalanine side chain intercalation to the TATA-box binding protein-DNA interaction: molecular dynamics and dispersion-corrected density functional theory studies. 2014 , 20, 2499	14
790	Shared memory multiprocessing implementation of resolution-of-the-identity second-order MllerPlesset perturbation theory with attenuated and unattenuated results for intermolecular interactions between large molecules. 2014 , 112, 836-843	10
789	Hydration of chloride anions in the NanC Porin from Escherichia coli: a comparative study by QM/MM and MD simulations. 2014 , 141, 22D521	2
788	van der Waals density functionals built upon the electron-gas tradition: facing the challenge of competing interactions. 2014 , 140, 18A539	86
787	Structure and dynamics of oligonucleotides in the gas phase. 2015 , 54, 467-71	18
786	Comparison of van der Waals corrected and sparse-matter density functionals for the metal-free phthalocyanine/gold interface. 2014 , 89,	33
7 ⁸ 5	Adsorption of CO2, N2, and CH4 in Cs-exchanged chabazite: a combination of van der Waals density functional theory calculations and experiment study. 2014 , 140, 084705	31
784	AgAg dispersive interaction and physical properties of Ag3Co(CN)6. 2014 , 90,	24
783	How important is self-consistency for the dDsC density dependent dispersion correction?. 2014 , 140, 18A516	23
782	Recommending Hartree-Fock theory with London-dispersion and basis-set-superposition corrections for the optimization or quantum refinement of protein structures. 2014 , 118, 14612-26	46
781	Tunable ferroelectric polarization and its interplay with spin-orbit coupling in tin iodide perovskites. 2014 , 5, 5900	215
780	Non-covalent functionalization of single wall carbon nanotubes and graphene by a conjugated polymer. 2014 , 105, 013103	17
779	The individual and collective effects of exact exchange and dispersion interactions on the ab initio structure of liquid water. 2014 , 141, 084502	223
778	A comparative synthetic, magnetic and theoretical study of functional MIIIL ubane-type Co(II) and Ni(II) complexes. 2014 , 43, 7847-59	37
777	B-DNA structure and stability: the role of hydrogen bonding, Estacking interactions, twist-angle, and solvation. 2014 , 12, 4691-700	51
776	Dispersion-correcting potentials can significantly improve the bond dissociation enthalpies and noncovalent binding energies predicted by density-functional theory. 2014 , 140, 18A542	20
775	Evaluating interaction energies of weakly bonded systems using the Buckingham-Hirshfeld method. 2014 , 140, 184105	2

(2021-2014)

774	Intermolecular symmetry-adapted perturbation theory study of large organic complexes. 2014 , 141, 094107	69
773	Quantum mechanical force field for hydrogen fluoride with explicit electronic polarization. 2014 , 140, 204501	8
772	Terahertz spectroscopy and solid-state density functional theory calculation of anthracene: effect of dispersion force on the vibrational modes. 2014 , 140, 174509	35
771	Multiple reaction pathways operating in the mechanism of vinylogous Mannich-type reaction activated by a water molecule. 2014 , 9, 305-12	12
770	Excitonic effects in oxyhalide scintillating host compounds. 2014 , 116, 133510	6
769	Spin-State Energetics of FeII Complexes IThe Continuing Voyage Through the Density Functional Minefield. 2014 , 2014, 4573-4580	35
768	Assessment of a Cost-Effective Approach to the Calculation of Kinetic and Thermodynamic Properties of Methyl Methacrylate Homopolymerization: A Comprehensive Theoretical Study. 2014 , 10, 5668-76	16
767	Dispersion forces in chirality recognition - a density functional and wave function theory study of diols. 2021 , 23, 12093-12104	1
766	Atom-surface van der Waals potentials of topological insulators and semimetals from scattering measurements. 2021 , 23, 7637-7652	8
765	Potential Visible-Light Driven PtO//GaN vdW Hetero-Bilayer Photocatalysts for Water Splitting Using First-Principles. 2021 , 9, 109510-109521	3
764	Pairing double hybrid functionals with a tailored basis set for an accurate thermochemistry of hydrocarbons 2021 , 11, 26073-26082	1
763	Ti-Decorated B/N-doped graphene as a high-capacity hydrogen storage material: a DFT study. 2021 , 50, 11398-11411	O
762	Interlayer Exciton Transport in MoSe/WSe Heterostructures. 2021 , 15, 1539-1547	21
761	Al-Decorated C 24N 24 Fullerene: A Promising Single-Atom Catalyst for CO Oxidation.	
760	Reactivity of dicationic N-heterocyclic chalcogen carbene analogues with methane and ethene: a theoretical investigation. 2021 , 23, 2419-2429	О
759	Tunable electronic and optical properties of a BAs/As heterostructure by vertical strain and external electric field 2021 , 11, 21824-21831	1
758	-Aminobenzoic acid protonation dynamics in an evaporating droplet by molecular dynamics. 2021 , 23, 19659-19672	2
757	Interplay between Locally Excited and Charge Transfer States Governs the Photoswitching Mechanism in the Fluorescent Protein Dreiklang. 2021 , 125, 757-770	5

756	Spot the difference: hydrogen adsorption and dissociation on unsupported platinum and platinum-coated transition metal carbides. 2021 , 23, 20255-20267	3
755	Replacing hybrid density functional theory: motivation and recent advances. 2021 , 50, 8470-8495	23
754	Utilization of electron-beam irradiation under atomic-scale chemical mapping for evaluating the cycling performance of lithium transition metal oxide cathodes. 2021 , 9, 2429-2437	3
753	First-principles calculations of hybrid inorganic-organic interfaces: from state-of-the-art to best practice. 2021 , 23, 8132-8180	11
75 ²	Effects of Doped N, B, P, and S Atoms on Graphene toward Oxygen Evolution Reactions. 2021 , 6, 5368-5378	6
751	Oxidative detoxification of nerve agent VX simulant by polyoxoniobate: Experimental and theoretical insights. 2021 , 394, 83-93	2
75°	First-principles study of structure, electronic, and magnetic properties of C sites vacancy defects in water adsorbed graphene/MoS van der Waals heterostructures. 2021 , 27, 82	5
749	Splitting dioxygen over distant binuclear transition metal cationic sites in zeolites. Effect of the transition metal cation. 2021 , 121, e26611	3
748	Electrocatalytic hydrogen evolution on the noble metal-free MoS/carbon nanotube heterostructure: a theoretical study. 2021 , 11, 3958	6
747	Formation Mechanism of PFN Dipole Interlayer in Organic Solar Cells. 2021 , 5, 2000753	9
746	Effect of AlEt2Cl on the polymerization of isoprene using TiCl4/MgCl2 type Ziegler-Natta catalyst: A DFT study. 2021 , 502, 111399	
745	Enormous Valley Splitting in Monolayer WS2 by Coupling with an N-Terminated GaN Substrate. 2021 , 15, 2000493	O
744	Splitting Dioxygen over Distant Binuclear Fe Sites in Zeolites. Effect of the Local Arrangement and Framework Topology. 2021 , 11, 2340-2355	4
743	Describing adsorption of benzene, thiophene, and xenon on coinage metals by using the Zaremba-Kohn theory-based model. 2021 , 154, 124705	1
742	High-throughput screening of transition metal single-atom catalyst anchored on Janus MoSSe basal plane for hydrogen evolution reaction. 2021 , 46, 10337-10345	8
741	Transport properties of Na-decorated borophene under CO/CO2 adsorption. 2021 , 1197, 113159	5
740	Adsorption of Formaldehyde on ZnO(0001) Surface Doped with Cr and Cu: A Density Functional Theory Study. 2021 , 95, 630-635	
739	Au-decorated semiconducting AlN nanosheet as an electronic sensor for theophylline drug. 2021 , 47, 500-509	1

738	Adsorption and separation of hexane isomers in metal-organic frameworks (MOFs): A computational study. 2021 , 1197, 113164	2
737	Sensing properties of Al- and Si-doped HBC nanostructures toward Gamma-butyrolactone drug: A density functional theory study. 2021 , 1197, 113163	5
736	New Syntheses, Analytic Spin Hamiltonians, Structural and Computational Characterization for a Series of Tri-, Hexa- and Hepta-Nuclear Copper (II) Complexes with Prototypic Patterns. 2021 , 3, 411-439	0
735	Insignificant Effect of Temperature on the Structure and Angular Jumps of Water near a Hydrophobic Cation. 2021 , 6, 8356-8364	2
734	From Monolayers to Nanotubes: Toward Catalytic Transition-Metal Dichalcogenides for Hydrogen Evolution Reaction. 2021 , 35, 6282-6288	2
733	Defective BC2N as an Anode Material with Improved Performance for Lithium-Ion Batteries. 2021 , 125, 4946-4954	4
732	Theoretical Study on P-coordinated Metal Atoms Embedded in Arsenene for the Conversion of Nitrogen to Ammonia. 2021 , 6, 8662-8671	5
731	Analyzing the interaction energy between dopaminergic agents and DRD2: Is there any difference between risperidone (antagonist), aripiprazole (partial agonist) and pramipexole (agonist)?. 2021 , 1197, 113125	5
730	Electronic structure modulation of MoS2 by substitutional Se incorporation and interfacial MoO3 hybridization: Implications of Fermi engineering for electrocatalytic hydrogen evolution and oxygen evolution. 2021 , 2, 011401	2
729	Theoretical prediction on the redox potentials of rare-earth ions by deep potentials. 2021 , 27, 2079-2088	6
728	Ni/Cu-catalyzed silylation of allylic alcohol: Theoretical studies on the mechanisms, regioselectivity, and role of ligand. 2021 , 504, 111456	
727	Theoretical screening of group IIIA-VIIA elements doping to promote hydrogen evolution of MoS2 basal plane. 2021 , 542, 148535	12
726	Accurate Receptor-Ligand Binding Free Energies from Fast QM Conformational Chemical Space Sampling. 2021 , 22,	4
725	Multivariate Sulfonic-Based Titanium Metal-Organic Frameworks as Super-protonic Conductors. 2021 , 13, 20194-20200	3
724	High storage capacity and small volume change of potassium-intercalation into novel vanadium oxychalcogenide monolayers V2S2O, V2Se2O and V2Te2O: An ab initio DFT investigation. 2021 , 546, 149062	18
723	Free H-Bonding Interaction Sites in Rigid-Chain Polymers and Their Filling Approach: A Molecular Dynamics Simulation Study. 2021 , 4, 2100016	O
722	Mechanism insights into direct conversion of syngas into C2 oxygenates via key intermediate C2O2 over Ni-Supported graphene. 2021 , 175, 322-333	2
721	Importance of the oxyl character on the IrO2 surface dependent catalytic activity for the oxygen evolution reaction. 2021 , 396, 192-201	3

720	Theoretical Prediction of Two-Dimensional Materials, Behavior, and Properties. 2021, 15, 5959-5976	8
719	Revealing the importance of kinetics in N-coordinated dual-metal sites catalyzed oxygen reduction reaction. 2021 , 396, 215-223	15
718	Experimental and Computational Studies on Structure and Energetic Properties of Halogen Derivatives of 2-Deoxy-D-Glucose. 2021 , 22,	2
717	SBS Thermoplastic Elastomer Based on Dynamic Metal-Ligand Bond: Structure, Mechanical Properties, and Shape Memory Behavior. 2021 , 306, 2000737	5
716	A novel biosensor for gabapentin drug detection based on the Pd-decorated aluminum nitride nanotube. 2021 , 32, 1961-1971	6
715	Concepts, models, and methods in computational heterogeneous catalysis illustrated through CO2 conversion. 2021 , 11, e1530	11
714	Beyond Chemical Accuracy for Alkane Thermochemistry: The DH Approach. 2021, 86, 5538-5545	3
713	Carbon Nitride Monolayers as Efficient Immobilizers toward Lithium Selenides: Potential Applications in LithiumBelenium Batteries. 2021 , 4, 3891-3904	5
712	A single-molecule van der Waals compass. 2021 , 592, 541-544	28
711	A DFT study on the electronic detection of mercaptopurine drug by boron carbide nanosheets. 2021 , 1198, 113166	12
710	Exploration of superhalogen nature of $Pt(CN)$ n complexes (n = 1 \overline{B}) and their abilities to form supersalts and superacids: a DFT \overline{D} 3 study. 1	1
709	Study the Adsorption of Letrozole Drug on the Silicon Doped Graphdiyne Monolayer: a DFT Investigation. 1	2
708	Predicting Hugoniot equation of state in erythritol with ab initio and reactive molecular dynamics. 2021 , 129, 195106	
707	Recent advancement on the mechanism of olefin metathesis by Grubbs catalysts: A computational perspective. 2021 , 200, 115096	1
706	How accurate is the determination of equilibrium structures for van der Waals complexes? The dimer NO?CO as an example. 2021 , 154, 194302	2
705	Crystal Structure Prediction and Dehydrogenation Mechanism of LiMg(BH4)3(NH3)2. 2021 , 125, 10235-10242	1
704	Photo-cycloreversion mechanism in diarylethenes revisited: A multireference quantum-chemical study at the ODM2/MRCI level. 2021 , 154, 204305	1
703	Cation-Anion Interactions, Stability, and IR Spectra of Dicationic Amino Acid-Based Ionic Liquids Probed Using Density Functional Theory. 2021 , 27, 180	2

(2021-2021)

702	A Key Piece in the Global N-Cycle: The NN Bond Formation Presented by Heme-Dependent Hydrazine Synthase. 2021 , 11, 6489-6498	3
701	Learning to Model G-Quadruplexes: Current Methods and Perspectives. 2021 , 50, 209-243	8
700	The hopping mechanism of the hydrated excess proton and its contribution to proton diffusion in water. 2021 , 154, 194506	1
699	C36 and C35E (E=N and B) Fullerenes as Potential Nanovehicles for Neuroprotective Drugs: A Comparative DFT Study. 2021 , 6, 4844-4858	O
698	Rh@C8N8 monolayer as a promising single-atom-catalyst for overall water splitting. 2021, 549, 149320	9
697	Complex formation of titanocene dichloride anticancer and Al12N12 nano-cluster: A quantum chemical investigation of solvent, temperature and pressure effects. 2021 , 20, 19-32	2
696	Computational insight of ZrS2/graphene heterobilayer as an efficient anode material. 2021 , 551, 149304	3
695	Diffusion quantum Monte Carlo study of argon dimer. 2021 , 3, 024010	1
694	Manipulation of the Magnetic Properties of Janus WSSe Monolayer by the Adsorption of Transition Metal Atoms. 2021 , 16, 104	1
693	Requirements for an accurate dispersion-corrected density functional. 2021 , 154, 230902	13
693 692	Requirements for an accurate dispersion-corrected density functional. 2021 , 154, 230902 Structural, electronic and magnetic properties of S sites vacancy defects graphene/MoS2 van der Waals heterostructures: First-principles study. 2021 , 10, 2150009	3
	Structural, electronic and magnetic properties of S sites vacancy defects graphene/MoS2 van der	
692	Structural, electronic and magnetic properties of S sites vacancy defects graphene/MoS2 van der Waals heterostructures: First-principles study. 2021 , 10, 2150009 Reduced Two-Electron Interactions in Anharmonic Molecular Vibrational Calculations Involving	3
692 691	Structural, electronic and magnetic properties of S sites vacancy defects graphene/MoS2 van der Waals heterostructures: First-principles study. 2021 , 10, 2150009 Reduced Two-Electron Interactions in Anharmonic Molecular Vibrational Calculations Involving Localized Normal Coordinates. 2021 , 17, 4383-4391 A mechanistic first-principles study on N reduction reaction catalyzed by Ni supported defective	3
692 691 690	Structural, electronic and magnetic properties of S sites vacancy defects graphene/MoS2 van der Waals heterostructures: First-principles study. 2021, 10, 2150009 Reduced Two-Electron Interactions in Anharmonic Molecular Vibrational Calculations Involving Localized Normal Coordinates. 2021, 17, 4383-4391 A mechanistic first-principles study on N reduction reaction catalyzed by Ni supported defective graphene. 2021, 105, 107890 Theoretical prediction on the local structure and transport properties of molten alkali chlorides by	3 0
692 691 690	Structural, electronic and magnetic properties of S sites vacancy defects graphene/MoS2 van der Waals heterostructures: First-principles study. 2021, 10, 2150009 Reduced Two-Electron Interactions in Anharmonic Molecular Vibrational Calculations Involving Localized Normal Coordinates. 2021, 17, 4383-4391 A mechanistic first-principles study on N reduction reaction catalyzed by Ni supported defective graphene. 2021, 105, 107890 Theoretical prediction on the local structure and transport properties of molten alkali chlorides by deep potentials. 2021, 75, 78-85 Enzymatic N N bond formation: Mechanism for the N-nitroso synthesis catalyzed by non-heme iron	3 0 1
692 691 690 689	Structural, electronic and magnetic properties of S sites vacancy defects graphene/MoS2 van der Waals heterostructures: First-principles study. 2021, 10, 2150009 Reduced Two-Electron Interactions in Anharmonic Molecular Vibrational Calculations Involving Localized Normal Coordinates. 2021, 17, 4383-4391 A mechanistic first-principles study on N reduction reaction catalyzed by Ni supported defective graphene. 2021, 105, 107890 Theoretical prediction on the local structure and transport properties of molten alkali chlorides by deep potentials. 2021, 75, 78-85 Enzymatic N N bond formation: Mechanism for the N-nitroso synthesis catalyzed by non-heme iron SznF enzyme. 2021, 398, 44-53 Novel Two-Dimensional Janus MoSiGeN and WSiGeN as Highly Efficient Photocatalysts for	3 0 1 12 2

684	Removal´of nitrous and carbon mono oxide´from flue gases´by Si-coordinated nitrogen doped C60-fullerene: A DFT approach. 2021 , 509, 111674	1
683	Impact of Orientational Glass Formation and Local Strain on Photo-Induced Halide Segregation in Hybrid Metal-Halide Perovskites. 2021 , 125, 15025-15034	4
682	Structural Studies of Aluminated form of Zeolites-EXAFS and XRD Experiment, STEM Micrography, and DFT Modelling. 2021 , 26,	0
681	The application of graphyne and its boron nitride analogue in Li-ion batteries. 2021 , 1200, 113243	2
680	Lithium-functionalized boron phosphide nanotubes (BPNTs) as an efficient hydrogen storage carrier. 2021 , 46, 20586-20593	7
6 7 9	Electrochemical and Structural Studies of LiNi0.85Co0.1Mn0.05O2, a Cathode Material for High Energy Density Li-Ion Batteries, Stabilized by Doping with Small Amounts of Tungsten. 2021 , 168, 060552	2
678	CrI3 revisited with a many-body ab initio theoretical approach. 2021 , 5,	4
677	A Halomanganates(II) with P,P'-Diprotonated Bis(2-Diphenylphosphinophenyl)ether: Wavelength-Excitation Dependence of the Quantum Yield and Role of the Non-Covalent Interactions. 2021 , 22,	3
676	The adsorption of cathinone drug on the platinum decorated silicon carbide nanosheets: DFT studies. 2021 , 27, 202	
675	Theoretical insights into catalytic CO2 hydrogenation over single-atom (Fe or Ni) incorporated nitrogen-doped graphene. 2021 , 48, 101532	6
674	A study of cation-dependent inverse hydrogen bonds and magnetic exchange-couplings in lanthanacarborane complexes. 2021 , 24, 102760	1
673	Dynamics of Ionic Liquid through Intrinsic Vibrational Probes Using the Dispersion-Corrected DFT Functionals. 2021 , 125, 6994-7008	6
672	Ultrasonication-assisted synthesis of 2D porous MoS/GO nanocomposite catalysts as high-performance hydrodesulfurization catalysts of vacuum gasoil: Experimental and DFT study. 2021 , 74, 105558	5
671	H-Bonding Networks Dictate the Molecular Mechanism of H2O2 Activation by P450. 2021 , 11, 8774-8785	9
670	Pressure-induced 1T to 3R structural phase transition in metallic VSe2: X-ray diffraction and first-principles theory. 2021 , 104,	3
669	CONI-Net: Machine Learning of Separable Intermolecular Force Fields. 2021 , 17, 4996-5006	1
668	Synthesis and Characterization of a Cobalt(III) Corrole with an S-Bound DMSO Ligand. 2021, 2021, 3540-3548	1
667	Enhancement of Structural, Electrochemical, and Thermal Properties of High-Energy Density Ni-Rich LiNiCoMnO Cathode Materials for Li-Ion Batteries by Niobium Doping. 2021 , 13, 34145-34156	11

(2021-2021)

666	Enhanced Sodium Metal/Electrolyte Interface by a Localized High-Concentration Electrolyte for Sodium Metal Batteries: First-Principles Calculations and Experimental Studies. 2021 , 4, 7376-7384	5
665	Stereospecific collision-induced dissociation and vibrational spectroscopy of protonated cyclo (Tyr-Pro). 2021 , 465, 116590	4
664	In situ construction of EMoC/VN heterostructured electrocatalysts with strong electron coupling for highly efficient hydrogen evolution reaction. 2021 , 416, 129130	11
663	Effect of strain on structural and electronic properties, and thermoelectric response of MXY (M=Zr, Hf and Pt; X/Y=S, Se) vdW heterostructures; A first principles study. 2021 , 299, 122189	6
662	Future directions of chemical theory and computation. 2021,	1
661	Coordination chemistry of platinum(II) and rhodium(I) complexes containing chiral monophosphacrown ether ligands. 2021 , 522, 120348	1
660	Exploration of the Activation Mechanism of the Epigenetic Regulator MLL3: A QM/MM Study. 2021 , 11,	0
659	A Quantitative Interpretation for the Difference of Terahertz Spectra of dl- and l-Alanine: Origins of Infrared Intensities in Terahertz Spectroscopy. 2021 , 125, 16175-16182	4
658	Aqueous Affinity and Interfacial Dynamics of Anisotropic Buckled Black Phosphorous. 2021 , 125, 7527-7536	4
657	Evaluate the potential utilization of B24N24 fullerene in the recognition of COS, H2S, SO2, and CS2 gases (environmental pollution). 2021 , 117041	1
656	Pushing Cu uphill of the volcano curve: Impact of a WC support on the catalytic activity of copper toward the hydrogen evolution reaction. 2021 , 46, 25092-25102	2
655	Graphene-hexagonal boron nitride van der Waals heterostructures: an examination of the effects of different van der Waals corrections. 2021 , 8, 085601	3
654	Ab-Initio Molecular Dynamics Simulation of the Electrolysis of Nucleobases. 2021 , 14, 5021	
653	Pyrophyllite dissolution at elevated pressure conditions: An ab initio study. 2021 , 307, 42-55	2
652	Structural, conductivity and DFT studies of L-Histidinium phosphite (Ferroelectric phosphite single crystal. 2021 , 300, 122211	
651	Layer dependent magnetism and topology in monolayer and bilayers Re(Br, I). 2021 , 33,	1
650	Defect engineering-induced porosity in graphene quantum dots embedded metal-organic frameworks for enhanced benzene and toluene adsorption. 2021 , 416, 125973	6
649	Induction of planar Li growth with designed interphases for dendrite-free Li metal anodes. 2021 , 39, 250-258	14

648	New Approach for Correcting Noncovalent Interactions in Semiempirical Quantum Mechanical Methods: The Importance of Multiple-Orientation Sampling. 2021 , 17, 5556-5567	3
647	Electronic structure and first hyperpolarizability of triple helicene compounds. 2021 , 1237, 130332	1
646	Gas Transport across Carbon Nitride Nanopores: A Comparison of van der Waals Functionals against the Random-Phase Approximation. 2021 , 125, 18896-18904	0
645	The strain and transition metal doping effects on monolayer Cr2O3 for hydrogen evolution reaction: The first principle calculations. 2021 ,	0
644	Switching the Local Symmetry from D5h to D4h for Single-Molecule Magnets by Non-Coordinating Solvents. 2021 , 9, 64	1
643	Observation and manipulation of valley polarization in two-dimensional H-Tl2O/CrI3 heterostructure. 2021 , 558, 149604	4
642	Investigating the property and strength of intermolecular interaction in saturated and unsaturated cyclic cations constructed ionic liquids. 2021 , 335, 116253	1
641	One-step laser fabrication of phosphorus-doped porous graphene electrodes for high-performance flexible microsupercapacitor. 2021 , 180, 56-66	19
640	Mechanism of over-stoichiometric oxidation of SO2 by iron oxides modified pyridinic N-doped carbonaceous materials. 2021 , 556, 149757	1
639	Controllable enormous valley splitting in Janus WSSe on CrN monolayer. 2021 , 54, 425304	O
638	Optical and tuning electronic properties of GeC/MoS2 van der Waals heterostructures by electric field and strain: A first-principles study. 2021 , 156, 106935	1
637	Effect of vacancy defects in 2D vdW graphene/h-BN heterostructure: First-principles study. 2021 , 11, 085218	4
636	First-principles investigation of CO2, CO, and O2 adsorptions on the (001)-reconstructed surfaces of CsPbX3 (X = Cl, Br, and I) perovskites. 2021 , 25, 101264	1
635	Hydrogen storage on Li-decorated B4N: a first-principle calculation insight. 2021 , 54, 445501	4
634	Viologen-Decorated TEMPO for Neutral Aqueous Organic Redox Flow Batteries. 2021 , 2021, 1-8	2
633	Interfacial optimization of PtNi octahedrons@Ti3C2MXene with enhanced alkaline hydrogen evolution activity and stability. 2021 , 291, 120100	21
632	CisErans isomerisation and absorption properties of the ring-extended azobenzene.	
631	Study of the molybdenum dichalcogenide crystals: recent developments and novelty of the P-MoS structure. 2021 , 27, 268	2

630	DFT Functionals for Modeling of Polyethylene Chains Cross-Linked by Metal Atoms. DLPNO-CCSD(T) Benchmark Calculations. 2021 , 125, 7382-7395	1
629	Synthesis of 0D SnO2 nanoparticles/2D g-C3N4 nanosheets heterojunction: improved charge transfer and separation for visible-light photocatalytic performance. 2021 , 871, 159561	8
628	Gas sensing properties of defective tellurene on the nitrogen oxides: A first-principles study. 2021 , 328, 112766	2
627	Methylphenidate drug adsorption on the pristine magnesium oxide nanotubes; a computational study. 2021 , 1203, 113351	1
626	Li-decorated B2O as potential candidates for hydrogen storage: A DFT simulations study. 2021 , 46, 33486-33	49Б
625	A reversible hydrogen storage material of Li-decorated two-dimensional (2D) C4N monolayer: First principles calculations. 2021 , 46, 32936-32948	6
624	Reaction between a NO Dimer and Dissolved SO: A New Mechanism for ONSO Formation and its Fate in Aerosol. 2021 , 125, 8468-8475	0
623	Computational investigation of sensing properties of Ca-doped zinc oxide nanotube toward formaldehyde. 2021 , 27, 303	Ο
622	Reduced-gradient analysis of van der Waals complexes.	1
621	Physical insights on transistors based on lateral heterostructures of monolayer and multilayer PtSe via Ab initio modelling of interfaces. 2021 , 11, 18482	1
620	Epoxidation of ethylene over an Ag atom embedded B-vacancy defective boron-nitride nanosheet via a trimolecular Langmuir inshelwood mechanism: A DFT investigation. 2021 , 514, 111843	O
619	Water-Assisted Chemical Route Towards the Oxygen Evolution Reaction at the Hydrated (110) Ruthenium Oxide Surface: Heterogeneous Catalysis via DFT-MD and Metadynamics Simulations. 2021 , 27, 17024-17037	2
618	Determination of kinetic properties in unimolecular dissociation of complex systems from graph theory based analysis of an ensemble of reactive trajectories. 2021 , 155, 124103	4
617	Theoretical analysis on reactions between syn-methyl Criegee intermediate and amino alcohols.	
616	Structural stability and electronic properties of graphene/germanene heterobilayer. 2021, 28, 104545	3
615	Effects of electric field and strain on the Schottky barrier of the bilayer van der Waals heterostructures of graphene and pure/hydrogenated PC3 monolayer. 2021 , 133, 114785	O
614	Investigation of molecular interactions by volumetric, transport, spectral and DFT studies in some liquid binaries of N-methyl-2-pyrrolidone with N-alkyl anilines in the temperature range 303.15B18.15 K. 2021 , 337, 116449	О
613	Modeling Liquid Water by Climbing up Jacob's Ladder in Density Functional Theory Facilitated by Using Deep Neural Network Potentials. 2021 , 125, 11444-11456	13

612	Probing metal-molecule contact at the atomic scale via conductance jumps. 2021 , 104,	1
611	vdW-DF-ahcx: a range-separated van der Waals density functional hybrid. 2021 , 34,	2
610	Highly stable TiOF monolayer as anode material for the applications of Li/Na-ion batteries. 2021 , 574, 151296	O
609	Temperature Dependence of Spin-Phonon Coupling in [VO(acac)]: A Computational and Spectroscopic Study. 2021 , 125, 22100-22110	5
608	Half-Pancake Bonding in Asphaltenes.	О
607	Mechanisms, challenges, and opportunities of dual Ni/photoredox-catalyzed C(sp2)ជ(sp3) cross-couplings. e1573	3
606	Comparison of optical response from DFT random phase approximation and a low-energy effective model: Strained phosphorene. 2021 , 104,	3
605	Al-decorated C24N24 fullerene: A robust single-atom catalyst for CO oxidation. 2021 , 115497	O
604	Van der Waals enhanced interfacial interaction in cellulose/zinc oxide nanocomposite coupled by graphitic carbon nitride. 2021 , 268, 118235	5
603	Theoretical evaluation of central ring doped Hexa-peri-hexabenzocoronene as Gamma-butyrolactone drug sensors. 2021 , 1204, 113412	
602	Hydroxyurea anticancer drug adsorption on the pristine and doped C70 fullerene as potential carriers for drug delivery. 2021 , 340, 117226	1
601	Ab-initio study of nanoporous phosphorene as anode material in rechargeable Li/Na ion batteries. 2021 , 564, 150155	2
600	Dispersion-corrected DFT design of nitrogen doped- or TMN4 embedded buckybowl-like porous carbon derived from zeolitic imidazolate frameworks as anode material of sodium-ion battery. 2021 , 562, 150156	1
599	Anharmonicity modeling in hydrogen bonded solvent dimers. 2021 , 339, 116735	
598	MXenes modified by single transition metal atom for hydrogen evolution reaction catalysts. 2021 , 562, 150151	5
597	Enhancing the hydrogen evolution reaction by non-precious transition metal (Non-metal) atom doping in defective MoSi2N4 monolayer. 2021 , 563, 150388	9
596	A DFT+U study about agglomeration of Au atoms on reduced surface of rutile TiO2 (110). 2021 , 271, 124944	2
595	Insight into the mechanism of nanoparticle induced suppression of interfacial tension. 2021 , 339, 117177	1

594	One-dimensional structures of three quinone molecules on Au(111). 2021, 713, 121911	О
593	Boron doped Ni-rich LiNi0.85Co0.10Mn0.05O2 cathode materials studied by structural analysis, solid state NMR, computational modeling, and electrochemical performance. 2021 , 42, 594-607	2
592	Catalytic CO oxidation reaction over N-substituted graphene nanoribbon with edge defects. 2021 , 108, 108006	1
591	Engineering the electronic and magnetic properties of nitrogene monolayer and bilayer by doping: A first-principles study. 2021 , 566, 150711	2
590	Theoretical study of the adsorption and sensing properties of pure and metal doped C24N24 fullerene for its potential application as high-performance gas sensor. 2021 , 134, 106035	2
589	Machine learning accelerates quantum mechanics predictions of molecular crystals. 2021 , 934, 1-71	4
588	Structural stability and electronic characteristics of cellulose nanowires on graphene-like systems. 2021 , 569, 150998	Ο
587	Explicit solvent effects on (1 1 0) ruthenium oxide surface wettability: Structural, electronic and mechanical properties of rutile RuO2 by means of spin-polarized DFT-MD. 2021 , 570, 150993	6
586	2D tellurene: Increase sensitivity toward toxic cyanide molecules. 2021 , 194, 110619	1
585	High-performance magnetic tunnel junctions based on two-dimensional Bi2O2Se. 2021 , 539, 168346	1
584	Identification of sulfur gases (environmental pollution) by BeO fullerenes: A DFT study. 2021 , 343, 117528	3
583	Theoretical study of the reaction mechanism between Criegee intermediates and hydroxyl radicals in the presence of ammonia and amine. 2022 , 287, 131877	Ο
582	Multiscale modeling studies for exploring lignocellulosic biomass structure. 2022 , 257-289	
581	Understanding delivery and adsorption of Flutamide drug with ZnONS based on: Dispersion-corrected DFT calculations and MD simulations. 2022 , 135, 114937	5
580	Computational survey on the Pt-decorated ZnO nanosheet as a chemical sensor for chlorobenzene: Explaining the experimental observations. 2022 , 161, 110379	O
579	Machine Learning Corrections for DFT Noncovalent Interactions. 2021 , 183-212	
578	The Statistical Mechanics of Solution-Phase Nucleation: CaCO(_3) Revisited. 2021, 101-122	1
577	Surface morphology controls water dissociation on hydrated IrO nanoparticles. 2021 , 13, 14480-14489	Ο

576	A high-temperature quantum anomalous Hall effect in electride gadolinium monohalides. 2021 , 9, 9539-9544	3
575	Experimental and DFT insights into nitrogen and sulfur co-doped carbon nanotubes for effective desulfurization of liquid phases: Equilibrium & kinetic study. 2021 , 15, 1	2
574	Cycloaddition mechanisms of CO2 and epoxide catalyzed by salophen han organocatalyst free from metals and halides. 2021 , 11, 2529-2539	3
573	Disentangling the complex network of non-covalent interactions in fenchone hydrates rotational spectroscopy and quantum chemistry. 2021 , 23, 20686-20694	5
572	Exploring organic semiconductors in solution: the effects of solvation, alkylization, and doping. 2021 , 23, 4841-4855	4
571	Computational and infrared spectroscopic investigations of N-substituted carbazoles. 2021 , 23, 8426-8438	
570	Computational modelling of Pd-catalysed alkoxycarbonylation of alkenes and alkynes. 2021 , 23, 15869-15880	1
569	Self-Healing of Broken Bonds and Deep Gap States in Sb2Se3 and Sb2S3. 2021 , 7, 2000908	4
568	New luminescent tetracoordinate boron complexes: an in-depth experimental and theoretical characterisation and their application in OLEDs. 2021 , 8, 3960-3983	3
567	Catalytic role of graphitic nitrogen atoms in the CO oxidation reaction over N-containing graphene: a first-principles mechanistic evaluation. 2021 , 45, 13822-13832	О
566	Machine-Learning-Driven Simulations on Microstructure and Thermophysical Properties of MgCl-KCl Eutectic. 2021 , 13, 4034-4042	18
565	Theoretical evaluation of the corrosion inhibition performance of aliphatic dipeptides. 2021 , 45, 3610-3629	6
564	Local energy decomposition analysis and molecular properties of encapsulated methane in fullerene (CH@C). 2021 , 23, 21554-21567	4
563	Study the adsorption process of 5-Fluorouracil drug on the pristine and doped graphdiyne nanosheet. 2021 , 27, 32	8
562	A Novel [OSSO]-Type Chromium(III) Complex as a Versatile Catalyst for Copolymerization of Carbon Dioxide with Epoxides. 2020 , 26, 5347-5353	7
561	Hohenberg-Kohn-Sham Density Functional Theory. 2007 , 153-201	1
560	Unraveling the Mechanisms of Ribozyme Catalysis with Multiscale Simulations. 2009, 377-408	1
559	Towards an Accurate Semi-Empirical Molecular Orbital Treatment of Covalent and Non-Covalent Biological Interactions. 2009 , 105-136	1

558	Molecular Models of Cation and Water Molecule Bridges in Humic Substances. 2014 , 107-115	3
557	On Quantum Chemical Topology. 2016 , 23-52	15
556	Electronic Properties of Iron Sites and Their Active Forms in Porphyrin-Type Architectures. 2019, 755-823	1
555	Endohedral Fullerene Complexes and In-Out Isomerism in Perhydrogenated Fullerenes. 2011 , 117-151	5
554	First Steps Towards Quantum Refinement of Protein X-Ray Structures. 2012 , 87-120	6
553	Weak Intermolecular Interactions: A Supermolecular Approach. 2015 , 1-27	2
552	Intermolecular Interactions. 2015 , 1-42	1
551	Molecular Mechanics: Principles, History, and Current Status. 2015 , 1-48	1
550	Structure and stability of sodium-doped helium snowballs through DFT calculations. 2020 , 139, 1	3
549	Insights into the Chemical Reactivity in Acetyl-CoA Synthase. 2020 , 59, 15167-15179	6
548	Three-Body Dispersion Corrections to the Spherical Atom Model: The PFD-3B Density Functional. 2020 , 124, 10296-10311	1
547	Performance of a Novel 3D GrapheneWS2 Hybrid Structure for Sodium-Ion Batteries. 2020 , 124, 3536-3541	4
546	Improving the Description of Interlayer Bonding in TiS2 by Density Functional Theory. 2020 , 124, 27592-27603	3 2
545	Enhanced conductivity of water at the electrified air-water interface: a DFT-MD characterization. 2020 , 22, 10438-10446	6
544	Amorphous molybdenum sulfide nanocatalysts simultaneously realizing efficient upgrading of residue and synergistic synthesis of 2D MoS2 nanosheets/carbon hierarchical structures. 2020 , 22, 44-53	71
543	Polymorphism and structural diversities of LiClO4臨lanine ionic co-crystals. 2020 , 22, 4427-4437	1
542	Adsorption of methane on single metal atoms supported on graphene: Role of electron back-donation in binding and activation. 2020 , 153, 244701	2
541	Exploration of MXene/polyaniline composites as promising anode materials for sodium ion batteries. 2021 , 54, 064001	4

540	TiO nanotube array-modified electrodes for L-cysteine biosensing: experimental and density-functional theory study. 2020 , 31, 505501	5
539	2D 1T?-MoS2-WS2 van der Waals heterostructure for hydrogen evolution reaction: dispersion-corrected density functional theory calculations. 2020 , 7, 075506	4
538	Stacking- and chirality-dependent collapse of single-walled carbon nanotubes: A large-scale density-functional study. 2019 , 100,	15
537	Interactions between copper and transition metal dichalcogenides: A density functional theory study. 2017 , 1,	4
536	Giant ferrimagnetism and polarization in a mixed metal perovskite metal-organic framework. 2018 , 2,	7
535	Design and analysis of machine learning exchange-correlation functionals via rotationally invariant convolutional descriptors. 2019 , 3,	29
534	Molecule-surface interaction from van der Waals-corrected semilocal density functionals: The example of thiophene on transition-metal surfaces. 2020 , 4,	12
533	CTM4DOC: electronic structure analysis from X-ray spectroscopy. 2016 , 23, 1264-71	19
532	Crystal structure, interaction energies and experimental electron density of the popular drug ketoprophen. 2018 , 5, 841-853	9
531	Photocrystallographic and spectroscopic studies of a model (N,N,O)-donor square-planar nickel(II) nitro complex: in search of high-conversion and stable photoswitchable materials. 2020 , 7, 1188-1198	4
530	Dataset for Modelling Reaction Mechanisms Using Density Functional Theory: Mechanism of ortho-Hydroxylation by High-Valent Iron-Oxo Species. 2014 , 2014, 1-7	3
529	Strain and Electric Field Controllable Schottky Barriers and Contact Types in Graphene-MoTe van der Waals Heterostructure. 2020 , 15, 180	10
528	How metal substitution affects the enzymatic activity of catechol-o-methyltransferase. 2012 , 7, e47172	21
527	Interfacial water molecules at biological membranes: Structural features and role for lateral proton diffusion. 2018 , 13, e0193454	7
526	Barrier to internal rotation, symmetry and carbonyl reactivity in methyl 3,3,3-trifluoropyruvate. 2020 , 234, 1383-1393	3
525	Computational Surface Modelling of Ices and Minerals of Interstellar Interest I hsights and Perspectives. 2021 , 11, 26	2
524	Assessment of the Performance of B2PLYP-D for Describing Intramolecular Hand III Interactions. 2011 , 32, 4195-4198	3
523	Theoretical Studies on Mechanisms and Origins of Stereocontrol in Chiral Phosphoric Acid Catalyzed Asymmetric Reactions. 2014 , 72, 580-595	1

522	Theoretical Study of Hydrogen Bond Formation in Trimethylene Glycol-Water Complex. 2012, 2012, 1-12	11
521	Terahertz spectrum study of organic electro-optic crystal 4-N, N-dimethylamino-4'-N'-methyl-stilbazolium tosylate. 2017 , 66, 244211	3
520	Path sampling for atmospheric reactions: formic acid catalysed conversion of SO3 + H2O to H2SO4. 2, e7	3
519	Benchmarking quantum mechanical methods for calculating reaction energies of reactions catalyzed by enzymes. 2, e8	7
518	-[(IBCH)Fe(IBCO)(ECO)], the poor relative between and tautomers. A theoretical study of the gas-phase Fe L-edge and C and O K-edge XAS of -/-[(IBCH)Fe(IBCO)(ECO)]. 2021 , 23, 24661-24668	1
517	Achieving an Ohmic contact in graphene-based van der Waals heterostructures by intrinsic defects and the inner polarized electric field of Janus AlGaSSe.	1
516	Tuning the Electronic Structure of Monolayer MgI2 by Biaxial Strain and External Electric Field. 2021 , 11, 99-108	O
515	Application of Computational Chemistry for Contaminant Adsorption on the Components of Soil Surfaces. 2022 , 171-213	O
514	Penta graphene: a superior anode material for Mg-ion batteries with high specific theoretical capacity. 2021 , 27, 4819-4828	О
513	Application of borophene as catechol sensor: a computational study. 2021 , 27, 310	О
512	Spin-Dependent Electronic Structure and Magnetic Properties of 2D JANUS Mn2CFCl/CuBiP2Se6 Van Der Waals Multiferroic Heterostructures. 2021 , 4, 2100302	1
511	Ferritin-based targeted delivery of arsenic to diverse leukaemia types confers strong anti-leukaemia therapeutic effects. 2021 ,	4
510	Advances in Low-Frequency Vibrational Spectroscopy and Applications in Crystal Engineering.	3
509	Condensed Phase Water Molecular Multipole Moments from Deep Neural Network Models Trained on Simulation Data. 2021 , 12, 10310-10317	5
508	Understanding the Catalytic Activity of the Preferred Nitrogen Configuration on the Carbon Nanotube Surface and Its Implications for LiD2 Batteries. 2021 , 125, 22570-22580	2
507	Computational Insights into the Role of External and Local Electric Fields in Macrocyclic Chemical and Biological Systems. 2021 , 22, 2484-2492	
506	Electron Flow Characterization of Charge Transfer for Carbonic Acid to Strong Base Proton Transfer in Aqueous Solution. 2021 , 125, 11473-11490	О
505	Stereochemistry, Conformational Dynamics, and the Stability of Liquid Crystal Phases. 2021 , 86, 15076-15084	2

504	Development of DNA intercalative, HSA binder pyridine-based novel Schiff base Cu(II), Ni(II) complexes with effective anticancer property: A combined experimental and theoretical approach. e6473	3
503	First-principles investigations of the geometric structures and electronic properties of pristine and Ag/Au-doped Janus MoSSe/C60 and WSSe/C60 heterostructures. 2021 , 575, 151660	1
502	Role of Hydration in Magnesium versus Calcium Ion Pairing with Carboxylate: Solution and the Aqueous Interface. 2021 , 125, 11308-11319	1
501	New Charge Transfer Complexes of K-Channel-Blocker Drug (Amifampridine; AMFP) for Sensitive Detection; Solution Investigations and DFT Studies. 2021 , 26,	
500	Pt-decorated BN nanosheets as chemical sensor for recognition of dopamine drug. 2021 , 134, 108990	O
499	Trimers of Nucleic Acid Bases. 2006 , 1493-1496	
498	Combined QM/MM methods for the simulation of condensed phase processes using an approximate DFT approach. 2008 , 381-405	
497	Conceptual Density Functional Theory. 2009,	
496	Ab Initio Quantum Chemistry and Semi-Empirical Description of Solid State Phases Under High Pressure: Chemical Applications. 2010 , 325-339	
495	Solving the Structure of Metakaolin. 2011 , 274-287	
494	Helical Compounds Forming Gas-Phase Dimers: A Dispersion-corrected Density Functional Investigation. 2011 , 32, 1231-1236	
493	First Principles DFT Studies of Metal- Based Biological and Biomimetic Systems. 2011 ,	
492	Theoretical Methods. 2012 , 23-39	
491	Intermolecular Potentials of the Carbon Tetrachloride and Trifluoromethane Dimers Calculated with Density Functional Theory. 2012 , 309-320	
490	Introduction. 2012 , 1-22	
489	Electron correlation methods based on the random phase approximation. 2012 , 103-120	
488	Adsorption of successive layers of H2 molecules on a model copper surface: performances of second- to fifth-rung exchange-correlation functionals. 2013 , 281-289	
487	Impact of DFT functionals on the predicted magnesium D NA interaction: an ONIOM study. 2013 , 271-279	

486	First-Principles Calculations of Physical Properties of Planetary Ices. 2013 , 149-169	
485	Theoretical study of adsorption of propanethiol on Au(111) surface at different coverages. 2013 , 62, 223101	1
484	Computational Methods. 2013 , 29-55	
483	Electronic Structure Methods. 105-125	
482	Energy Conversion: Heterogeneous Catalysis. 187-229	1
481	Benchmarking the Performance of DHDFs for the Main Group Chemistry. 2014 , 47-77	
480	Electronic Properties of Iron Sites and Their Active Forms in Porphyrin-Type Architectures. 2014 , 711-782	
479	The Scanning Tunneling Microscopy of Adsorbed Molecules on Semiconductors: Some Theoretical Answers to the Experimental Observations. 2014 , 1-44	
478	Direct Dynamics Simulations of Ir(_2)(dimen)(_4^{2+}). 2015 , 75-97	
477	Modelling the Structure and Vibrational Properties of Layered Double Hydroxides. 2015 , 317-323	1
476	Computational Techniques. 2015 , 19-77	
475	Understanding the Exohedral Functionalization of Endohedral Metallofullerenes. 2015, 67-99	
474	Analyzing Interaction Energy of Polycyclic Aromatic Hydrocarbons (PAH) Dimers. 2016 , 113-126	
473	Computational Modeling of DNA and RNA Fragments. 2016 , 1-24	
472	Nitrogen Gas on Graphene: Pairwise Interaction Potentials. 2018 , 563-578	1
471	Including London Dispersion Forces in Density Functional Theory (DFT + D): Applications to Molecule(Atom)/Surface Phenomena. 2018 , 1-9	
470	CHAPTER 18:Noncovalent Interactions in Olefin Polymerization Catalysis Promoted by Transition Metals. 2019 , 393-414	
469	Binding Energies of N-Bearing Astrochemically-Relevant Molecules on Water Interstellar Ice Models. A Computational Study. 2020 , 683-692	О

Van der Waals Interactions in Material Modelling. **2020**, 259-291

467	Theoretical Insights About the Chemical Dependent Role of Exchange-Correlation Functionals: A Case Study. 2020 , 341-357	О
466	Influence of Membrane Phase on the Optical Properties of DPH. 2020, 25,	2
465	Non-enzymatic glucose sensors based on Hexa-peri-hexabenzocoronene: A computational study. 2021 , 553, 111388	O
464	Fluorinated Graphite (FG)-Modified Li-S Batteries with Superhigh Primary Specific Capacity and Improved Cycle Stability. 2021 ,	0
463	DFT studies on PbO2 and binary PbO2/SnO2 thin films. 2021 , 136, 115037	1
462	Resolving the Structural Debate for the Hydrated Excess Proton in Water. 2021 , 143, 18672-18683	5
461	Structure of Electrode-Electrolyte Interfaces, Modeling of Double Layer and Electrode Potential. 2020 , 1439-1472	
460	Low-Energy CO Scattering at the Gaslliquid Interface: Experimental/Theoretical Evidence for a Novel Subthermal Impulsive Scattering (STIS) Channel. 2020 , 124, 28006-28017	3
459	Theoretical Study on Aluminum Oxide Cluster Anions A12Ox[(x=2B) with Rhombus Structure. 2020 , 5, 15137-15147	
458	Novel CuTe monolayer as promising anode material for Na-ion batteries: A theoretical study. 2022 , 573, 151550	2
457	Analysis of the combustion mechanism of diesel surrogate fuel under CO2/O2 atmosphere. 2022 , 309, 122223	0
456	Towards tuning the modality of hierarchical macro-nanoporous metals by controlling the dealloying kinetics of close-to-eutectic alloys. 2021 , 23, 25388-25400	0
455	Prismatic Edge Dislocations in Graphite.	
454	Chapter 3. Theoretical Approaches. 2020 , 99-224	1
453	Nanotechnology for Water and Wastewater Treatment Using Graphene Semiconductor Composite Materials. 2020 , 1-34	1
452	10-Porphyrin Nanorings with Copper(II) and Zinc(II) Centres. 2020 , 25-68	
451	Energy Trends in Adsorption at Surfaces. 2020 , 1321-1341	

450 Controlled Growth of Monolayer WS2 on GaN Substrate and Its Optical Properties. **2020**, 10, 412-421

449	Haeckelite phosphorus: an emerging 2D allotrope of phosphorus for potential use in LIBs/SIBs. 2021 , 23, 26547-26560	Ο
448	Spin resonance amplitude and frequency of a single atom on a surface in a vector magnetic field. 2021 , 104,	2
447	Rational design of a novel two-dimensional porous metal-organic framework material for efficient benzene sensor. 2021 ,	1
446	Study on Structure, Stability, and Phase Transformation of Dufulin Polymorphs.	0
445	Molecular simulation for physisorption characteristics of O2 in low-rank coals. 2021 , 242, 122538	1
444	Symmetry induced phonon renormalization in few layers of 2H-MoTe transistors: Raman and first-principles studies. 2021 , 32, 045202	1
443	Hg adatoms on graphene: A first-principles study. 2020 , 4, 015002	
442	Defect induced electrocatalytic hydrogen properties of pentagonal PdX (X = S, Se) 2021 , 11, 38478-38485	1
441	Polyaniline-based gas sensors: DFT study on the effect of side groups. 2022 , 1207, 113526	1
440	Phase-separated indenofluorene arrays stabilized by hydrogen and halogen bonds on Au(111). 2022 , 40, 013201	0
439	Three decades of unveiling the complex chemistry of C-nitroso species with computational chemistry.	1
438	Adsorption behaviour of NO, NO2, CO and CS2 molecules on the surface of carbon-doped gallium nitride nanosheet: A DFT study. 2022 , 717, 121988	1
437	Low-cost single-atom transition metals on two-dimensional SnO nanosheets for efficient hydrogen evolution catalysis in all pH-range. 2022 , 578, 152021	1
436	Functionalized semiconducting carbon nanotube arrays for gas phase explosives detection. 2022 , 717, 121998	О
435	Prediction of functionalized graphene as potential catalysts for overall water splitting. 2022 , 578, 151989	1
434	NH3-SCR catalysts for heavy-duty diesel vehicles: Preparation of CHA-type zeolites with low-cost templates. 2022 , 303, 120928	1
433	CO2-assisted ethane aromatization over zinc and phosphorous modified ZSM-5 catalysts. 2022 , 304, 120956	3

432 Combining Metal Nanoparticles with an Ir(III) Photosensitizer. **2021**, 125, 25765-25773

431	Molecular dynamics simulations of lanthanum chloride by deep learning potential. 2021 , 111014	4
430	Parametrization of Nonbonded Force Field Terms for Metal-Organic Frameworks Using Machine Learning Approach. 2021 ,	0
429	Enhancing the Accuracy of Ab Initio Molecular Dynamics by Fine Tuning of Effective Two-Body Interactions: Acetonitrile as a Test Case. 2021 , 125, 10475-10484	О
428	2,4,6-Trinitro-N-(m-tolyl)aniline: A New Polymorphic Material Exhibiting Different Colors. 2021 , 21, 7269-7284	2
427	Revisiting the Structural Evolution of MoS2 During Alkali Metal (Li, Na, and K) Intercalation.	2
426	Large valley polarization in a novel two-dimensional semiconductor H-ZrX(XCl, Br, I). 2021, 34,	2
425	Mimicking Elementary Reactions of Manganese Lipoxygenase Using Mn-hydroxo and Mn-alkylperoxo Complexes. 2021 , 26,	
424	Electronic properties, stability, and lattice thermal conductivity of bulk Janus 3R-PtXY (X, Y=S, Se, Te) transition-metal dichalcogenide. 2021 , 94, 1	0
423	Interfacial nitrogen engineering of robust silicon/MXene anode toward high energy solid-state lithium-ion batteries. 2021 ,	9
422	Prismatic edge dislocations in graphite. 2021 , 188, 401-401	O
421	2-Substituted Perimidines: Zwitterionic Tauterism in Solid State, Substituent Effect on their Crystal Packing and Biological Activity 2021 , 1252, 132056	O
420	Enhanced OER activity of FePc molecule by substrate effects: A first principles study. 2021 , 717, 122000	0
419	Design of Metal-Decorated Beryllium Carbide (Be 2C) As a High-Capacity Hydrogen Storage Material with Strong Adsorption Characteristics.	
418	Application of Docking and Quantum Chemistry to the Search for Inhibitors of SARS-CoV-2 Main Protease. 2021 , 17-28	
4 ¹ 7	Low-Cost Hydrocarbon Membrane Enables Commercial-Scale Alkaline-Based Flow Batteries for Long-Duration Energy Storage.	
416	Experimental study and simulation analysis of terahertz absorption spectra of ⊞actose aqueous solution. 2021 , 70, 243202	0
415	Electrospun Cu-doped In2O3 hollow nanofibers with enhanced H2S gas sensing performance. 1	6

414	Ab Initio Molecular Dynamics Study of Aqueous Solutions of Magnesium and Calcium Nitrates: Hydration Shell Structure, Dynamics and Vibrational Echo Spectroscopy 2022 ,	2
413	Antiferromagnetic Coupling Supported by Metallophilic Interactions: Theoretical View 2022 , 61, 1401-1417	О
412	Role of Computational Science in Materials and Systems Design for Sustainable Energy Applications: An Industry Perspective. 1	
411	CO2 Capture and Separation from H2/CH4/N2 gas mixtures by a Novel Ternary Pentagonal Monolayer Penta-BCNEFirst Principles Investigation. 2022, 348, 118474	О
410	Study the role of MgONTs on adsorption and detection of carbon dioxide: First-principles density calculations. 2022 , 1208, 113572	0
409	Strain effect on the electronic and photocatalytic properties of GaN-MSSe (M=Mo, W). 2022 , 306, 122798	О
408	Sc functionalized boron-rich C60 fullerene for efficient storage and separation of CO2 molecules: A DFT investigation. 2022 , 1208, 113557	О
407	2D IR spectra of the intrinsic vibrational probes of ionic liquid from dispersion corrected DFT-MD simulations. 2022 , 348, 118390	2
406	Defect stabilized Fe atom on porous BN sheet as a potential electrocatalyst for oxygen reduction reaction: A first-principles investigation. 2022 , 580, 152271	О
405	Nonmetal doped carbon nitride nanosheet as photocatalyst for degradation of 4, 5-dichloroguaiacol 2022 , 207, 112623	O
404	Modified fullerenes as acceptors in bulk heterojunction organic solar cells - a theoretical study. 2021 ,	O
403	Screening of Transition Metal Single-Atom Catalysts Doped on EGraphyne-Like BN Sheet for Efficient Nitrogen Reduction Reaction.	
402	Molecular Features Behind Formation of ⊕r ¶Co-Crystalline and Nanoporous-Crystalline Phases of PPO 2021 , 9, 809850	2
401	Cooperativity of Halogen- and Chalcogen-Bonding Interactions in the Self-Assembly of 4-lodoethynyl- and 4,7-Bis(iodoethynyl)benzo-2,1,3-chalcogenadiazoles: Crystal Structures, Hirshfeld Surface Analyses, and Crystal Lattice Energy Calculations. 2022 , 22, 1299-1311	1
400	Deep learning-driven molecular dynamics simulations of molten carbonates: 1. Local structure and transport properties of molten Li2CO3-Na2CO3 system. 2022 , 28, 1231	1
399	A metallic Cu2N monolayer with planar tetracoordinated nitrogen as a promising catalyst for CO2 electroreduction. 2022 , 10, 1560-1568	2
398	A journey toward the heaven of chemical fidelity of intermolecular force fields.	1
397	A cost-effective water-in-salt electrolyte enables highly stable operation of a 2.15-V aqueous lithium-ion battery. 2022 , 3, 100688	O

396	Rotational analysis of naphthol-aromatic ring complexes stabilized by electrostatic and dispersion interactions 2021 ,	O
395	Suppressing electrolyte-lithium metal reactivity via Li-desolvation in uniform nano-porous separator 2022 , 13, 172	9
394	Second-Sphere Lattice Effects in Copper and Iron Zeolite Catalysis 2022,	2
393	A new MoCN monolayer containing stable cyano structural units as a high-efficiency catalyst for the hydrogen evolution reaction 2022 ,	O
392	B-DNA Structure and Stability: The Role of Nucleotide Composition and Order 2022, e202100231	
391	Controllable spin direction in nonmagnetic BX/MX2 ($M = Mo$ or W ; $X = S$, Se and Te) van der Waals heterostructures by switching between the Rashba splitting and valley polarization. 2021 , 10, 312-320	1
390	First-Principles Calculations of Graphene-WS2 Nanoribbons As Electrode Material for Magnesium-Ion Batteries. 2022 , 51, 978-984	0
389	Hydrogen-bonded organic molecular ferroelectrics/antiferroelectrics. 2022, 47-84	О
388	The reaction of Criegee intermediates with formamide and its implication to atmospheric aerosols 2022 , 296, 133717	0
387	Co Anchored B 36 Cluster as a Novel Single Atom Catalyst for Removing Toxic CO Molecules: A Mechanistic First-Principles Study. 2022 , 7,	O
386	Alkali metal decorated C fullerenes as promising materials for delivery of the 5-fluorouracil anticancer drug: a DFT approach 2022 , 12, 3948-3956	2
385	Double-hybrid density functionals for the condensed phase: Gradients, stress tensor, and auxiliary-density matrix method acceleration 2022 , 156, 074107	1
384	Theoretical Study on Si I Il Bond Activation in Pd-Catalyzed Cross-Coupling of Chlorosilanes with Organoaluminum. 2022 , 2022,	2
383	A computational study on the potential application of carbon nitride nanosheets in Na-ion batteries 2022 , 28, 40	
382	Synthesis, Characterization and DFT-D Studies of 2-Aminoethoxycalix[4]resorcinarenes: A Novel Heterogeneous Organocatalyst. 1	
381	Unraveling the Role of Estacking Interactions in Ligand Binding to the Thiamine Pyrophosphate Riboswitch with High-level Quantum Chemical Calculations and Docking Study 2022 ,	2
380	Quantum chemical study the interaction between thiotepa drug and silicon doped graphdiyne. 2022 , 1209, 113612	1
379	Hydrophilic oxygen radical absorbance capacity values of low-molecular-weight phenolic compounds containing carbon, hydrogen, and oxygen 2022 , 12, 4094-4100	1

378	Employing Pseudopotentials to Tackle Excited-State Electron Spill-Out in Frozen Density Embedding Calculations 2022 ,	2
377	Janus MoPC Monolayer with Superior Electrocatalytic Performance for the Hydrogen Evolution Reaction 2022 ,	O
376	Carbon dioxide storage and separation using all-boron B38 fullerene: DFT calculations. 2022, 790, 139361	0
375	Selective sensing of NH3 and CH2O molecules by novel 2D porous hexagonal boron oxide (B3O3) monolayer: A DFT approach. 2022 , 29, 101767	O
374	Robust valley polarization induced by super-exchange effects in HfNX ($X = Cl$, Br, I)/FeCl2 two-dimensional ferrovalley heterostructures. 2022 , 120, 063103	6
373	Application of aluminum nitride nanotubes as a promising nanocarriers for anticancer drug 5-aminosalicylic acid in drug delivery system. 2022 , 118676	3
372	Key Piece in the Wolfe Cycle of Methanogenesis: The SB Bond Dissociation Conducted by Noncubane [Fe4S4] Cluster-Dependent Heterodisulfide Reductase. 2606-2622	
371	Ultrafast charge transfer dynamics in 2D covalent organic frameworks/Re-complex hybrid photocatalyst 2022 , 13, 845	6
370	Analysis of vibronic coupling in a 4f molecular magnet with FIRMS 2022 , 13, 825	7
369	Lone pair driven anisotropy in antimony chalcogenide semiconductors 2022,	3
369 368	Lone pair driven anisotropy in antimony chalcogenide semiconductors 2022, Density Functional Theory for Transition Metal Catalysis. 2022,	3
		3
368	Density Functional Theory for Transition Metal Catalysis. 2022 , Surface Functionalization of Penta-Siligraphene Monolayer for Nanoelectronic, Optoelectronic and	0
368 367	Density Functional Theory for Transition Metal Catalysis. 2022, Surface Functionalization of Penta-Siligraphene Monolayer for Nanoelectronic, Optoelectronic and Photocatalytic Water-Splitting: A First-Principles Study. A combination of proton spin diffusion NMR and molecular simulations to probe supramolecular	
368 367 366	Density Functional Theory for Transition Metal Catalysis. 2022, Surface Functionalization of Penta-Siligraphene Monolayer for Nanoelectronic, Optoelectronic and Photocatalytic Water-Splitting: A First-Principles Study. A combination of proton spin diffusion NMR and molecular simulations to probe supramolecular assemblies of organic molecules in nanoporous materials 2022, X-ray wavefunction refinement and comprehensive structural studies on bromo-substituted	
368 367 366 365	Density Functional Theory for Transition Metal Catalysis. 2022, Surface Functionalization of Penta-Siligraphene Monolayer for Nanoelectronic, Optoelectronic and Photocatalytic Water-Splitting: A First-Principles Study. A combination of proton spin diffusion NMR and molecular simulations to probe supramolecular assemblies of organic molecules in nanoporous materials 2022, X-ray wavefunction refinement and comprehensive structural studies on bromo-substituted analogues of 2-deoxy-d-glucose in solid state and solution 2022, 12, 8345-8360 Exploring a novel two-dimensional metallic YC sheet applied as an anode material for sodium-ion	0
368 367 366 365 364	Density Functional Theory for Transition Metal Catalysis. 2022, Surface Functionalization of Penta-Siligraphene Monolayer for Nanoelectronic, Optoelectronic and Photocatalytic Water-Splitting: A First-Principles Study. A combination of proton spin diffusion NMR and molecular simulations to probe supramolecular assemblies of organic molecules in nanoporous materials 2022, X-ray wavefunction refinement and comprehensive structural studies on bromo-substituted analogues of 2-deoxy-d-glucose in solid state and solution 2022, 12, 8345-8360 Exploring a novel two-dimensional metallic YC sheet applied as an anode material for sodium-ion batteries 2022, Energy decomposition analysis of cationic carbene analogues with group 13 and 16 elements as a	0

360	Effects of Heterocyclic Ring Fusion and Chain Elongation on Chiroptical Properties of Polyaza[9]helicene: A Computational Study 2022 , 126, 1412-1421	2
359	Improving the transferability of density functional theory predictions through correlation analysis: Structural and energetic properties of NiX alloys (X=C, Si, . 2022, 105,	O
358	In-plane magnetization and electronic structures in BiFeO3/graphene superlattice. 2022, 120, 084002	О
357	Understanding Poor Milling Behavior of Voriconazole from Crystal Structure and Intermolecular Interactions 2022 ,	2
356	Computational Investigation of Chemisorption of Thiophosgene on Co@B\$\$_{8}^{ - }\$\$. 2022 , 96, 267-272	
355	Thermal Desorption of Interstellar Ices: A Review on the Controlling Parameters and Their Implications from Snowlines to Chemical Complexity. 2022 , 6, 597-630	5
354	Orientational Effects on the Electronic Structure and Polarization in ScN@C 2022,	
353	Zn Metal D rganic Framework with High Stability and Sorption Selectivity for CO2. 2022 , 41, 829-835	2
352	Classical nuclear motion: Does it fail to explain reactions and spectra in certain cases?.	О
351	The PM6-FGC Method: Improved Corrections for Amines and Amides 2022 , 27,	1
350	The electronic response of the aluminum phosphide nanotube to different concentrations of carbon disulfide molecules. 2022 , 153, 339-345	
349	Electronic properties of germanene on pristine and defective MoS2 : A first-principles study. 2022 , 105,	
348	Controlling the Formation of Two Concomitant Polymorphs in Hg(II) Coordination Polymers 2022 , 61, 4965-4979	1
347	A Theoretical Study on the Structural, Electronic, and Magnetic Properties of Bimetallic PtNi (N = 0, 3, 6, 9, 13) Nanoclusters to Unveil the Catalytic Mechanisms for the Water-Gas Shift Reaction 2022 , 10, 852196	
346	How Symmetry Influences the Dissociation of Protonated Cyclic Peptides. 2022 , 14, 679	О
345	Liquid-phase sintering enabling mixed ionic-electronic interphases and free-standing composite cathode architecture toward high energy solid-state battery. 1	O
344	Interfacial coupling enhanced photocatalytic activity: an experimental/DFT combined study of porous graphitic carbon nitride/carbon composite material. 1	Ο
343	Stereoisomeric Tris-BINOL-Menthol Bulky Monophosphites: Synthesis, Characterisation and Application in Rhodium-Catalysed Hydroformylation 2022 , 27,	O

342	Adsorption of water on C sites vacancy defected graphene/h-BN: First-principles study 2022, 28, 107	0
341	StructureIntioxidant activity (oxygen radical absorbance capacity) relationships of phenolic compounds. 1	Ο
340	Hydrogen storage on superalkali NLi4 decorated \$\frac{1}{2}\$-borophene: A first principles insights. 2022 ,	1
339	Low-cost hydrocarbon membrane enables commercial-scale flow batteries for long-duration energy storage. 2022 ,	4
338	Ternary Cu(OH)2/P(g-C3N4)/MoS2 Nanostructures for Photocatalytic Hydrogen Production.	1
337	Modulation of the B4N monolayer as an efficient electrocatalyst for hydrogen evolution reaction. 2022 , 47, 11511-11519	O
336	How the Chalcogen Atom Size Dictates the Hydrogen-Bond Donor Capability of Carboxamides, Thioamides, and Selenoamides 2022 ,	0
335	Influence of Dimensionality on the Charge Density Wave Phase of 2H-TaSe 2. 2100329	
334	DNA Nucleobase Interaction with Silicon Carbide Nanosheet. 1	Ο
333	Optimal Tuning Perspective of Range-Separated Double Hybrid Functionals 2022 , 18, 2331-2340	1
332	Interfacial Properties of Two-Dimensional CdS/GO from DFT. 2022 , 101960	0
331	Study of Two-Dimensional Janus WXY (XIY= S, Se, and Te) Trilayer Homostructures for Photovoltaic Applications Using DFT Screening of Different Stacking Patterns 2022 , 7, 12947-12955	1
330	Enhanced reversible hydrogen storage performance of light metal-decorated boron-doped siligene: A DFT study. 2022 ,	0
329	Different metal-decorated aluminum phosphide nanotubes as hydrazine sensors for biomedical applications 2022 , 28, 112	
328	First-principles study on haeckelite hexagonal monolayer with high specific capacity for sodium-ion battery. 2022 , 378, 115898	0
327	A phenomenological model of diesel combustion characteristics under CO2/O2 atmosphere. 2022 , 229, 107167	
326	Superionic conductivity and large capacitance behaviors of two-metal MXenes WCrC in sodium ion battery. 2022 , 200, 111054	1
325	Investigation on the local structure and properties of molten Li2CO3-K2CO3 binary salts by machine learning potentials. 2022 , 356, 118979	Ο

324	Design of metal-decorated beryllium carbide (Be2C) as a high-capacity hydrogen storage material with strong adsorption characteristics. 2022 , 589, 152960	2
323	Screening of transition metal single-atom catalysts doped on Egraphyne-like BN sheet for efficient nitrogen reduction reaction. 2022 , 908, 164675	2
322	The Density Functional Theory Account of Interplaying Long-Range Exchange and Dispersion Effects in Supramolecular Assemblies of Aromatic Hydrocarbons with Spin 2021 , 27,	1
321	2D NbSBr and TaSBr: Experimentally Achievable Janus Photocatalysts with Robust Coexistence of Strong Optical Absorption, Intrinsic Charge Separation, and Ultrahigh Solar-to-Hydrogen Efficiency 2021 ,	1
320	Terahertz Spectroscopic Measurements and Solid-State Density Functional Calculations on CH3NH3PbBr3 Perovskites: Short-Range Order of Methylammonium. 2022 , 126, 339-348	2
319	Drug Discovery for Using Structure-Based Computer-Aided Drug Design Approach 2021 , 22,	4
318	Magnetic moment quenching in small Pd clusters in solution. 2021 , 75, 1	
317	Study of the Electronic Structure of M2(CH2CMe3)6 (M = Mo, W) by Photoelectron Spectroscopy and Density Functional Theory. 2022 , 41, 29-40	1
316	Energy transfer, pre-reactive complex formation and recombination reactions during the collision of peroxy radicals 2022 ,	0
315	Bipolar fluorinated covalent triazine framework cathode with high lithium storage and long cycling capability 2022 , 12, 11484-11491	O
314	Kinetic Separation of C2H6/C2H4 in A Cage-Interconnected Metal-Organic Framework: An Interaction-Screening Mechanism.	1
313	Adsorption of Water Molecule in Graphene/MoS2 Heterostructure with Vacancy Defects in Mo Sites. 2022 , 2022, 1-18	
312	Toxic hydrazoic acid vapor detection and adsorption by different metal-decorated BN nanotubes: a first-principles study. 2022 , 113721	1
311	Exploring Photoswitchable Properties of Two Nitro Nickel(II) Complexes with (,,)-Donor Ligands and Their Copper(II) Analogues 2022 ,	2
310	Systematically theoretical investigation the effect of nitrogen and iron-doped graphdiyne on the oxygen reduction reaction mechanism in proton exchange membrane fuel cells. 2022 ,	O
309	Modeling magnesium surfaces and their dissolution in an aqueous environment using an implicit solvent model 2022 , 156, 174702	
308	Poly (O-Aminophenol) Produced by Plasma Polymerization Has IR Spectrum Consistent with a Mixture of Quinoid & Education Structures. 2022 , 5, 196-205	
307	Double Hybrids and Noncovalent Interactions: How Far Can We Go?. 2022 ,	1

306	Gallium and scandium doping effect on the sensing performance of aluminum phosphide nanotubes toward toxic ethylene oxide gas. 2022 , 128145	O
305	Impact of covalent modifications on the hydrogen bond strengths in diaminotriazine supramolecules 2022 ,	O
304	Defect Physics of the Quasi-Two-Dimensional Photovoltaic Semiconductor GeSe.	
303	Tracing the Primordial Chemical Life of Glycine: A Review from Quantum Chemical Simulations 2022 , 23,	O
302	Dipole-dipole interactions of sulfone groups as a tool for self-assembly of a 2D Covalent Organic Framework derived from a non-linear diboronic acid. 2022 , 337, 111914	O
301	Theoretical investigations of Janus WSeTe monolayer and related van der Waals heterostructures with promising thermoelectric performance. 2022 , 593, 153402	O
300	Silicon-doped boron nitride graphyne-like sheet for catalytic NO reduction: A DFT study 2022 , 114, 108186	1
299	Data_Sheet_1.PDF. 2019 ,	
298	Organic ferroelectric Croconic Acid: A concise survey from bulk single crystals to thin films.	1
297	FeP2 monolayer: Isoelectronic analogue of MoS2 with excellent electronic and optical properties.	O
296	Noncovalently bound excited-state dimers: a perspective on current time-dependent density functional theory approaches applied to aromatic excimer models 2022 , 12, 13014-13034	4
295	Direct Electron Transfer between Aromatic Molecules inside and outside the ZSM-5 Zeolite Channels: An Identification of the EPR Spectra of 1,3,5-Trimethylbenzene Radical Cations. 2022 , 126, 7421-7430	
294	Comparison of approximate intermolecular potentials for ab initio fragment calculations on medium sized N-heterocycles <i>Journal of Computational Chemistry</i> , 2022 ,	1
293	LFDFTA Practical Tool for Coordination Chemistry. 2022, 10, 70	1
292	A sensitive non-enzymatic glucose sensor based on MgO entangled nanosheets decorated with CdS nanoparticles: Experimental and DFT study. 2022 , 119366	O
291	A theoretical investigation of nonlinear optical and electronic molecular parameters of hexabutyloxytryphenylene and halogenated hexabutyloxytryphenylene molecules using density functional theory (DFT) for nonlinear device applications. 2022 , 97, 065808	1
290	Accurate Deep Learning-Aided Density-Free Strategy for Many-Body Dispersion-Corrected Density Functional Theory 2022 , 13, 4381-4388	1
289	Atomic-scale interactions between quorum sensing autoinducer molecules and the mucoid P. aeruginosa exopolysaccharide matrix 2022 , 12, 7724	O

288	Anisotropic Impact Sensitivity of Metal-Free Molecular Perovskite High-Energetic Material (C6H14N2)(NH2NH3)(ClO4)3 by First-Principles Study.	
287	Two-dimensional TeX(X=C, Si, Ge) monolayers with strong intrinsic electric field for efficiency hydrogen evolution reaction. 2022 , 102011	O
286	Triggering the Direct CII Coupling of Gaseous CO into C2 Oxygenates by Synergizing Interfacial Interactions and Reversible Spatial Dynamic Confinement.	О
285	First principles calculations investigation of optoelectronic properties and photocatalytic CO2 reduction of (MoSi2N4)5-n/(MoSiGeN4)n in-plane heterostructures. 2022 , 37, 105549	2
284	Two-dimension black arsenic-phosphorus as a promising NO sensor: A DFT study. 2022 , 1213, 113727	
283	Strain and electric field dependent spin polarization in two-dimensional arsenene/CrI3 heterostructure. 2022 , 912, 165093	
282	Development of moderately fluorescence active salen type chemosensor for judicious recognition and quantification of Zn(II), Al(III) and SO4=: Demonstration of molecular logic gate formation and live cell images studies. 2022 , 1263, 133214	1
281	Exciton moir[potential in twisted WSe₂ homobilayers modulated by electric field. 2022 ,	
280	Betulinic acid and 3-o-acetyl-betulinic acid interactions with external and internal surface of boron-nitride nanotubes: A DFT and MD investigation. 2022 , 113738	O
279	Magnesium oxide nanotube as a promising material for detection of methamphetamine drug: theoretical study 2022 , 28, 150	О
278	Theoretical evaluation of Al-doped biphenylene nanosheet sensing properties toward gamma-butyrolactone.	
277	Dangling Octahedra Enable Edge States in 2D Lead Halide Perovskites 2022 , e2201666	3
276	Connection between water's dynamical and structural properties: Insights from ab initio simulations 2022 , 119, e2121641119	1
275	First-principles investigations to evaluate monolayer Mo2B as promising two-dimensional anode materials for Mg-ion batteries.	
274	Tribology at the Atomic Scale with Density Functional Theory.	О
273	Analysis of the hostguest complex formation involving bridged hexameric pyridiniumphenyl rings in the HexaCage6+ host in suit[3]ane: insights from dispersion-corrected DFT calculations for a nanometric mechanically interlocked device.	О
272	Identification of potential inhibitors against FemX of Staphylococcus aureus: A hierarchial in-silico drug repurposing approach. 2022 , 115, 108215	2
271	Ti2co2/Ti2cf2 Van Der Waals Heterostructure with Robust Schottky Barriers Under Electric Fields.	

270	Mechanistic Insight into the Promotional Effect of CO2 on Propane Aromatization over Zn/ZSM-5.	О
269	Fundamental mechanisms of hexagonal boron nitride sensing of dopamine, tryptophan, ascorbic acid, and uric acid by first-principles study. 2022 , 28,	
268	A highly sulfur resistant and stable heterogeneous catalyst for liquid-phase hydrogenation. 2022 , 121566	2
267	Modeling the Adsorption of Polycyclic Aromatic Hydrocarbons on Graphynes: An Improved Lennard-Jones Formulation.	O
266	Propylthiouracil drug adsorption on pristine, Cu, Ag, and Au decorated AlP nanosheets. 2022 , 128236	1
265	First-principles Calculations of Bulk WX2 (X = Se, Te) as Anode Materials for Na Ion Battery.	1
264	Metal Coordination Determines the Catalytic Activity of IrO2 Nanoparticles for the Oxygen Evolution Reaction. 2022 ,	О
263	Study to molecular insight into the role of Aluminum nitride nanotubes on to deliver of 5-Fluorouracil (5FU) drug in smart drug delivery. 2022 , 109617	1
262	Density functional theory-based quantum-computational analysis on the strain-assisted phononic, electronic, photocatalytic properties and thermoelectric performance of monolayer Janus SnSSe. 2022 , 128,	O
261	Tailoring the electronic and optical properties of ZrS2/ZrSe2 vdW heterostructure by strain engineering. 2022 , 139332	O
260	Impact of linker/metal tuning on the performance of two-dimensional Ni3(HITP)2 MOF-based Mg ion batteries. 2022 , 34, 100382	1
259	Density functional theory study of P-embedded SiC monolayer as a robust metal free catalyst for N2O reduction and CO oxidation. 2022 , 527, 112392	
258	In-situ engineered heterostructured nickel tellur-selenide nanosheets for robust overall water splitting. 2022 , 446, 137297	O
257	Deep neural network based quantum simulations and quasichemical theory for accurate modeling of molten salt thermodynamics.	1
256	Structural and Photoelectrochemical Dynamics of In-Situ Hydrogenated Anatase Tio2 Thin Films Grown by Dc Reactive Magnetron Sputtering.	
255	Computational mechanistic insights on Ag2O as a host for Li in lithium-ion batteries.	
254	Graphene-based polymer composites in corrosion protection applications. 2022 , 559-581	
253	Enhanced Fluorescence with Tunable Color in Doped Diphosphine-Protected Gold Nanoclusters. 5873-5880	2

252 Porphyrins: Electronic Structure and Ultraviolet/Visible Absorption Spectroscopy. **2022**, 505-586

251	Potential application of some metal decorated AlP nano-sheet for detection of boron trichloride. 2022 , 113792	O
250	A Peculiar Binding Characterization of DNA (RNA) Nucleobases at MoOS-Based Janus Biosensor: Dissimilar Facets Role on Selectivity and Sensitivity. 2022 , 12, 442	1
249	A first principle study on sensing properties of quasi-planer born (B36 borophene) towards COS, SO2, H2S and CS2 gases. 2022 , 115364	
248	Efficient and Accurate Description of Diels-Alder Reactions using Density Functional Theory.	О
247	Effect of Boron Doping on the Interlayer Spacing of Graphite. 2022 , 15, 4203	1
246	Not a Mere Decoration: Impact of Submonolayer Coverages of Nickel on Fundamental Properties of Platinum. 2022 , 126, 10167-10180	O
245	Theoretical study of metal-free catalytic for catalyzing CO-oxidation with a synergistic effect on P and N co-doped graphene. 2022 , 12,	O
244	Revealing the regioselective N-acylation of 5-bromo-2-aminobenzimidazole using experiment and theoretical calculation. 2022 , 132905	O
243	Benchmark Density Functional Theory Approach for the Calculation of Bond Dissociation Energies of the MD2 Bond: A Key Step in Water Splitting Reactions. 2022 , 7, 20800-20808	2
242	Improved proton-transfer barriers with van der Waals density functionals: Role of repulsive non-local correlation. 2022 , 156, 244106	О
241	First-principles calculations on CO2 hydrogenation to formic acid over a metal-doped boron phosphide. 2022 , 527, 112412	
240	Theoretical insights into the mechanism of photocatalytic reduction of CO2 over semiconductor catalysts. 2022 , 52, 100538	3
239	Al- and Ga-embedded boron nitride nanotubes as effective nanocarriers for delivery of rizatriptan. 2022 , 361, 119662	1
238	Developing Dipole-scheme heterojunction photocatalysts. 2022 , 599, 153942	О
237	Electrocatalytic activity of 版b two-dimensional surface for hydrogen evolution reaction.	1
236	Coordination Modulated Passivation for Stable Organic-Inorganic Perovskite Solar Cells.	
235	Voltage Prediction of Vanadium Redox Flow Batteries from First Principles.	

234	Cationic palladium(ii)-indenyl complexes bearing phosphines as ancillary ligands: synthesis, and study of indenyl amination and anticancer activity.	
233	Performance of Dispersion-Inclusive Density Functional Theory Methods for Energetic Materials. 2022 , 18, 4456-4471	О
232	Rutin precursor for the synthesis of superparamagnetic ZnFe2O4 nanoparticles: experimental and density functional theory. 2022 , 128,	1
231	Anodic SnO2 Nanoporous Channels Functionalized with CuO Quantum Dots for Selective H2O2 Biosensing.	О
230	Post-synthetic halogen incorporation in Zr-based MOF for enhancement of the catalytic oxidation reactions. 2022 , 136, 104438	
229	How Reproducible Are QM/MM Simulations? Lessons from Computational Studies of the Covalent Inhibition of the SARS-CoV-2 Main Protease by Carmofur.	2
228	Effects of Ag-decoration on the adsorption and detection of toxic OF2 gas on a GaN nanotube. 1-9	О
227	Potential application of different metal-decorated boron nitride nanosheets as chemical sensors for trichlorosilane detection. 2022 , 128303	
226	Synthesis and antiviral properties of biomimetic iminosugar-based nucleosides. 2022, 114618	
225	Mechanism for the Halogenation and Azidation of Lysine Catalyzed by Non-heme Iron BesD Enzyme.	О
224	Computational study of the effect of Fe-doping on the sensing characteristics of BC3 nano-sheet toward sulfur trioxide. 2022 , 113805	O
223	Atomic imaging of zeolite-confined single molecules by electron microscopy.	7
222	Investigation of structural properties of Mg-doped twisted bilayer graphene for phosphine gas detection. 1-9	
221	Multiphase nanosheet-nanowire cerium oxide and nickel-cobalt phosphide for highly-efficient electrocatalytic overall water splitting. 2022 , 316, 121678	1
220	Cooperativity in Diiron(III)porphyrin Dication Diradical-Catalyzed Oxa-DielsAlder Reactions: Spectroscopic and Mechanistic Insights. 9589-9601	1
219	Intermolecular Interactions of Pyrene and Its Oxides in Toluene Solution.	1
218	NMR and computational studies of ammonium ion binding to dibenzo-18-crown-6.	
217	Ti2CO2/Ti2CF2 van der Waals heterostructure with robust Schottky barriers under electric fields. 2022 , 602, 154313	

216	A litmus test for the balanced description of dispersion interactions and coordination chemistry of lanthanoids.	
215	Supercomputer Search for the New Inhibitors of the Coagulation Factor XIIa. 2022 , 43, 895-903	Ο
214	Ionic Dynamics and Vibrational Spectral Diffusion of a Protic Alkylammonium Ionic Salt through Intrinsic Cationic NH Vibrational Probe from FPMD Simulations. 2022 , 126, 5134-5147	1
213	Tunable Topological Phase Transition in Two-Dimensional Ternary Transition Metal Halides TiXI (X = P and As). 9,	
212	Band versus Polaron: Charge Transport in Antimony Chalcogenides. 2954-2960	1
211	Multilevel Computational Studies Reveal the Importance of Axial Ligand for Oxygen Reduction Reaction on FeNជ Materials.	10
210	Effects of thermal, elastic, and surface properties on the stability of SiC polytypes. 2022, 106,	1
209	Periodic Density Matrix Embedding for CO Adsorption on the MgO(001) Surface. 2022 , 13, 7483-7489	1
208	Computational Prediction of Tc-99 NMR Chemical Shifts in Technetium Complexes with Radiopharmaceutical Applications. 2022 , 126, 5434-5448	
207	Exploring the application of AlN graphyne in calcium ion batteries. 2022,	
207	Exploring the application of AlN graphyne in calcium ion batteries. 2022, Atomically Reconstructed Palladium Metallene by Intercalation-Induced Lattice Expansion and Amorphization for Highly Efficient Electrocatalysis.	7
Í	Atomically Reconstructed Palladium Metallene by Intercalation-Induced Lattice Expansion and	7
206	Atomically Reconstructed Palladium Metallene by Intercalation-Induced Lattice Expansion and Amorphization for Highly Efficient Electrocatalysis.	
206	Atomically Reconstructed Palladium Metallene by Intercalation-Induced Lattice Expansion and Amorphization for Highly Efficient Electrocatalysis. Al-, Ga-, and In-decorated BP nanotubes as chemical sensors for 2-chloroethanol. 2022, 153, 589-596 Deriving force fields with a multiscale approach: from ab initio calculations to molecular-based	
206	Atomically Reconstructed Palladium Metallene by Intercalation-Induced Lattice Expansion and Amorphization for Highly Efficient Electrocatalysis. Al-, Ga-, and In-decorated BP nanotubes as chemical sensors for 2-chloroethanol. 2022, 153, 589-596 Deriving force fields with a multiscale approach:from ab initio calculations to molecular-based equations of state. Inverse spin crossover in fluorinated Fe(1,10-phenanthroline)2(NCS)2 adsorbed on Cu (001) surface.	1
206 205 204 203	Atomically Reconstructed Palladium Metallene by Intercalation-Induced Lattice Expansion and Amorphization for Highly Efficient Electrocatalysis. Al-, Ga-, and In-decorated BP nanotubes as chemical sensors for 2-chloroethanol. 2022, 153, 589-596 Deriving force fields with a multiscale approach:from ab initio calculations to molecular-based equations of state. Inverse spin crossover in fluorinated Fe(1,10-phenanthroline)2(NCS)2 adsorbed on Cu (001) surface. 2022, e00735	0
206 205 204 203	Atomically Reconstructed Palladium Metallene by Intercalation-Induced Lattice Expansion and Amorphization for Highly Efficient Electrocatalysis. Al-, Ga-, and In-decorated BP nanotubes as chemical sensors for 2-chloroethanol. 2022, 153, 589-596 Deriving force fields with a multiscale approach:from ab initio calculations to molecular-based equations of state. Inverse spin crossover in fluorinated Fe(1,10-phenanthroline)2(NCS)2 adsorbed on Cu (001) surface. 2022, e00735 Coordination Modulated Passivation for Stable Organic-Inorganic Perovskite Solar Cells. 2022, 138740 Density Functional Response Calculations of Dispersion Coefficients C6 and C9 of Closed- and	0

198	Charge Transfer in Metallocene Intercalated Transition Metal Dichalcogenides. 2022, 126, 13994-14002	
197	Synergistic effect of Si-doping and Fe2O3-encapsulation on drug delivery and sensor applications of Egraphyne nanotube toward favipiravir as an antiviral for COVID-19: A DFT study. 2022 , 99, 100666	O
196	Ordered double transition metal MBene: the hexagonal ScTiB2 monolayer as a superior anode material for lithium-ion batteries. 2022 , 214, 111736	
195	Functional complexed zincate ions enable dendrite-free long cycle alkaline zinc-based flow batteries. 2022 , 102, 107697	O
194	Structure effect in the demulsification performance of cationic surfactants. 2022, 218, 110895	
193	First principle study of benzoquinone based microporous conjugated polymers as cathode materials for high-performance magnesium ion batteries. 2022 , 214, 111757	
192	Structural and spectroscopic studies of Na+ IQuercetin-5?-sulfonic acid polymeric complexes obtained via solvothermal synthesis. 2022 , 226, 116083	
191	Enhancing the kinetics of vanadium oxides via conducting polymer and metal ions co-intercalation for high-performance aqueous zinc-ions batteries. 2022 , 628, 204-213	O
190	Photodegradation of dye using Polythiophene/ZnO nanocomposite: A computational approach. 2022 , 117, 108285	0
189	Building Metal-Molecule Interface towards Stable and Reversible Zn Metal Anodes for Aqueous Rechargeable Zinc Batteries. 2206695	4
188	Tunable electronic structures in Type-II PtSe2/HfS2 van der Waals heterostructure by external electric field and strain. 2022 , 144, 115456	1
187	A Type-II WSe2/BP heterostructure with adjustable electronic properties under external electric field and biaxial strain. 2022 , 251, 119256	O
186	Chlorine trifluoride gas adsorption on the Fe, Ru, Rh, and Ir decorated gallium nitride nanotubes. 2022 , 356, 114945	0
185	Metal-decorated BN monolayer as potential chemical sensors for detection of purinethol drug. 2022 , 145, 109919	O
184	Sarin chemical warfare agent detection by Sc-decorated XN nanotubes (X´=´Al or Ga). 2022 , 145, 109941	0
183	High solar-to-hydrogen efficiency photocatalytic hydrogen evolution reaction with the HfSe2/InSe heterostructure. 2022 , 547, 232008	5
182	Desulfurization reactions of methanethiol on defect CeO2 surfaces. 2022 , 605, 154738	0
181	Structural and photoelectrochemical dynamics of in-situ hydrogenated anatase TiO2 thin films grown by DC reactive magnetron sputtering. 2023 , 607, 155023	O

180	Rationally designed oxygen vacancy for achieving effective and kinetically boosted Na-Se batteries. 2023 , 451, 139062	O
179	Achieving high-rate and high-capacity Zn metal anodes via a three-in-one carbon protective layer. 2022 , 10, 17440-17451	4
178	Capture and detection of SO2 using a chemically stable Mg(ii)MOF. 2022, 10, 18636-18643	O
177	Doping of the Mn vacancy of Mn2B2 with a single different transition metal atom as the dual-function electrocatalyst. 2022 , 24, 20988-20997	1
176	2D NbIrTe4 and TaRhTe4 Monolayers: Two Fascinating Topological Insulators as Electrocatalysts for Oxygen Reduction.	O
175	Reaction mechanism of the PuDddK dimethylsulfoniopropionate lyase and cofactor effects of various transition metal ions. 2022 , 51, 14664-14672	O
174	Ni-Decorated Graphene Oxide Nanosheet as an Adsorption Surface of Toxic Molecules (So2, No2 and O3): A Theoretical Study.	O
173	Theoretical study of 36Adz based alkaline earthides M+(36Adz)MI(M+ = Li & Na; MI± Be, Mg & Ca) with remarkable nonlinear optical response. 2023 , 153, 107119	O
172	Reaction Kinetics of Criegee Intermediates with Nitric Acid. 2022 , 126, 6160-6170	1
171	Investigation on the catalytic activity and Na tolerance performance of rare earth element decorated ZSM-5 zeolite: a first-principle study. 2022 , 596, 203-213	O
170	Strain-induced structural, elastic, and electronic properties of 1L-MoS2.	O
169	Enabling structural and interfacial stability of 5 V spinel LiNi0.5Mn1.5O4 cathode by a coherent interface. 2022 ,	1
168	P-type conductivity in Sn-doped Sb2Se3. 2022 , 4, 045006	O
167	Sensing of Acetaminophen Drug Using Silicon-Doped Graphdiyne: a DFT Inspection.	O
166	Resolving the amine-promoted hydrolysis mechanism of N 2 O 5 under tropospheric conditions. 2022 , 119,	О
165	Atomistic insight into the initial stage of graphene formation on SiC(0001) surfaces. 2022, 6,	O
164	Multiscale Pseudoatomistic Quantum Transport Modeling for van der Waals Heterostructures. 2022 , 18,	O
163	An overview of SnO2 based Z scheme heterojuctions: Fabrication, mechanism and advanced photocatalytic applications. 2022 ,	O

162	Cheap Turns Superior: A Linear Regression-Based Correction Method to Reaction Energy from the DFT.	O
161	Organic crystal structure prediction and its application to materials design.	O
160	Unraveling the Role of the Tyrosine Tetrad from the Binding Site of the Epigenetic Writer MLL3 in the Catalytic Mechanism and Methylation Multiplicity. 2022 , 23, 10339	О
159	Graphene grown on transition metal substrates: Versatile templates for organic molecules with new properties and structures. 2022 , 100575	O
158	HYDROGEN ADSORPTION AND STORAGE ON PALLADIUM-FUNCTIONALIZED C20 BOWL AND C20H10 BOWL MOLECULE INCLUDING HYDROGEN SATURATION. 2022 , 63, 1399-1408	O
157	Two-dimensional intrinsic ferrovalley Janus 2H-VSeS monolayer with high Curie temperature and robust valley polarization. 2022 , 6,	O
156	Structural, Electronic, and Vibrational Properties of N 2 O 4 under Pressure from First-Principles Study. 2200264	О
155	MoS2/TiO2 van der Waals heterostructures for promising photocatalytic performance: a first-principles study.	0
154	Method to Compute the SoluteBolvent Dispersion Contribution to the Electronic Excitation Energy in Solution.	O
153	H2 and CO adsorption ability of cationic lithiated carbenes: A computational study. 2022,	O
152	Sugar-cane based biorefineries: The butadiene synthesis from ethanol employing ZnZr/SiO2 catalyst. 2022 , 531, 112690	0
151	Reaction Mechanisms for Chiral Phosphate Catalyzed Transformations Involving Cationic Intermediates and Protic Nucleophiles.	O
150	Natural Lignin: a Sustainable and Cost-Effective Electrode Material for High-Temperature Na-Ion Battery.	О
149	Computational identification of bifunctional metal-modified ZSM-5 catalysts to boost methanehethanol coupling.	O
148	Enabling dual aromaticity in fused nanobelts: evaluation of the magnetic behavior of fused [10]CPP units.	О
147	Photoinduced electron transfer in hostguest complexes of double nanohoops.	O
146	Systematic Evaluation of Counterpoise Correction in Density Functional Theory.	3
145	Quantum chemical simulation of hydrogen adsorption in pores: A study by DFT, SAPT0 and IGM methods. 2022 , 12, 363-372	O

144	Looking beyond Adsorption Energies to Understand Interactions at Surface using Machine Learning. 2022 , 7,	0
143	Accurate Nonempirical Range-Separated Hybrid van der Waals Density Functional for Complex Molecular Problems, Solids, and Surfaces. 2022 , 12,	О
142	Mononuclear Oxidovanadium(IV) Complexes with BIAN Ligands: Synthesis and Catalytic Activity in the Oxidation of Hydrocarbons and Alcohols with Peroxides. 2022 , 12, 1168	0
141	M2(CHOO)4 paddlewheel of metal organic frameworks (M = Co, Mo, Ir) with open metal sites as anode materials of Na/K ion batteries: a theoretical study.	o
140	Tuning transport properties of B and C sites vacancy defects Graphene/h-BN heterostructures: first-principles study. 2022 , 95,	0
139	Bilayer Heterostructure of Boron Nitride and Graphene for Hydrogen Storage: A First-Principles Study. 2022 , 36, 13307-13316	О
138	Mechanisms of Reactions between HOI and HY (Y = Cl , Br , I) on a Water Nanodroplet Surface. 2022 , 126, 8028-8036	0
137	Alkaline earthides based on 15-crown-5 ether with remarkable NLO response. 2022 , 137,	О
136	Pressure-induced topological and structural phase transitions in natural van der Waals heterostructures from the (SnTe)m(Bi2Te3)n. 2022 , 106,	0
135	Formation of C60-SnI4 Adducts. Insights of the role of Ehole and Tetrel-bonding in the Strength and Interaction Nature from DFT calculations. 2022 , 121277	o
134	Endowing homodimeric carbamoyltransferase GdmN with iterative functions through structural characterization and mechanistic studies. 2022 , 13,	0
133	Exploring the role of Stone-Wales defect in boron nitride nano-sheet as a anode Mg-ion batteries. 2022 , 146, 110098	o
132	A density functional theory study of the CO oxidation on Pt1 supported on PtX2 (X´=´S, Se, Te). 2023 , 609, 155341	0
131	Boosted charge transfer in ReS2/Nb2O5 heterostructure by dual-electric field: Toward superior electrochemical reversibility for lithium-ion storage. 2023 , 630, 76-85	o
130	Tailoring the sensing capability of 2H-MoSe2 via 3d transition metal decoration. 2023, 610, 155399	0
129	Antioxidant mechanisms and products of four 4屆,7-trihydroxyflavonoids with different structural types.	o
128	Perspectives on weak interactions in complex materials at different length scales.	О
127	Mechanistic views and computational studies on transition-metal-catalyzed reductive coupling reactions.	O

126	Speciation and Structures in Pt Surface Sites Stabilized by N-Heterocyclic Carbene Ligands Revealed by Dynamic Nuclear Polarization Enhanced Indirectly Detected 195Pt NMR Spectroscopic Signatures and Fingerprint Analysis.	1
125	Electronic band gap on graphene induced by interaction with hydrogen cyanide. An DFT analysis. 2022 , 111744	0
124	Evaluation of the role perfect and defect boron nitride monolayer in calcium ion batteries as a anode. 2022 , 113940	0
123	Anodic SnO2 Nanoporous Structure Decorated with Cu2O Nanoparticles for Sensitive Detection of Creatinine: Experimental and DFT Study.	1
122	Structure and stability of Au, Au2 and Au8 cluster on Ni(111) supported h-BN sheet: Role of size and support towards oxygen bond activation. 2022 , 115561	0
121	Role of External Electric Field in Carrier Mobility of Graphene/ZnO Heterojunction Adsorbed H 2 O and O 2 Molecules. 2022 , 7,	O
120	Realizing a strong visible-light absorption band in piezoelectric 2D carbon nitride sheets for enhanced piezocatalysis. 2022 , 104, 107983	2
119	Chelidamic acid tautomers in copper(II) compounds. One-pot synthesis, crystal structure, spectroscopic and DFT studies. 2022 , 116210	O
118	Internal doping of metallic carbon nanotubes for chemiresistive sensing of explosive molecules. 2022 , 111773	0
117	DFT study about capturing of toxic sulfur gases over cyclic tetrapyrrole. 2023 , 1219, 113966	0
116	On the stability of peptide secondary structures on the TiO2 (101) anatase surface: a computational insight. 2022 , 25, 392-401	0
115	How do density functionals affect the Hirshfeld atom refinement?.	O
114	DFT calculations in solution systems: solvation energy, dispersion energy and entropy.	0
113	First principles investigation on Na-ion storage in two-dimensional boron-rich B2N, B3N, and B5N.	O
112	Theoretical design of two-dimensional AMInP2X3Y3 (AM = Li, Na, K; $X/Y = S$, Se, Te) monolayers for highly efficient excitonic solar cells.	0
111	Ab initio molecular dynamics study of proton transport in imidazolium-based ionic liquids with added imidazole.	o
110	Synthesis of novel and tunable Micro-Mesoporous carbon nitrides for Ultra-High CO2 and H2S capture. 2023 , 456, 140973	0
109	Nonvolatile electrical control of valley splitting by ferroelectric polarization switching in two-dimensional AgBiP2S6/CrBr3 multiferroic heterostructure.	O

108	Sulphur vacancy-rich PCdS/NiCoLDH promotes highly selective and efficient photocatalytic CO2 reduction to MeOH. 2023 , 67, 102332	О
107	Semirigid discotic dimers: flexible but not flexible enough?.	1
106	Tunable electronic properties and related functional devices for ferroelectric In2Se3/MoSSe van der Waals heterostructures. 2022 , 13, 228-238	О
105	Tinning the carbon: hydrostannanes strike back. 2022 , 52, 29-36	O
104	Magneto-structural correlations of dinickel(II) complexes with phenoxido/azido coligands: A theoretical investigation. 2023 , 811, 140241	1
103	4-BNP2 layered materials as auspicious anodes for Lithium batteries. 2023, 295, 127146	O
102	The Cd-decorated AlN nanotube as a potential chemical sensor for chloropicrin: DFT studies. 2023 , 1220, 113982	O
101	Hollow nano-CaCO3's VOC sensing properties: A DFT calculation and experimental assessments. 2023 , 313, 137334	O
100	First principles screening of transition metal single-atom catalysts for nitrogen reduction reaction. 2023 , 612, 155916	0
99	A comparative analysis of different van der Waals treatments for molecular adsorption on the basal plane of 2H-MoS2. 2023 , 729, 122226	O
98	Influence of nitro group on solvatochromism, nonlinear optical properties of 3-morpholinobenzanthrone: Experimental and theoretical study. 2023 , 437, 114434	O
97	Nonadiabatic molecular dynamics study of a complete photoswitching cycle for a full-size diarylethene system. 2023 , 438, 114513	O
96	Role of electronic correlations in room-temperature ferromagnetism of monolayer MnSe2. 2022 , 106,	O
95	Scavenging of Organic Pollutant and Fuel Generation through Cost-Effective and Abundantly Accessible Rust: A Theoretical Support with DFT Simulations. 2023 , 16, 142	O
94	Biodegradation of 2,5-Dihydroxypyridine by 2,5-Dihydroxypyridine Dioxygenase and Its Mutants: Insights into OD Bond Activation and Flexible Reaction Mechanisms from QM/MM Simulations. 2022 , 61, 20501-20512	O
93	New Au(III)- and Fe(III)-based complexes of bio-pharmacological interest: DFT and in silico studies. 2023 , 142,	O
92	Manganese(II) Bromide Compound with Diprotonated 1-Hydroxy-2-(pyridin-2-yl)-4,5,6,7-tetrahydrobenzimidazole: Dual Emission and the Effect of Proton Transfers. 2022 , 10, 245	2
91	Single-step extraction of small-diameter single-walled carbon nanotubes in the presence of riboflavin. 13, 1564-1571	O

90	Understanding X-ray Photoelectron Spectra of Ionic Liquids: Experiments and Simulations of 1-Butyl-3-methylimidazolium Thiocyanate. 2022 , 126, 10500-10509	О
89	Understanding the Atomic and Defective Interface Effect on Ruthenium Clusters for the Hydrogen Evolution Reaction. 49-59	2
88	Outstanding performance of transition-metal decorated BC3 nanotubes for high capacity CH4 storage. 2022 , 156062	О
87	Near-Infrared-Induced Photothermal Enhanced Photocatalytic H2 Production for 3D/2D Heterojunctions of Snowflake-like CuS/g-C3N4 Nanosheets.	O
86	Metallocenes and Beyond for Propene Polymerization: Energy Decomposition of Density Functional Computations Unravels the Different Interplay of Stereoelectronic Effects. 2022 , 41, 3872-3883	O
85	Pristine, Co, Rh, and, Ir decorated aluminum phosphide nano-sheet semiconductors as viable chemical sensors for cathinone. 2022 , 110305	O
84	Interexcited State Photophysics I: Benchmarking Density Functionals for Computing Nonadiabatic Couplings and Internal Conversion Rate Constants.	O
83	Uncovering Compounds with Promising Piezoresistive Properties via High-Throughput First-Principles Survey. 2022 , 105240	O
82	Application of pure and Ti-decorated AlP nano-sheet in the dacarbazine anti-cancer drug delivery: DFT calculations. 2022 , 113999	O
81	Transition Metals Incorporated on Phosphorene Sheet as Cost-Effective Single Atom Catalysts for Hydrogen Evolution Reaction: A DFT Study. 2022 , 113998	O
80	Electronic and optical properties of Janus-like hexagonal monolayer materials of group IV-VI. 2023 , 7,	O
79	Computational Studies of Auto-Active van der Waals Interaction Molecules on Ultra-Thin Black-Phosphorus Film. 2023 , 28, 681	1
78	Glass-box molecular dynamics simulation for teaching the van der Waals interaction.	O
77	Solvent-free oxidation of toluene to benzaldehyde using electron-rich Au clusters confined in Silicalite-1. 2023 , 141446	O
76	Atomistic insight into the effects of electrostatic fields on hydrocarbon reaction kinetics.	О
75	Improving Lurasidone Hydrochloride Solubility and Stability by Higher-Order Complex Formation with Hydroxypropyl-tyclodextrin. 2023 , 15, 232	O
74	[4FeßS]-Mediated Proton-Coupled Electron Transfer Enables the Efficient Degradation of Chloroalkenes by Reductive Dehalogenases. 1173-1185	О
73	Studying Ga and Ge-doped AlP nanotube as a drug carrier for ciclopirox anticancer drug using DFT. 2023 , 114025	O

72	Novel metallic titanium fluoride: A promising high capacity and superionic conductivity anode in Li-, Na-, and K-ion batteries. 2023 , 210, 111822	O
71	Investigate the effect of Zn12O12, AlZn11O12, and GaZn11O12 nanoclusters in the carbamazepine drug detection in gas and solvent phases: a comparative DFT study.	O
70	Discriminating and understanding molecular crystal polymorphism.	O
69	Mechanistic insights into hydrogen production from formic acid catalyzed by Pd@N-doped graphene: The role of the nitrogen dopant. 2023 ,	1
68	Cs 2 XI 2 Cl 2 (X = Pb, Sn) All-Inorganic Layered Ruddlesden Popper Mixed Halide Perovskite Single Junction and Tandem Solar Cells: Ultra-High Carrier Mobility and Excellent Power Conversion Efficiency. 2201050	О
67	Janus Ga2SeTe and In2SeTe nanosheets: Excellent photocatalysts for hydrogen production under neutral pH. 2023 ,	O
66	Facile modification of phosphole-based aggregation-induced emission luminogens with sulfonyl isocyanates.	O
65	The influence of N?pnicogen bonding in Estacked parallel displaced geometry of nitrobenzene dimers: Evidence using matrix isolation infrared spectroscopy and ab initio computations. 2023 , 1279, 135022	O
64	Infinitene as two fused helicoidal trails of fused rings: evaluation of the magnetic behavior of [12]infinitene and anionic species displaying global aromaticity and antiaromaticity. 2023 , 25, 8190-8197	O
63	Calculation of electric field gradients in Cd(II) model complexes of the CueR protein metal site.	O
62	Synthesis and Optical Properties of a Series of Push-Pull Dyes Based on Pyrene as the Electron Donor. 2023 , 28, 1489	O
61	Interaction of 5-Fluorouracil on the Surfaces of Pristine and Functionalized Ca12O12 Nanocages: An Intuition from DFT.	O
60	Theoretical evaluation of boron carbide nanotubes as non-enzymatic glucose sensors. 2023, 140510	O
59	Electronic and optical properties of transition-metal (TM=Sc, Ni, Cu, Zn) adsorbed monolayer SnSe2. 2023 , 177, 207548	O
58	The coupling of graphene, graphitic carbon nitride and cellulose to fabricate zinc oxide-based sensors and their enhanced activity towards air pollutant nitrogen dioxide. 2023 , 324, 138325	О
57	Preferred intermolecular cation manion interactions within the [EMIM][DCA] ionic liquid and its interaction with a water co-solvent molecule. 2023 , 381, 121804	O
56	2D CrMoC2S6/Sc2CO2 multiferroic heterostructure with robust antiferromagnetic ordering, switchable electronic properties and magnetic anisotropy. 2023 , 952, 169962	O
55	Emerging Trends of Computational Chemistry and Molecular Modeling in Froth Flotation: A Review.	O

54	A computational study on the potential application of metal-doped AlN nanotubes for chloroform detection. 2023 , 1222, 114047	O
53	Theoretical design of buckled honeycomb binary ZrX (X=S, Se, Te) monolayers and valley splitting of heterostructures constructed with MoTe2. 2023 , 660, 414899	О
52	Projected Hybrid Density Functionals: Method and Application to Core Electron Ionization. 2023 , 19, 837-847	0
51	Cooperative effect of strain and electric field on Schottky barriers in van der Waals heterostructure of graphene and hydrogenated phosphorus carbide. 2023 , 148, 115665	О
50	On the Trail of Molecular Hydrophilicity and Hydrophobicity at Aqueous Interfaces. 2023, 14, 1301-1309	О
49	The potential of pure and atom-decorated AlP nano-sheet as a drug delivery system for procarbazine: A DFT approach. 2023 , 1222, 114048	О
48	On the Cation-lapabilities of infinitene (II Evaluation of bonding and circular dichroism properties for Infinitene-Ag(I)n (n´=´1l4) complexes from relativistic DFT calculations. 2023 , 234, 116323	0
47	Interaction between [(ြ6-p-cym)M(H2O)3]2+ (MII = Ru, Os) or [(ြ5-Cp*)M(H2O)3]2+ (MIII = Rh, Ir) and Phosphonate Derivatives of Iminodiacetic Acid: A Solution Equilibrium and DFT Study. 2023 , 28, 1477	O
46	Direct synthesis of Al-rich ZSM-5 nanocrystals with improved catalytic performance in aromatics formation from methane and methanol. 2023 , 351, 112485	1
45	Molecular dynamics simulation studies of 1,3-dimethyl imidazolium nitrate ionic liquid with water. 2023 , 158, 084505	О
44	Generalized Many-Body Dispersion Correction through Random-Phase Approximation for Chemically Accurate Density Functional Theory. 2023 , 14, 1609-1617	O
43	Atomistic simulations for investigation of substrate effects on lipid in-source fragmentation in secondary ion mass spectrometry. 2023 , 18, 011003	О
42	A metallic La3C2 monolayer with remarkable activity for the hydrogen evolution reaction: a first-principles study. 2023 , 11, 6394-6402	0
41	Cyclophosphamide drug sensing characteristics by using pure and Ti-doped graphyne-like BN-yne. 2023 , 150, 110535	O
40	Extending density functional theory with near chemical accuracy beyond pure water. 2023, 14,	O
39	Single Atom Catalysis for Hydrogen Evolution Reaction using Transition-metal Atoms Doped g-C 3 N 3 : A Density Functional Theory Study. 2023 , 8,	O
38	Investigation on the potential application of some metal oxide nanoclusters in the detection of phenytoin in gas and solvent phases through density functional theory calculations. 2023 , 150, 110526	O
37	NAP-XPS Probes the Electronic Structure of the MgAlal Layered Double Hydroxide upon Controlled Hydration. 2023 , 127, 4144-4153	O

36	Rh-doped ultrathin NiFeLDH nanosheets drive efficient photocatalytic water splitting. 2023,	O
35	Identifying Ordered OH/F Anions in Hydroxyfluorides by a Terahertz Spectroscopic Approach. 2023 , 127, 4367-4373	O
34	Decoupling Planarizing and Steric Energetics to Accurately Model the Rigidity of Econjugated Polymers. 2023 , 127, 2092-2102	O
33	A DFT study on the selective adsorption and separation of CO2/CH4 on the Mg-decorated 2-D covalent organic framework (COF-5). 2023 , 100, 100949	O
32	Delivery of Cisplatin Anti-cancer Drug by Si-Decorated Al24N24 Nanocage: DFT Evaluation of Electronic and Structural Features. 2023 , 52, 3281-3290	O
31	Boron-embedded C3N nanosheets as efficient electrocatalysts for reduction of nitric oxide. 2023,	O
30	Metal-coordinated polybenzimidazole membranes with preferential K+ transport. 2023, 14,	0
29	Electrocatalytic reduction of N2 on FeRu dual-atom catalyst anchored in N-doped phosphorene. 2023 , 539, 113032	O
28	Mechanism for the synthesis of medium-chain 1-alkenes from fatty acids catalyzed by binuclear iron UndA decarboxylase. 2023 , 420, 123-133	O
27	Strong reactivity and electronic sensitivity of Au-decorated BC3 nanotubes toward the phenylpropanolamine drug. 2023 , 129,	O
26	Anthracite based activated carbon impregnated with HMTA as an effectiveness adsorbent could significantly uptake gasoline vapors. 2023 , 254, 114698	0
25	Gas phase electronic spectra of xylene-water aggregates. 2023 , 393, 111761	O
24	Potential Energy Surfaces Sampled in Cremer B ople Coordinates and Represented by Common Force Field Functionals for Small Cyclic Molecules. 2023 , 127, 2646-2663	0
23	9-Borafluoren-9-yl and diphenylboron tetracoordinate complexes of F- and Cl-substituted 8-quinolinolato ligands: synthesis, molecular and electronic structures, fluorescence and application in OLED devices. 2023 , 52, 4933-4953	O
22	A density functional theory study of van der Waals interaction in carbon nanotubes. 2023 , 70, 759-769	0
21	Influence of Capping Ligands, Solvent, and Thermal Effects on CdSe Quantum Dot Optical Properties by DFT Calculations. 2023 , 8, 11467-11478	O
20	High production of furfural by flash pyrolysis of C6 sugars and lignocellulose by Pd-PdO/ZnSO4 catalyst. 2023 , 14,	О
19	A Buckycatcher in Solution A Computational Perspective. 2023 , 28, 2841	O

18	Application of Pure and Au-Decorated YN (Y = B, Al, and Ga) Nanotubes as Good Media for Toxic Phosgene Oxime Gas Adsorption.	O
17	Role of molecular modelling in the development of metal-organic framework for gas adsorption applications. 2023 , 135,	0
16	Biphenylene Nanotube: A Promising Anode Material for Sodium-Ion Batteries.	О
15	A Tetraiodomanganate(II) Compound with P,P?-Diprotonated Bis(2-Diphenylphosphinophenyl)Ether Manifesting Unexpected Short Luminescence Lifetime. 2023 , 64, 398-409	O
14	Chemically circular, mechanically tough, and melt-processable polyhydroxyalkanoates. 2023, 380, 64-69	1
13	FeC6N monolayer with ideal properties for water splitting. 2023 , 626, 157203	O
12	Investigating Hydrogenation of Aldehyde and Heck Reaction on the Surface of Recyclable Palladium Decorated Functionalized Mica.	0
11	Dehydration of a crystal hydrate at subglacial temperatures. 2023 , 616, 288-292	O
10	Breaking BEP Relationship with Strong CO Binding and Low CL Coupling Barriers for Ethanol Synthesis on Boron-Doped Graphyne: Bond Order Conservation and Flexible Orbital Hybridization.	0
9	Synergy of Small Antiviral Molecules on a Black-Phosphorus Nanocarrier: Machine Learning and Quantum Chemical Simulation Insights. 2023 , 28, 3521	O
8	Quantum Mechanical and Classical Calculation of the Transport and Relaxation Properties of HeCO2 Complex Using a New PES.	0
7	MagnetoEtructural maps and bridged-ligand effect for dichloro-bridged dinuclear copper(ii) complexes: a theoretical perspective. 2023 , 13, 12430-12437	O
6	L-Histidine-based computation devices. 2023 , 97,	О
5	Rapid Detection of Cd2+ Ions in the Aqueous Medium Using a Highly Sensitive and Selective Turn-On Fluorescent Chemosensor. 2023 , 28, 3635	O
4	Characterizing Soft Matter Self-Assembly and Material Properties with Advanced Molecular Dynamics and Data-Driven Methods. 2023 , 1197-1220	0
3	Density functional theory (DFT)-based molecular modeling. 2023 , 115-133	О
2	Thermogravimetric analysis of flax, jute, and UHMWPE fibers and their composites with melamine and phenol formaldehyde resins. 2023 , 10,	0
1	Performance of Functionals and Basis Sets in Calculating Redox Potentials of Nitrile Alkenes and Aromatic Molecules using Density Functional Theory. 2023 , 8,	Ο